ABSTRACT

Title of Document: KINETICS OF *DEHALOBACTER* AND *DEHALOCOCCOIDES* STRAINS AND THEIR EFFECTS ON COMPETITION FOR GROWTH SUBSTRATES.

YenJung Lai, Doctor of Philosophy, 2010

Directed By: Associate Professor, Jennifer G. Becker, Department of Environmental Science and Technology

The chlorinated solvents tetrachloroethene (PCE) and trichloroethene (TCE) are common groundwater contaminants. Reductive dechlorination of PCE and TCE at contaminated sites is commonly carried out by dehalorespiring bacteria that utilize these compounds as terminal electron acceptors, but often results in the accumulation of *cis*-1,2-dichloroethene (cDCE) and vinyl chloride (VC), rather than non-toxic ethene. This project focused on evaluating how interactions among dehalorespiring populations that may utilize the same electron acceptors, electron donors and/or carbon source may affect the extent of PCE dechlorination *in situ*. These interactions may be particularly important if both *Dehalococcoides ethenogenes* (*Dhc. ethenogenes*) and *Dehalobacter restrictus* (*Dhb. restrictus*) are present because these bacteria utilize the same electron donor (H_2) and both respire PCE and TCE. However, unlike *Dhc*. *ethenogenes*, *Dhb*. *restrictus* cannot dechlorinate PCE beyond cDCE. Therefore, the outcome of the population interactions may determine the extent of detoxification achieved.

Monod kinetic parameter estimates that describe chlorinated ethene and electron donor utilization by *Dhc. ethenogenes* and *Dhb. restrictus* at non-inhibitory substrate concentrations were obtained in batch assays. Substrate inhibition effects on both populations were also evaluated. Highly chlorinated ethenes negatively impacted dechlorination of the lesser chlorinated ethenes in both populations. In *Dhc. ethenogenes*, cometabolic transformation of VC was also inhibited by the presence of other chlorinated ethenes. PCE and TCE dechlorination by *Dhb. restrictus* was strongly inhibited by VC.

The microbial interactions between *Dhc. ethenogenes* and *Dhb. restrictus* was investigated using reactors and mathematical models under engineered bioremediation and natural attenuation conditions. Under engineered bioremediation conditions, *Dhc. ethenogenes* became the dominant population, and the modeling predictions suggested that the inhibition of *Dhb. restrictus* by VC was a key factor in determining this outcome. Dechlorination rates by *Dhb. restrictus* appeared to be affected very little by low acetate concentrations under natural attenuation conditions, giving it an advantage over *Dhc. ethenogenes*, which requires relatively high acetate concentrations. This study highlighted that substrate interactions among dehalorespiring bacteria can influence their performance and contaminant fate under common bioremediation scenarios. A better understanding of the factors affecting the outcomes of these microbial interactions was achieved, which should aid in the design of successful bioremediation strategies.

Kinetics of Tetrachloroethene-Respiring *Dehalobacter* and *Dehalococcoides* Strains and Their Effects on Competition for Growth Substrates

By

YenJung Lai

Dissertation submitted to the Faculty of the Graduate School of the
University of Maryland, College Park, in partial fulfillment
of the requirements for the degree of
Doctor of Philosophy
2010

Advisory Committee:
Associate Professor: Jennifer G. Becker/Advisor
Professor: Kevin Sowers
Associate Professor: Hubert Montas
Associate Professor: Eric A. Seagren
Assistant Professor: Stephanie Lansing

Acknowledgements

I deeply appreciate my advisor, Dr. Jennifer Becker for her advice, encouragement, and patience throughout the project. Under her direction, I am able to explore amazing microbial world and learn how to interpret the findings. I also appreciate Drs. Kevin Sowers, Bruce James, Eric Seagren, Hubert Montas and Stephanie Lansing for their willing and time to serve my committee members. Especially, I appreciate Dr. Montas for his guidance and patience on parts of my modeling work.

I am thankful to my lab mates, Kyla Gregoire, Deyang Huang, Preston Postl, Gayle Davis, and Emily Devillier for sharing their lab experience with me and work together to fix equipments in the lab. Furthermore, I am also thankful of my friend, Hsuan-Chen Wu, for unselfishly sharing his knowledge in molecular techniques with me.

I am thankful of the National Science Foundation (NSF) for providing research funding and Environmental Science and Technology Department for providing the assistantships during this period.

Finally, I am especially thankful of my wife, HoChing Lin, for her complete understanding and consideration during the overnight sampling and weekend/holiday culturing. I am also grateful of my parents for their love and financial support. Furthermore, I am very grateful to have a lot of brothers and sisters in Christ around us to make our life so joyful and invaluable.

Table of Contents

List of Tables

List of Figures

Chapter 1 Introduction

Chlorinated solvents such as tetrachloroethene (PCE) and trichloroethene (TCE) are commonly used in a variety of industrial and commercial applications including dry cleaning of fabrics and for metal-degreasing. Because of their long histories of use and improper disposal, they are among the most abundant contaminants found at numerous industrial, residential, and military sites. PCE and TCE have been found in at least 852 of the 1,430 National Priority List (NPL) sites identified by the Environmental Protection Agency (EPA), and they are included on the Comprehensive Environmental Response, Compensation, and Liability Act (CERCLA) list of priority substances that are most commonly found at facilities on the NPL and pose the greatest potential threat to human health due to their known or suspected toxicity (U.S. EPA, 2005).

PCE and TCE are highly oxidized compounds, and consequently reduction of these compounds is thermodynamically favorable under anaerobic conditions (Vogel et al., 1987). Since Freedman and Gossett (1989) first demonstrated that PCE could be converted to non-toxic ethene via reductive dechlorination under anaerobic conditions, the application of in-situ bioremediation of PCE and TCE based on this microbial process has expanded significantly. In fact, it is now known that a number of bacterial strains are able to conserve energy through the reductive dechlorination of PCE, TCE, and/or other halogenated hydrocarbons through an anaerobic form of respiration known as dehalorespiration (Furukawa, 2003; Smidt et al., 2000; Holliger et al., 1999). However, the abundance of appropriate electron donors and microorganisms, nutrient availability, redox potential, pH and temperature are often not ideal at contaminated sites. Therefore, complete dechlorination of PCE and TCE rarely occurs without engineering intervention

at many contaminated sites (Christ et al., 2005; Bradley, 2003; Stuart et al., 1999; Mohn and Tiedje, 1992).

To achieve successful bioremediation, an improved understanding of the factors controlling the extent and efficiency of PCE and TCE dechlorination is needed. In particular, engineered bioremediation of chlorinated ethene-contaminated sites often involves increasing the availability of the electron donor, because many contaminated sites are electron donor-limited (Gossett and Zinder, 1997; McCarty and Semprini, 1994). Hydrogen is generally considered to be the ultimate electron donor for the reductive dechlorination process. However, increasing the supply of hydrogen does not always guarantee successful clean-up of PCE and TCE contamination in part because many hydrogenotrophs i.e., sulfate reducing bacteria and methanogens may compete with dehalorespirers for hydrogen. Thus, the microbial ecology of contaminated sites may play an important role in determining the outcome of bioremediation applications. In recent years, several laboratory and field studies indicated that multiple dehalorespiring populations may also be present at contaminated sites (Yang et al., 2005; Lendvay et al., 2003; Löffler et al. 2000). Under these conditions, competitive or complementary interactions may arise among the dehalorespiring populations depending on the physiological and kinetic characteristics of the populations and substrate availability (Becker, 2006). The goals of this study are to evaluate some of the substrate interactions that may arise among dehalorespiring populations under conditions that are relevant to bioremediation practice and to improve our understanding of the factors controlling the outcome of these interactions and, ultimately, contaminant fate.

Chapter 2 Literature review

2.1 Background

The high stability and low flammability of chlorinated hydrocarbons make them very useful in a wide variety of industrial and commercial applications, and they have been extensively used, particularly as solvents, since the 1920s. In the past decades it was commonly known that chlorinated hydrocarbons were released into the environment primarily via anthropogenic processes, although biogenic sources of these compounds do exist. Consequently, chlorinated hydrocarbons are now among the most common where they pose a health threat owing to their suspected or known carcinogenicity and mutagenicity. The properties of chlorinated hydrocarbons that make them so popular in industrial and commercial applications (high stability and low flammability) also render them very stable in the environment, particularly under aerobic conditions. However, biodegradation of chlorinated hydrocarbons under anaerobic conditions has been shown to be promising as the basis of several bioremediation strategies for the clean-up of sites contaminated with these compounds. To date several bacteria have been isolated that have the unique property of being able to use chlorinated hydrocarbons as their terminal electron acceptors in a form of anaerobic respiration called dehalorespiration (Furukawa, 2003; Smidt et al., 2000; Holliger et al., 1999).

2.2 Biodegradation mechanisms

The biodegradation of chlorinated hydrocarbons is simply classified into aerobic and anaerobic processes for this review. Due to the electronegativity of the chlorine substitutes, chlorinated hydrocarbons are oxidized compounds and tend to serve as

electron acceptors in redox reactions. In particular, highly chlorinated compounds, such as tetrachloroethene (PCE) do not react readily under aerobic conditions.

In the presence of oxygen molecules, chlorinated hydrocarbons are mainly transformed via cometabolic degradation. Cometabolism refers to a mode of biodegradation in which the microorganism is not able to conserve energy from the transformation of the cometabolic substrate and thus requires additional substrates that serve as a source of energy and/or carbon (Grady et al., 1985). Generally, cometabolism involves monooxygenases or dioxygenases with relaxed substrate specificities that allow them to oxidize chlorinated hydrocarbons (or other cometabolic substrates), as well as metabolic substrates that serve as sources of carbon and energy, such as methane, ammonia, phenol, or toluene (Wackett et al., 1985). However, cometabolic transformation of chlorinated hydrocarbons generally forms unexpected byproducts such as epoxides, which are toxic to the organisms. The less chlorinated hydrocarbons, such as dichloroethene and vinyl chloride, may also be directly metabolized as a source of carbon and energy by microorganisms under aerobic conditions, (e.g., Verce et al., 2002; Coleman et al., 2002).

In the absence of oxygen, the chlorinated hydrocarbons can undergo reductive dechlorination by either a hydrogenolysis or a dihaloelimination mechanism. The latter occurs only in chlorinated hydrocarbons in which two carbons with chlorine substituents are joined by a single bond. Although anaerobic oxidation of cDCE and VC have been observed under methanogenic, sulfidogenic, Fe(III)-reducing, Mn(IV)-reducing conditions (Bradley, 2003), the most relevant anaerobic biodegradation pathway is of reductive dechlorination. Recently, research on the biodegradation of chlorinated

compounds has made considerable progress due to the isolation of an increasing number of anaerobic bacteria that can use these compounds as terminal electron acceptors for generating energy for microbial growth.

2.3 Metabolic diversity of dehalorespiring bacteria

A large variety of chlorinated hydrocarbons are now known to undergo dehalorespiration, ranging from chlorinated alkanes and alkenes, halogenated benzenes, and phenols, to polychlorinated biphenyls and dioxins. Dehalorespiring strains are affiliated with several distinct phyla (Figure 2.1; Smidt and de Vos, 2004). Isolates that belong to the genera *Anaeromyxobacter, Desulfitobacterium, Sulfurospirillum, Desulfomonile, Desulfuromonas, Desulfovibrio*, and *Trichlorobacter* are metabolically versatile with respect to their spectrum of electron donors and acceptors, as summarized in Table 2.1 (Maillard, 2004). Of particular note is *Dehalococcoides ethenogenes* strain 195, which is the only organism currently known to have the ability to completely detoxify PCE in pure culture via a series of reductive dechlorination reactions using hydrogen as the sole electron donor (Maymó-Gatell et al., 1997). The last step, reductive dechlorination of VC, is cometabolic in *Dhc. ethenogenes*. In contrast, VC is metabolically transformed by *Dehalococcoides* strains VS and BAV1 using hydrogen as the electron donor (Müller et al., 2004; He et al., 2003). Like the *Dehalococcoides* strains, *Dehalobacter restrictus* is, as its name suggests, restricted to the utilization of hydrogen as the electron donor and chlorinated hydrocarbons as the terminal electron acceptors (Holliger et al., 1998). However, unlike *Dhc. ethenogenes, Dhb. restrictus* can convert PCE only to *cis*-DCE (cDCE) and cannot completely dechlorinate the parent

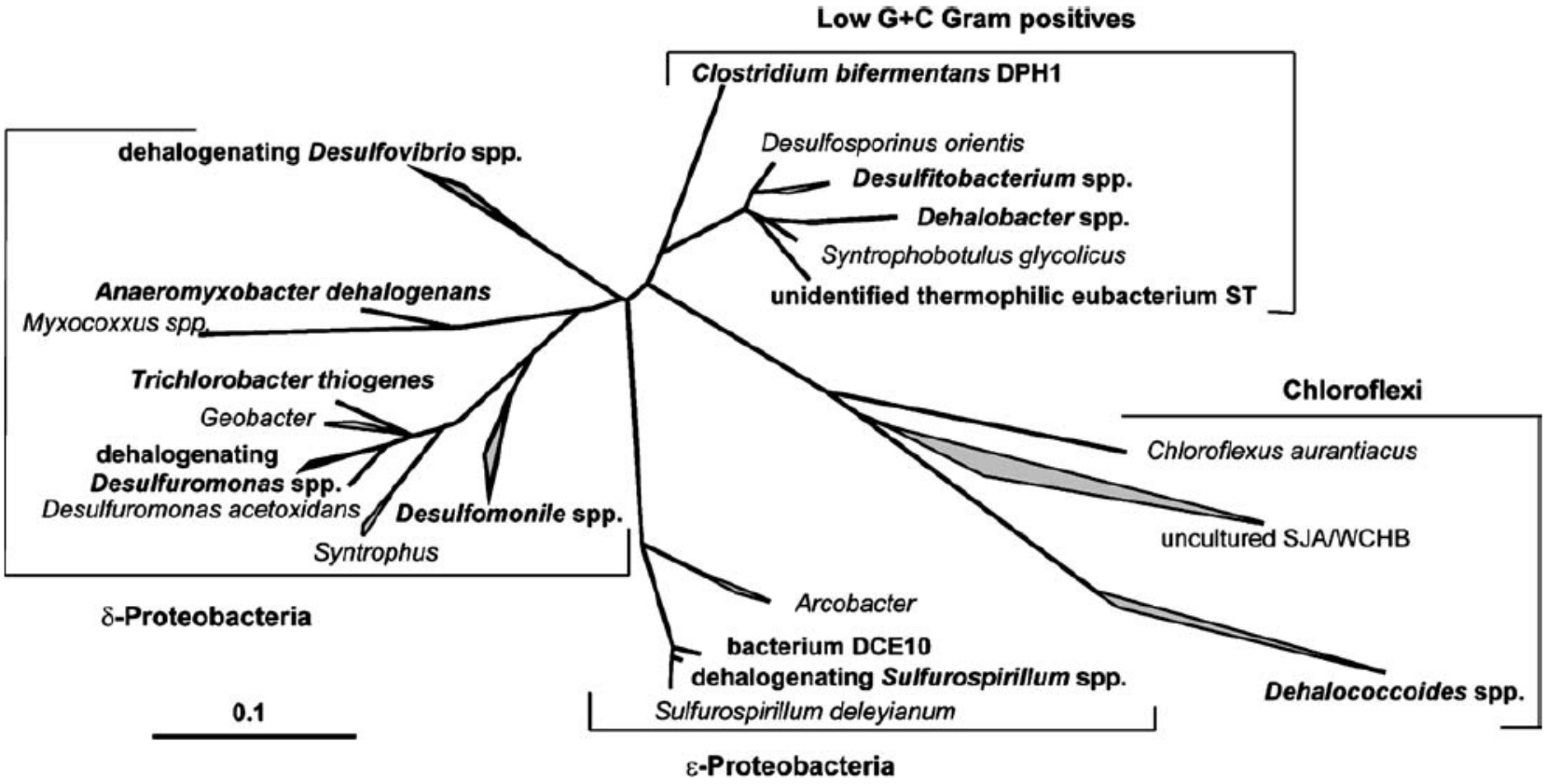

Figure 2.1 Phylogenetic tree of dehalorespiring isolates (in bold) based on bacterial SSU rRNA sequences. The reference bar indicates the branch length that represents 10% diversity (Source: Smidt and de Vos, 2004).

Table 2.1 Phylogenetic affiliation, electron donors and acceptors used by dehalorespiring bacteria (Source: Maillard, 2004).

Isolate	Electron donors	Chlorinated electron acceptors	Products	Non-Chlorinated electron acceptors	Reference
Low G + C Gram positive					
Dehalobacter restrictus strains PER-K23 and isolate TEA	H_2	PCE, TCE	*cis*-1,2-DCE	none	Holliger et al 1998; Wild et al, 1997
Desulfitobacterium hafniense strain TCE1	H_2, formate, pyruvate, lactate, butyrate	PCE, TCE	*cis*-1,2-DCE	nitrate, fumarate, sulfite, thiosulfate	Gerritse et al., 1999
Desulfitobacterium sp. strain PCE-S	H_2, formate, pyruvate, yeast extract	PCE, TCE	*cis*-1,2-DCE	fumarate, sulfite	Miller et al., 1997
Desulfitobacterium sp. strain Y51	pyruvate, lactate, formate	PCE, TCE, HCA, PCA, TeCAs, hepta-CPa	*cis*-1,2-DCE, 1,1-DCE, PCP	fumarate, nitrite, sulfite	Suyama et al., 2001
Desulfitobacterium dehalogenans strain JW/IU-DC1	H_2, formate, lactate, pyruvate, butyrate, ethanol	Cl-OHPA, PCP, TeCPs, TCPs, DCPs	OHPA, TCPs, DCPs, CPs	nitrate, fumarate, sulfite, sulfur, thiosulfate	Utkin et al., 1994
Desulfitobacterium strain PCE1	formate, pyruvate, lactate, butyrate, crotonate, succinate, ethanol, serine	PCE, Cl-OHPA, 2,4,6-TCP, 2,4-DCP, 2-CP	TCE, OHPA, phenol, 4-CP	fumarate, sulfite, thiosulfate	Gerritse et al., 1996
Desulfitobacterium dichloroeliminans strain DCA1	H_2, formate, lactate	1,2-DCA, 1,1,2-TCA, vicinal DCP & DCB	ethene, VC, corresponding alkenes	nitrate, sulfite, thiosulfate	de Wildeman et al., 2003
δ-Proteobacteria					
Desulfomonile tiedjei strain DCB-1	H_2, formate, pyruvate	3-CBe	Benzoate	sulfate, sulfite, thiosulfate	deWeerd et al., 1990.
Desulfuromonas michiganensis strains BB1	Acetate	PCE, TCE	cis-1,2-DCE	fumarate, malate, iron(III), sulfur	Sun et al., 2000
Geobacter thiogenes strain K1	Acetate	TCA	Dichloroacetic acid	sulfure	deWever et al., 2000
Geobacter lovleyi sp. nov. strain SZ	H_2, pyruvate, acetate	PCE, TCE,	*cis*-DCE	nitrate, fumarate,	Sung et al., 2006

				Fe(III), malate	
Desulfuromonas chloroethenica strain TT4B	acetate, pyruvate	PCE, TCE	*cis*-1,2-DCE	fumarate, iron(III), sulfur	Krumholz et ., 1997
ε-Proteobacteria					
Sulfurospirillum multivorans	H_2, formate, pyruvate, lactate, ethanol, glycerol, sulfide	PCE, TCE	*cis*-1,2-DCE	nitrate, fumarate, arsenate, selenate	Scholz-Muramatsu., 1995
Sulfurospirillum halorespirans strain PCE-M2	H_2, formate, lactate, pyruvate	PCE, TCE	*cis*-1,2-DCE	fumarate	Luijten et al., 2003
Green nonsulfur bacteria					
Dehalococcoides ethenogenes strain 195	H_2	PCE, TCE, *cis*-DCE, 1,1-DCE, 1,2-DCA, VC*	VC, ethene	none	Maymó-Gatell et al., 1997
Dehalococcoides sp. strain CBDB1	H_2	TeCBs, TCBs	1,3,5-TCB, DCBs	none	Adrian et al., 2000
Dehalococcoides sp. strain BAV1	H_2	cis-DCE, trans-DCE, 1,1-DCE, VC, 1,2-DCA, VB	ethene	none	He et al., 2003
Dehalococcoides sp. strain VS	H_2	1,1-DCE, VC	ethene	n.d.	Müller, et al., 2004
ultramicrobacterium DF-1	H_2, formate	2,3,4,5-TeCB, Aroclor 1260, HCB, chlorinated ethenes	Less-chlorinated benzenes/ethenes	n.d.	Wu et al., 2002(a,b); May et al., 2008

n.d. = not determined.
CB: chlorobenzoate; Cl-OHPA: 3-chloro-4-hydroxyphenyl acetate; CP: chlorophenol; CPa: chloropropane; DCA: dichloroethane; DCB: dichlorobenzene; DCBa: dichlorobutane; DCE: dichloroethene; DCP: dichlorophenol; DCPa: dichloropropane; HCA: hexachloroethane; PCA: pentachloroethane; PCE: tetrachloroethene; PCP: pentachlorophenol; PCPe: pentachloropropene; TCA: trichloroethane; TCB: trichlorobenzene; TCE: trichloroethene; TCP: trichlorophenol; TeCA: tetrachloroethane; HCB, hexachlorobenzene; Aroclor 1260: Commercial PCB mixtures composed of 60 to 100 different congeners; TeCB: tetrachlorobenzene; TeCP: tetrachlorophenol; VC: vinyl chloride.

compound to produce non-toxic ethene. Dehalorespiring members of the *Desulfitobacterium* genus(such as strain PCE1) are more metabolically versatile. These strains can use a variety of organic electron donors, such as formate, pyruvate and lactate, and non-chlorinated terminal electron acceptors (such as sulfite) (Gerritse et al., 1999; 1996).

2.4 Competition for resources

Microorganisms, whether they live in nutrient-rich sediment or nutrient-poor subsurface, actively compete for available resources. Microorganisms that have physiological characteristics suitable to the conditions of a given environment usually have a competitive advantage and will thrive and may dominate in that environment. In contrast, microorganisms whose physiological features are not suitable in a given environment may not compete effectively for available resources and thus tend to be out competed in the environment.

2.5 Competition case studies of dehalorespiring bacteria

Microbial dehalorespiration using chlorinated compounds as terminal electron acceptors is a promising bioremediation strategy for the clean-up of chlorinated contaminants. A member of the genus *Dehalococcoides*, *Dhc. ethenogenes* strain 195, is a unique dehalorespiring bacteria because of its ability to completely detoxify PCE to non-toxic ethene. Other PCE-dehalorespiring bacteria including *Desulfitobacterium*, *Desulfuromonas*, *Geobacter* and *Dehalobacter* strains are capable of dechlorinating PCE only to the level of TCE or cDCE (Sung et al., 2006; He et al., 2002; Holliger et al., 1998; Gerritse et al., 1996). Recently, the coexistence of *Dehalococcoides* species and

other dehalorespiring bacteria has been of concern due to competitive and complementary associations (He et al., 2007; Grostern and Edwards, 2006ab; Becker, 2006; Yang et al., 2005; Fennell et al., 2001). For example, organisms that dechlorinate PCE to cDCE, including *Dehalobacter restrictus* and *Desulfuromonas michiganensis* tend to have fast substrate utilization kinetics. Therefore, these PCE-to-cDCE dechlorinators are expected to out compete *Dhc. ethenogenes* for PCE, at least under certain conditions, whereas *Dhc. ethenogenes,* which exhibits slower substrate utilization rates, is expected to specialize in dechlorination of cDCE (this work, Chapter 3; Huang and Becker, 2009; Becker, 2006). Co-cultures of *Dehalobacter* and *Dehalococcoides* strains can completely detoxify co-contaminants including 1,1,1-trichloroethane (1,1,1-TCA), 1,1-dichloroethane (1,1-DCA) and TCE to monochloroethane (CA) and ethene in a synergistic fashion with *Dehalobacter* respiring the chlorinated ethanes via dihaloelimination and the *Dehalococcoides* strain respiring the cDCE and VC produced by these reactions. Because the *Dehalobacter* strains cannot respire cDCE and VC and *Dehalococcoides* cannot respire chlorinated ethanes, one population alone would not be able to completely detoxify these contaminants (Grostern et al., 2009; Grostern and Edwards, 2006ab). The heterotroph *Desulfitobacterium* strain PCE1 can utilize lactate as a electron donor and produces acetate (Gerritse et al., 1996). Thus, if it is present along with hydrogentrophic strains like *Dhc. ethenogenes*, it may directly compete with the other dehalorespirers for PCE but could also enhance their performance by providing the acetate these strains require as a carbon source. Based on these examples, it is clear that under certain conditions, coexistence of multiple dehalorespiring bacteria may be possible and could be important in achieving successful engineered bioremediation.

Nevertheless, in situations where the availability of growth substrates, carbon sources, and/or nutrients is limited, especially at sites undergoing natural attenuation, the presence of *Dehalococcoides* strains and PCE-respiring bacteria with similar niches will lead to substrate competition. If *Dehalococcoides* strains are out competed, it may lead to toxic daughter product accumulation, i.e., cDCE or VC (Becker, 2006).

Microcosm studies conducted with subsurface materials obtained at sites contaminated with chlorinated ethenes demonstrated that acetate addition could enhance PCE-to-cDCE dechlorination activity, which was carried out by *Desulfuromonas* strains that utilize acetate as an electron donor (He et al., 2002). Further, this work suggested either acetate or hydrogen alone may be sufficient to achieve complete dechlorination through the action of a homoacetogen working in reverse, that is converting acetate to CO_2 and hydrogen that could be utilized as an electron donor by *Dehalococcoides* strains. In another study, it was shown that maintaining a lactate fermentor, *Acetobacterium woodii*, in co-culture with *Dhc. ethenogenes* could enhance the dechlorination activity by *Dhc. ethenogenes* due primarily to the high levels of vitamin B_{12} produced by *A. woodii* (He et al., 2007). Continuous-flow column studies were conducted using lactate as the electron donor, PCE as the electron acceptor, and an enrichment culture containing *Dehalococcoides* (Azizian et al., 2008). These studies showed that lactate-fermentors were the key to maintaining hydrogen and acetate availability in the column. These electron donors were utilized by *Dehalococcoides* and iron-reducing bacteria in the column, and moreover, dechlorination of cDCE to VC and ethene improved when lactate was increased to 1.35 mM compared with experiments done with 0.35 to 0.67 mM lactate. Interestingly, the effluent hydrogen and acetate levels were maintained at or

above 20 nM and 0.2 mM, respectively. The effluent hydrogen concentrations exceeded the typical hydrogen thresholds for dehalorespiration (Cupples et al., 2004; Fennell and Gossett, 1998; Yang and McCarty, 1998). The *Dehalococcoides* population was not consistently dominant and its percentage within the total microbial population dropped from 74 at the head of the column to 4% at the outlet. In another study, *Dehalobacter* spp. were out competed by *Dehalococcoides* spp. and the dehalorespirer *Geobacter lovleyi* strain SZ in a continuous-flow column supplied with 0.30 mM PCE and 20 mM lactate, but the researchers could not conclude whether a competition effect or inhibition due to intermediates negatively impacted dechlorination by the *Dehalobacter* spp. Furthermore, the *Geobacter* population was typically more than one order of magnitude higher than the population of *Dehalococcoides* (Amos et al, 2009). However, the lack of hydrogen experimental data reported in this study made it difficult to clarify whether the presence of *Geobacter lovleyi* strain SZ had a negative impact on dechlorination by *Dehalococcoides* due to competition.

As noted by Huang (2009), competition among dehalorespiring bacteria may occur not only for electron donor and acceptors, but also for organic carbon sources, especially in the presence of heterotrophic dehalorespiring bacteria. The media formulations generally suggested for maintaining *Dhc. ethenogenes* and *Dhb. restrictus* include high (millimolar) concentrations of acetate, which is provided as the carbon source for these hydrogenotrophic organisms (Holliger et al., 1998; Maymó-Gatell et al. 1997). Interestingly, carbon dioxide assimilation has also been observed in both dehalorespiring bacteria (Tang et al., 2009; Holliger et al., 1993). Analysis of the genome sequence of *Dhc. ethenogenes* confirmed that this organism lacks key enzymes

needed for autotrophic growth (Seshadri et al., 2005), and Holliger et al. (1998) reported that *Dhb. restrictus* could not grow on hydrogen, PCE, and peptone without providing acetate as the carbon source. However, so far few studies have clearly quantified the effect of carbon source availability on dechlorination by *Dhc. ethenogenes* and *Dhb. restrictus*. This information could improve our ability to overcome limitations on dehalorespiration in the field because carbon source availability may be insufficient at contaminated sites undergoing natural attenuation and thus negatively impact dechlorination rates.

Overall, the current lack of understanding of the factors affecting the outcome of microbial competition, particularly involving carbon source utilization, limits the rational design of bioremediation strategies to achieve successful clean-up. Often, in engineered bioremediation, excess electron donor is added in an attempt to improve dechlorination activity, but this approach can create concerns about costs and biofouling (Fennell and Gossett, 1999). More relevant to this study, bioaugmentation and supply of excess substrate may not guarantee that all key dehalorespiring bacteria are successfully stimulated and sustained if their interactions and physiological requirements are not well understood (Amos et al., 2009; Azizian et al., 2008).

2.6 Dehalorespiration kinetic model

Under non-inhibitory conditions, dehalorespiration of chlorinated ethenes can be described using the dual Monod equation (Bagley, 1998; Fennell and Gossett, 1998; Haston and McCarthy, 1999).

$$\frac{dS_{e\text{-}\,acceptor}}{dt} = -q_{\max} X \left(\frac{S_{e\text{-}donor}}{K_{s,e\text{-}donor} + S_{e\text{-}donor}} \right) \left(\frac{S_{e\text{-}acceptor}}{K_{s,e\text{-}acceptor} + S_{e\text{-}acceptor}} \right) \qquad (2.1)$$

where q_{max} [$M_S M_X^{-1} \cdot T^{-1}$] is the maximum specific substrate utilization rate; X [$M_X \cdot L^{-3}$] is the biomass concentration; $S_{e\text{-}donor}$ and $S_{e\text{-}acceptor}$ [$M_S \cdot L^{-3}$] are the aqueous concentrations of electron donor and acceptor, respectively; and $K_{S,e\text{-}donor}$ and $K_{S,e\text{-}acceptor}$ [$M_S \cdot L^{-3}$] are the half-saturation constants for the electron donor and acceptor, respectively. When the electron donor is provided in excess and the electron acceptor is the limiting substrate, the dual Monod equation can be simplified to a single Monod equation

$$\frac{dS_{e\text{-}acceptor}}{dt} = -q_{\max} X \left(\frac{S_{e\text{-}acceptor}}{K_{s,e\text{-}acceptor} + S_{e\text{-}acceptor}} \right) \quad (2.2)$$

A similar equation can be written for the electron donor when the electron acceptor is provided in excess. Therefore, when conducting batch kinetic experiments (described in Chapter 4), one substrate was maintained in excess, and the concentration of the limited substrate was monitored over time to obtain a single substrate depletion curve.

2.7 Intrinsic and extant kinetics

Equations 2.1—2.2 can be used to accurately describe dehalorespiration kinetics only if meaningful estimates of $q_{\max}$ and K_S can be obtained. To be meaningful, the kinetic parameter estimates must reflect the relevant physiological state of the cells and the microbial community composition, and the estimates must be unique and identifiable (Liu and Zachara, 2001). For example, in most environments, cell growth is restricted by substrate availability. In mixed cultures, low substrate availability tends to select for slow-growing populations with a high affinity for the substrate (Grady et al., 1996). In pure cultures, low substrate availability means that the organism's physiological state (basically the protein synthesis system), and consequently the rate of biodegradation, is

less than optimal and dependent on the culture's history. This means that if we want to describe the in situ activity of microorganisms in a particular contaminated site or bioreactor, the batch assays used to obtain the kinetic parameter estimates must be designed so that the cells cannot be able to alter their enzyme synthesis system. In other words, they must not be able to grow. This is achieved by providing a small S_0 relative to the X_0. Grady et al. (1996) recommends that cells will exhibit their currently existing (or *extant*) kinetics without changing their biomass if $S_0/X_0 \leq 0.025$, when both parameters are expressed in terms of chemical oxygen demand (COD). On the other hand, parameter estimates that describe microbial activity during unrestricted growth, i.e., the intrinsic kinetics of the population, then a large S_0 must be provided relative to X_0 in the batch kinetic assays. This condition selects for fast-growing, high affinity populations, and allows individual cells to optimize their enzyme synthesis system. Most importantly, the optimal biodegradation expressed in the batch kinetic assay will be optimal and independent of the culture history. A S_0/X_0 ratio ≥ 20 is recommended to estimate intrinsic kinetics (Grady et al., 1996). A common bioremediation scenario in which intrinsic kinetic parameter estimates may be needed is the application of engineered bioremediation due to relatively large amounts of electron donor substrate provided to enhance the growth of dehalorespirers.

The meaning of kinetic parameters obtained at intermediate ratios of the initial substrate concentration to initial biomass concentration ($0.025 \leq S_0/X_0 \leq 20$) are not clear. Unfortunately, many kinetic parameters obtained under intermediate conditions may not reflect the microbial kinetics of interest. In addition to not being reflective of the appropriate physiological state and microbial community composition, many of the

Monod kinetic parameters reported in the literature have a high degree of correlation, which further impedes efforts to obtain reliable kinetic parameter estimates.

Previous studies have highlighted the need to carefully select the initial conditions (S_0/K_S and S_0/X_0) in batch assays in order to minimize the amount of correlation between Monod kinetic parameter estimates (Liu and Zachara, 2001; Ellis et al., 1996; Grady et al., 1996; Robinson and Tiedje, 1983). Some studies suggested that it may be difficult to obtain independent estimates of q_{max} and K_S at small S_0/K_S ratios ($S_0 < K_S$) (Ellis et al., 1996; Robinson and Tiedje, 1983). These findings were of particular concern with respect to the feasibility of obtaining independent model parameters at the low initial substrate concentrations (S_0) required for extant conditions. Therefore, a former member of the Becker research group conducted a systematic numerical evaluation of the effects of a range of S_0/X_0 values (at a constant S_0/K_S) and a range of S_0/K_S values (at a constant S_0/X_0) on the correlation and identifiability of q_{max} and K_S parameter estimates (Huang, 2009). Parameter correlation is described using the correlation coefficient (R^2), and parameter identifiability is quantified using the collinearity index (γ_K). Both of these measures are described in greater detail below, but it is important to note that if $R^2 = 1$, the parameters are highly correlated, and previous studies (Brockmann et al., 2008; Brun et al., 2002) suggest that parameter estimates for which γ_K>10-15 are poorly identifiable. The results of the numerical evaluations are shown in Tables 2.2 and 2.3 and show that an S_0/K_S ratio of at least 4 is needed to obtain identifiable parameter estimates. Correlation coefficient values (R^2) for parameter estimates with $15 < \gamma_K$ ranged from 0.8401 to 0.9853. The amount of parameter correlation decreases with increasing S_0/K_S. Increasing S_0/X_0 does not reduce parameter correlation at a constant S_0/K_S ratio. In order to

adequately describe the kinetics under natural attenuation and engineered bioremediation scenarios and obtain reliable parameter estimates, the initial substrate-to-biomass ratios must be carefully controlled if batch kinetic assays are used. Analyses of parameter identifiability should also be performed to verify whether parameters are reliable and are described in the next section.

Table 2.2 Correlation coefficients (R^2) for q_{max} and K_S parameter values of that were fit to numerically simulated data for a range of initial conditions in the batch culture assays involving *Desulfuromonas michiganensis* strain BB1 (From Huang, 2009)

		S_0/K_s							
		0.04	0.1	0.4	1	4	10	20	40
S_0/X_0	0.025	1	0.9996	0.9958	0.9883	0.9434	0.8984	0.8705	0.8401
	0.1	1	0.9999	0.9971	0.9869	0.9432	0.9065	0.8747	0.8462
	1	1	1	0.999	0.9925	0.9581	0.9231	0.8968	0.8783
	5	1	1	1	0.9959	0.9738	0.9524	0.9375	0.9280
	10	1	1	1	0.9968	0.9793	0.9633	0.9525	0.9449
	20	1	1	1	0.9970	0.9829	0.9701	0.962	0.9558
	50	1	1	1	0.9968	0.9853	0.9749	0.9673	0.9601

Table 2.3 Collinearity index values (γ_K) calculated for q_{max} and K_S parameter values that were fit to numerically simulated data for a range of initial conditions in the batch culture assays involving *Desulfuromonas michiganensis* strain BB1 (From Huang, 2009)

		S_0/K_s							
		0.04	0.1	0.4	1	4	10	20	40
S_0/X_0	0.025	∞	∞	32.12	21.35	9.69	7.51	6.78	6.27
	0.1	∞	∞	58.17	17.86	9.73	7.97	6.92	6.40
	1	∞	∞	38.23	23.19	10.82	8.36	7.32	6.78
	5	∞	∞	∞	24.01	12.54	9.37	8.56	8.06
	10	∞	∞	∞	32.36	13.18	10.18	9.34	8.56
	20	∞	∞	∞	29.43	13.24	11.02	9.80	9.16
	50	∞	∞	∞	28.11	13.24	11.34	9.92	9.30

2.8 Outlook

The roles of dehalorespiring populations might be dynamic at different times and under different substrate conditions, rather than constant. Some species which are metabolically versatile with respect to various electron donors and acceptors definitely play a significant role in bioremediation. However, few meaningful Monod kinetic

studies have been conducted to understand their ability to degrade contaminants and describe their interactions using mathematical models, although molecular studies have highlighted that their interactions may influence the outcome of bioremediation. Therefore, further quantitative study of substrate interactions between dehalorespiring populations is needed to improve our understanding when conducting bioremediation of chlorinated hydrocarbon contaminants.

Chapter 3 Research objectives

3.1 Conceptual models of substrate interactions among dehalorespiring populations

Members of the genus *Dehalococcoides* are currently the only bacteria known to be capable of dehalorespiring the lesser chlorinated ethenes (cDCE and/or VC). PCE-dehalorespiring bacteria belonging to other genera, including *Desulfitobacterium*, *Desulfuromonas*, and *Dehalobacter* are capable of dechlorinating PCE only to the level of TCE or cis-DCE, which are not acceptable end-products in bioremediation. Recently, the detection of both *Dehalococcoides* strains and other dehalorespiring bacteria has been reported in studies involving natural environments or laboratory systems (Nijenhuis et al., 2007; Duhamel and Edwards, 2006; Yang et al., 2005; Fennell et al., 2001; Löffler et al., 1999;). When multiple dehalorespiring bacteria are present, competitive and/or complementary interactions may arise due to the range of chlorinated ethene electron acceptors and electron donors used by the organisms. Becker (2006) formulated conceptual models of competition among several representative PCE-respiring organisms including *Dsf.* strain PCE1, *Dsm. michiganensis*, *Dhc. ethenogenes* and *Dhb. restrictus*. Substrate interactions involving *Dhc. ethenogenes* and *Dhb. restrictus* are the focus of the current study and are shown in Fig. 3.1.

In each of the scenarios, *Dhc. ethenogenes*, which is capable of completely dechlorinating PCE to ethene (Maymó-Gatell et al., 1997) competes directly for the

electron donor (hydrogen) with *Dhb. restrictus*, which can utilize only hydrogen as an electron donor (Holliger et al. 1998). In fact, competition for hydrogen is inevitable if both organisms are present. In addition, it is also possible that *Dhc. ethenogenes* and *Dhb. restrictus* could compete for PCE and TCE, which both organisms can utilize as terminal electron acceptors (Fig. 3.1 A). Alternatively, it is possible that the two organisms could interact in a complementary manner, with *Dhb. restrictus* converting PCE to cDCE and *Dhc. ethenogenes* specializing in dechlorination of cDCE and VC (Fig 3.1B).

The overall hypothesis of this study is that multiple dehalorespiring populations may be present in contaminated groundwater environments. Competitive interactions (Figure 3.1A) may negatively impact the outcome of bioremediation if dehalorespiring populations that partially dechlorinate PCE out compete *Dehalococcoides* strains for limited substrates. Complementary interactions could enhance bioremediation efforts by promoting complete dechlorination of PCE due to the relatively fast PCE utilization kinetics of *Dhb. restrictus* and the ability of *Dhc. ethenogenes* to "clean-up" the products of dehalorespiration by *Dhb. restrictus*.

3.2 Research objectives

The current lack of meaningful kinetic parameter estimates for dehalorespiring bacteria limits our understanding and ability to predict which of the interactions shown in

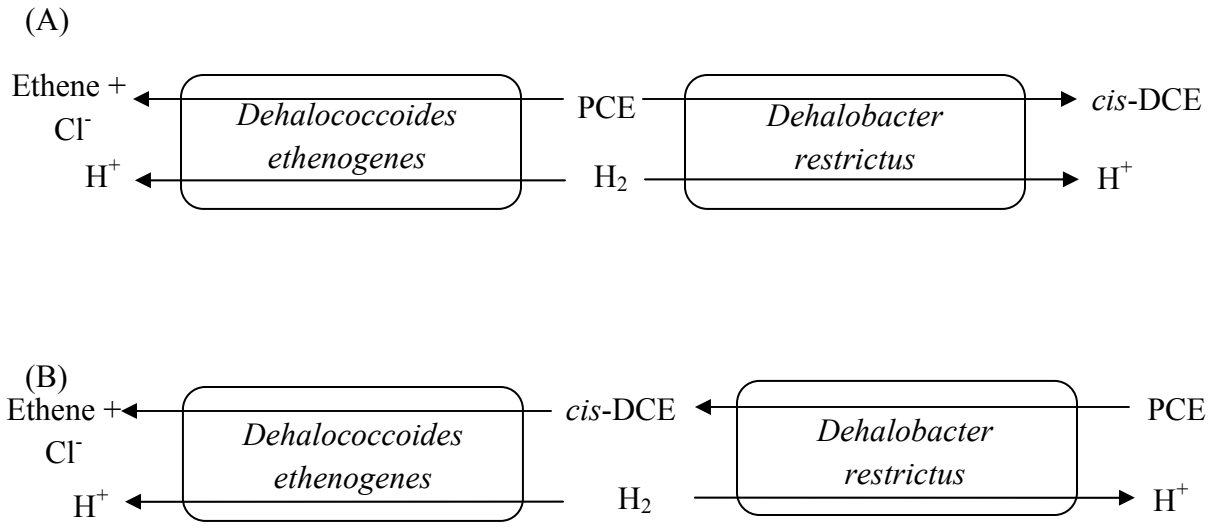

Figure 3. 1 Potential substrate interactions between *Dhc. ethenogenes* and *Dhb. restrictus*. (A) The two populations compete for H_2, PCE and TCE (not shown). Adapted from Becker (2006); (B) The two populations compete for H_2 and *Dhb. restrictus* converts PCE to cDCE, which is consumed by *Dhc. ethenogenes*.

Fig 3.1 will dominate under various conditions and their impact on the outcome of bioremediation. Therefore, the current study focused on estimating meaningful biokinetic parameters for both key dehalorespiring organisms under conditions that are relevant to groundwater bioremediation. Sites undergoing natural attenuation typically have low aqueous chlorinated ethene concentrations and are electron donor limited. In contrast, electron donor is typically provided in excess at sites where engineered bioremediation is being applied to alleviate electron donor limitation. The kinetic parameters were needed to refine a mathematical model and improve our understanding of the factors controlling the interactions between dehalorespiring populations and how these interactions affect contaminant fate. Experimental evaluations of competition were

conducted in continuous-flow reactors so that microbial growth and substrate utilization could reach a steady-state. Steady-state conditions improve our ability to evaluate population interactions and compare model predictions with experimental results by avoiding the transient processes observed in batch reactors.

The specific objectives of the proposed research are to:

(1) Obtain reliable estimates of Monod kinetic parameters for two dehalorespiring organisms, *Dhc. ethenogenes* and *Dhb. restrictus* under intrinsic and extant conditions.

(2) Estimate inhibition kinetic parameters to describe the effects of other chlorinated ethenes on dechlorination rates as well as self-inhibition kinetic constants to describe the dechlorination of high concentrations of PCE by *Dhc. ethenogenes* and *Dhb. restrictus*.

(3) Characterize the effect of carbon source availability on dechlorination rates by *Dhc. ethenogenes* and *Dhb. restrictus* through estimation of $K_{s,acetate}$ values and electron donor thresholds when different levels of carbon source are supplied.

(4) Predict the outcome of substrate interactions involving *Dhc. ethenogenes* and *Dhb. restrictus* using a mathematical model and kinetic parameters estimated in this study under both natural attenuation and engineered bioremediation conditions

(5) Compare the modeling predictions by experimentally evaluating substrate interactions in the scenarios described under objective (1) using continuous-flow stirred tank reactors.

Chapter 4 Materials and methods

4.1 Chemicals

PCE (99%, Spectrum Chemical Mfg. Corp.), TCE (99.9%, Fisher Scientific), *cis*-DCE (99.9%, Supelco), VC (2000 μg/mL in methanol, Supelco) were used as microbial growth substrates and/or for preparation of analytical standards. Sodium acetate (Certified ACS) was obtained from Fisher Scientific Inc. [1,2-^{14}C]sodium acetate ([^{14}C]acetate, 98.8%, 110 mCi/mmol) was obtained from Moravek Biochemicals and Radiochemicals (Brea, CA), and [1,2-^{14}C]sodium lactate ([^{14}C] lactate, >95%, 110 mCi/mmol) was obtained from Sigma-Aldrich Co. (St. Louis, MO).

4.2 Cultures

Dehalobacter restrictus (DSM 9455) was purchased from the German Collection of Microorganisms and Cell Cultures (DSMZ). *Dehalococcoides ethenogenes* strain 195 was provided by Dr. Steven Zinder (Cornell University), *Dhb. restrictus* and *Dhc. ethenogenes* were grown as described in DSMZ medium 732 except that the high vitamin solution was used as described by Maymó-Gatell et al. (1997).

4.3 Semi-continuous cultures

To ensure all cultures used for batch kinetic determinations and competition experiments had the same culture history and were at the same physiological state, all batch cultures were maintained on a semi-continuous basis in 160-ml serum bottles with

sealed with black butyl rubber septa and crimp caps (Fisher). The bottles were incubated at 30°C for *Dhb. restrictus* and at 35°C for *Dhc. ethenogenes*. As described in Chapter 3, the competition experiments were conducted in continuous-flow stirred tank reactors (CSTRs) maintained at 20-day solid retention time (SRT). To ensure that the extant kinetic parameters estimated using the semi continuous stock culture described population activity in the CSTRs, the semi-continuous cultures were also maintained at a 20-day SRT. To accomplish this, 20-mL of 100-mL cultures was wasted and replaced with fresh medium every four days. During this procedure, the cultures were purged with ultra-high pure (UHP) grade $N_2/C0_2$ (80%:20%) to remove any residual chlorinated ethenes and for *Dhb. restrictus* and *Dhc. ethenogenes* $N_2/C0_2$ was replaced with H_2/CO_2 (80%:20%) at 24.7 psi to maintain a neutral pH and supply H_2 (approximately 3.3 mM) as the electron donor for *Dhb. restrictus* and *Dhc. ethenogenes*. *Dhc. ethenogenes* was routinely fed 50 μmol of PCE (resulting in aqueous concentration of 315 μM), and *Dhb. restrictus* was supplied with 60 μmol of PCE (resulting in aqueous concentration of 380 μM). Prior to running batch kinetic determinations and competition experiments, semi-continuous cultures were maintained at least 60 days (or at least 3 SRTs) to ensure that the cultures were at a steady-state.

4.4 Analytical methods

4.4.1 Chlorinated ethene analysis

Chlorinated ethenes were analyzed using headspace gas chromatography (GC). Two different GC systems were used. Routine analyses were performed using Hewlett-Packard 5890 Series II Plus gas chromatograph equipped with a flame ionization detector (FID), stainless-steel column packed with 1% SP-1000 on 60/80 Carbopack-B (2.4 m by 3.2 mm, Supelco Inc.). Ultra pure carrier grade helium from Airgas East (Greenbelt, MD) was used as the carrier gas and supplied at a flow rate of 40 ml/min. Ultra purity carrier grade hydrogen and air obtained from Airgas East were supplied at 60 ml/min and 260 ml/min, respectively, to maintain the FID. The injector and detector temperatures were set at 200 °C and 250 °C, respectively. As suggested by Gossett (1985), the oven was programmed at an initial temperature of 60 °C (for 2 min), and then the temperature was increased at a rate of 20 °C/min to 150 °C, followed by an increase at a rate of 10 °C/min to 200 ºC. The total run time is 15.9 min. The retention times for ethene, VC, *cis*-DCE, TCE and PCE approximately are 0.7, 2.6, 7.2, 10.2 and 15.3 min, respectively. The output signals from GC were analyzed via the software Chemstation (version 10.03, Agilent Technologies).

The gas samples (0.5 ml) taken from the headspace of batch reactors were obtained using a 1-ml gastight syringe equipped with a push-button valve (Dynatech, A-2 Pressure Lok) and sterile needle and manually injected directly onto the GC. The

concentrations of chlorinated ethenes and ethene in samples determined by comparison with calibration curves that were prepared using standards of known concentrations. Standards were prepared by adding different amounts measured gravimetrically of a stock methanol solution containing known concentrations of chlorinated compounds to 6 ml D.I. water in an amber vial (11.84 ml) sealed with a Teflon septum and crimp cap. A standard solution of VC (2000 μg/mL), was added directly to an amber vial. The other stock solutions were prepared by gravimetric method that added neat PCE, TCE, *cis*-DCE to 10 ml methanol in an amber vial sealed with a Teflon septum and crimp cap. The aqueous concentrations of standards were determined according to.

$$M_t = C_w V_w + C_g V_g = C_w (V_w + H_c V_g) \quad (4.1)$$

where M_t [M] is the total mass of chlorinated hydrocarbon; C_w [M/L^3] is the aqueous concentration of the chlorinated hydrocarbon; V_w [L^3]; is the volume of the liquid phase; C_g [M/L^3] is the concentration of chlorinated hydrocarbon in the gas phase; V_g [L] is the volume of the gas phase; and H_C is the dimensionless Henry's constant of the given compound. The dimensionless Henry's constants for PCE, TCE, *cis*-DCE and VC at 30ºC are 0.917, 0.491, 0.190 and 1.262, respectively (Gossett, 1987). The standards were equilibrated at 30 ºC for at least 12 hours and then were analyzed by GC-FID. The R^2 obtained for each calibration curve was > 0.995. Chlorinated ethenes were analyzed in samples from the reactors using following procedures; aqueous samples (1-ml) were obtained from the reactors through sampling ports using 1-ml disposable sterile syringes

(Becton-Dickinson) equipped with sterile needles and transferred to 11.84-ml autosampler vials sealed with Teflon-lined caps. Samples were incubated at 30 °C for at least 30 min, and 0.5 ml of the headspace was injected onto GC. Experiments were conducted to demonstrate that dechlorination activity in the sample vials ceased immediately due to exposure to oxygen (data not shown). Therefore, continued biodegradation of the chlorinated ethenes was not a concern during the incubation period.

4.4.2 Hydrogen analysis

Hydrogen was also quantified by a headspace technique via a Peak Performer 1 GC (Peak Laboratories, Mountain View, CA) equipped with a reducing compound photometer (RCP) detector and two columns, a 31 inch UNI 1S guard column, to filter out the chlorinated ethenes, and a 31 inch Molecular Sieve 13X column to separate reduced components. The column and detector were set at 105°C and 265°C, respectively and the temperature program was held constant at 265°C. Ultra pure carrier grade nitrogen (Airgas East) was used as a carrier gas at a flow rate of 20 ml/min under these conditions, the retention time of hydrogen is 48 to 54 seconds. New hydrogen calibration curves were prepared prior to each experiment. Two glass beads were added to a 160-ml serum bottle to enhance the mixing of gases and the bottle was sealed with a black butyl septum and a crimp cap. Then, the serum bottle was flushed with 18.7 ppm hydrogen standard (balanced with nitrogen, Air Gas) for 20 minutes. Five samples, ranging in volumes from 100 to 500 μL (corresponding to 7.77×10^{-2} to 3.89×10^{-1} nmol

H_2), were withdrawn from the 18.7 ppm H_2 standard using either a 100-µL or 1-ml gastight syringe equipped with a push-button valve (Supelco, Pressure-Lok®, Series A-2) and injected onto the GC. The R^2 obtained for calibration curves generally exceed 0.994. The aqueous concentrations of hydrogen were calculated using Equation 4.2 (Löffler et. al., 1999)

$$C_{L,H_2} = \frac{OP}{RT} \tag{4.2}$$

where C_{L,H_2} is the aqueous concentration of hydrogen (mole per liter), O is Ostwald coefficient for H_2 solubility, which is 0.01895 at 30ºC (Wilhelm et al., 1977), P is the partial pressure of H_2 (atm), R is the universal gas constant (0.0821 $L \cdot atm \cdot K^{-1} \cdot mol^{-1}$), and T is the absolute temperature (K).

4.4.3 Organic acids analysis

Standard chromatographic analytical techniques such as gas chromatography and high performance liquid chromatography (HPLC) are unsuitable for quantifying free organic acids at the µM or nM level, as required in this research. Therefore, the concentrations of organic acids, such as acetate and lactate were determined radiometrically using ^{14}C-labeled compounds. ^{14}C-labeled acetate and lactate were separated using HPLC as discussed by He and Sanford (2004). An autosampler (Fraction Collector III Waters Corporation, Milford, MA) was used to collect the organic acids in

the HPLC system effluent. The trapping interval for acetate was 11.0-12.0 min. ^{14}C activity in each 0.5 min fraction was quantified, and ≥75 % of the injected ^{14}C activity was recovered in the above trapping intervals. These effluent collection intervals were determined by injecting 0.3 M of ^{14}C-labeled acetate on the HPLC and collecting the effluent at 0.5 min intervals. The 3-ml effluent samples were collected in 7 ml scintillation vials containing 4 ml of scintillation cocktail (Ecoscint XR; National Diagnostics Inc; Atlanta, GE). ^{14}C activity was determined by counting samples for 10 min in a Perkin Elmer Tri-Carb Liquid Scintillation Counter (Boston, MA).

4.4.4 Biomass analysis

The biomass concentrations of cultures in batch cultures were estimated based on the protein content, which was measured using the Bradford assay because of its compatibility with the reducing agent used in this study. Aqueous samples (1 ml) were withdrawn from the serum bottles using sterile luer-lock syringes and needles transferred to glass centrifuge tubes. 0.05 ml of 4.4 N NaOH was added to each tube and the samples were incubated at 85°C for 20 min to achieve cell lysis. After the samples cooled down to room temperature, 0.05 ml of 4.4N HCl was added to neutralize the contents. Protein standards (2.5 to 20 mg/L) were prepared using bovine serum albumin (BSA, Lyophilized powder; Acros Organics) and D.I. water or freshly prepared media was used as the blank. Assays were performed according to manufacturer's instructions. Briefly, 1 ml of lysed sample or standard was mixed with 1 ml of Bradford reagent in a 5-ml

centrifuge tube by vortexing and then incubated at room temperature for 20 min. The samples were then transferred to quartz and absorbance was measured at 595 nm in a spectrophotometer (DR/4000V HACH, Loveland, CO). The R^2 obtained for calibration curve was greater than 0.995. The volatile suspended solid (VSS) content was calculated assuming that the VSS contained 55% protein by weight (Grady et al. 1996).

4.4.5 DNA extraction and real-time PCR analysis

DNA was extracted from 10-ml culture samples using the DNeasy Blood & Tissue Kit (QIAGEN; Valencia, CA) following the protocol provided by the manufacturer, except that an enzyme lysis buffer (20 mM Tris-HCl (pH 8.0), 2 mM EDTA, 20 mg/mL Lysozyme, 2.5 % (w/v) SDS and 1.2 % Triton X-100), was used to enhance cell lysis (Krajmalnik-Brown, 2005). The DNA was eluted using 120 µL AE Buffer provided in the DNA extraction kit and stored at –20ºC. The concentration of extracted DNA was determined spectrophotometrically (λ=260 nm), and the purity of the DNA was assessed by comparing the spectrophotometric absorbance at 260 nm to that measured at 280 nm. Samples with A_{260}/A_{280} ratio of 1.8 – 2.0 were considered to be sufficiently pure for real-time PCR analysis. Real-time PCR amplification of 16S rRNA gene sequences was performed in a Roche LightCycler® 480 System (Roche Diagnostics Corporation, Indianapolis, IN) in order to either quantify the abundance of individual populations in competition experiments conducted using the continuous-flow reactor or

in the growth yield (Y) determinations in pure culture batch assays. The specific 16S rRNA gene primers used for amplification of each species are shown in Table 4.1. The reaction mixture consisted of (per 15 µL reaction volume): 10 µL of 2X LightCycler® 480 SYBR Green I Master Mix (Roche Diagnostics Corporation, Indianapolis, IN), 2 µL of a primer solution containing 5 µM of each primer, 3 µL of PCR-grade water (Roche Diagnostics Corporation, Indianapolis, IN). DNA template (5 µL) was added to each tube. All samples were analyzed in using the following temperature program: 15 min at 94 ºC, followed by 45 cycles of 30 s at 94ºC, 20 s at 58ºC, and 30 s at 72ºC. The estimation of the gene copy number assumed an average molecular weight of 660 g/mol for a base pair in double-stranded DNA and one gene copy per 1.5 Mbp genome for *Dhc. ethenogenes* (He et al., 2003). The genome size of *Dhb. restrictus* (Villemur et al., 2006) was assumed to be equal to that of *Desulfitobacterium hafniense* strain Y51 (5.7 Mbp; Nonaka et al., 2006).

Table 4.1 16S rRNA gene primers for each species

Species	Primer Name[a]	Primers	Reference
Dehalobacter restrictus	Dre 441F	GTTAGGGAAGAACGGCATCTGT	Smits et al. (2004)
	Dre 645R	CCTCTCCTGTCCTCAAGCCATA	
Dehalococcoides ethenogenes strain 195	Dhc 730 F	GCGGTTTTCTAGGTTGTC	Ritalahti et al. (2004)
	Dhc 1350R	CACCTTGCTGATATGCGG	

[a] Numbers refer to position in *Escherichia coli* 16S rRNA gene sequence.

Calibration curves (log 16S rRNA gene copy concentration versus an arbitrarily set cycle threshold value [C_T]) for each strain were obtained by using serial dilutions of pure culture genomic DNA. The gene copy number in the standards containing known DNA concentration was calculated according to the equation 4.3 (Ritalahti et. al., 2006).

$$\text{Gene copies} = \left(\text{volume of DNA [}\mu\text{L]}\right)\left(\text{DNA concentration [ng/}\mu\text{L]}\right)\times \left(\frac{1\text{g}}{1{,}000^3\,\text{ng}}\right)\left(\frac{1\text{ mol bp DNA}}{660\text{g DNA}}\right)\left(\frac{6.023\times10^{23}\text{ bp}}{\text{mol bp}}\right)\left(\frac{1\text{ copy}}{\text{genome size [bp]}}\right) \tag{4.3}$$

The number of target genes per ml of sample was determined by equation 4.4,

$$\text{Gene copies per ml sample} = \left(\frac{\left(\text{gene copies per reaction mix}\right)\times\left(\text{volume of DNA [}\mu\text{l]}\right)}{\left(5\ \mu\text{l DNA per reaction mix}\right)\times\left(\text{ml sample used}\right)}\right) \tag{4.4}$$

The volume of extracted DNA was 120 µl. The volume of DNA per reaction was 5 µl. A set of standards was routinely analyzed with each sample set and compared with previous calibration curves to ensure consistency between runs.

4.5 Reactor Experimental System

The reactor system (Figure 4.1) consisted of (1) duplicate bioreactors, (2) a waste collection vessel, (3) media and PCE feeding reservoirs, and (4) a gassing system. These components were connected with either stainless steel tubing and companion fittings or 1/8″ (I.D.) Teflon tubing (Cole-Parmer; City, State) and Teflon fittings. All of the Teflon tubing was covered with 1/4″-Viton tubing to reduce oxygen diffusion into the reactor system. The bioreactors were constructed from 2-L Pyrex bottles with an inlet and outlet

fused to the bottles with glass-to-Teflon connector (1/4″-28 threaded fitting, Supelco, Bellefonte, PA). A pair of glass flanges was fused to the top of the reactor, and a gas-tight seal was formed with a flanged lid with an O-ring and metal clamp. Sample ports were located at the side and top of the reactor and were sealed with black butyl rubber septa and aluminum crimp caps. The bioreactor effluent flowed to the waste collection vessel via a glass-to-Teflon connector and Teflon tubing. The effluent waste collection vessel was fitted with a carbon trap to capture volatile organic compounds. The fresh medium in the feeding reservoir was pumped into the bioreactors at a flow rate of 80 μL/min using a syringe pump (corresponding to a 20-d SRT) using a syringe pump (Standard pump 22, Harvard Bioscience Inc; Holliston, MA) equipped with 100 ml gas-tight syringes (Hamilton, Reno, NV). The feeding reservoir was maintained under a positive pressure, a mix of $H_2/CO_2/N_2$ (6%/10%/84%, certified grade; Air Gas) for natural attenuations or a mixture of H_2/CO_2 (80%/20%, Air gas) for engineered bioremediation conditions. This prevented oxygen from entering feed reservoir, and when H_2 was included provided the electron donor needed by *Dhc. ethenogenes* and *Dhb. restrictus*. According to equation (4.5), at 1 atm, these gas mixtures provided theoretical aqueous H_2 concentration of 40 μM and 645 μM, respectively. The real H_2 concentration supplied by gas mixtures was verified by hydrogen analysis (Section 4.4.2).

$$X_g = K_H P_g \tag{4.5}$$

where X_g = mole fraction of gas in liquid phase at equilibrium, K_H = Henry's law constant [atm^{-1}], and P_g = partial pressure of gas in atmosphere [atm].

All gases used in the reactor system were passed through oxygen traps (TTO100-2, Trigon Technologies, Shingle Springs, CA) and a sterile filter (0.2 μM diameter, PTFE, Millipore Corporation, Billerica, MA). The PCE stock solution (3.6 mM) was pumped into the bioreactors at a flow rate of 0.4 μl/min by the second syringe pump (Model 355 Sage Instruments; Freedom, CA) to maintain the PCE influent concentration at 15 μM. All components of the reactor system were autoclaved at least 0.75 hr before assemblage. Fresh medium was also autoclaved at least 1.5 hrs and cooled to room temperature under 80% N_2/20% CO_2.

4.6 Determination of Monod kinetic parameters for substrates

As noted in Chapter 2, when one substrate is provided in excess and the other substrate is the limiting substrate, the dual Monod equation can be simplified to a single Monod equation (Equation 2.2). When conducting batch kinetic experiments, the concentration of the limiting substrate was monitored over time to obtain a single substrate depletion curve. The chlorinated ethenes and hydrogen have partition between the gas and aqueous phases. At equilibrium, the distribution of chlorinated ethenes and hydrogen in the aqueous and gas phases can be described by Henry's Law

$$H_c = \frac{S_G}{S_L} \tag{4.6}$$

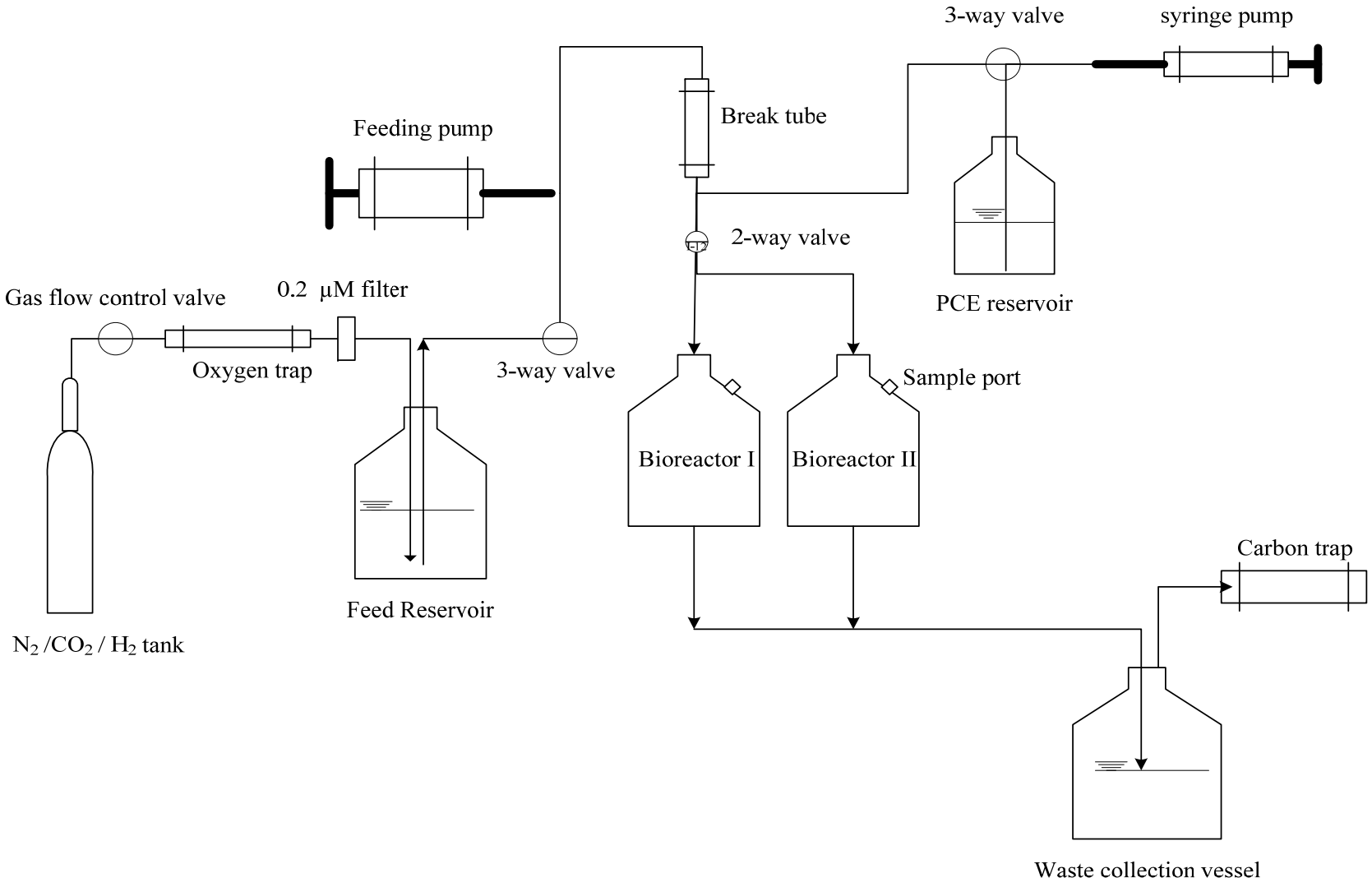

Figure 4.1 A diagram of the reactor experimental system to evaluate substrate interaction between dehalorespiring populations.

where H_C is the dimensionless Henry's Law constant, and S_G [$M_S \cdot L^{-3}$] and S_L [$M_S \cdot L^{-3}$] are the gaseous and aqueous concentrations, respectively, of a chlorinated ethene or hydrogen. The total mass of a chlorinated ethene, M_T [M_S] can be expressed as

$$M_T = S_L V_L + S_G V_G \tag{4.7}$$

where V_G [L^3] and V_L [L^3] are the volumes of the gas and aqueous phases, respectively. By substituting equation 4.6 into equation 4.7, S_L can be determined according to

$$S_L = \frac{M_T}{V_L + H_C V_G} \tag{4.8}$$

The cell yield (Y) [$M_X M_S^{-1}$] can be defined as

$$Y = \frac{X - X_0}{S_0 - S} \tag{4.9}$$

where X_0 is the initial biomass concentration [$M_X L^{-3}$] and S_0 is the initial substrate concentration [$M_S L^{-3}$]. Equation 4.9 can be rearranged and substituted for X in the integrated form of the single Monod model (equation 2.2) according to

$$t = \frac{1}{q_{\max}} \left[\frac{Ks}{X_0 + YS_0} \ln \frac{(X_0 + YS_0 - YS)}{X_0 S} + \frac{1}{Y} \ln \frac{X_0 + YS_0 - YS}{X_0} \right] \tag{4.10}$$

The parameters q_{max} and Ks were estimated using nonlinear regression analysis to fit equation 4.10 to a substrate depletion curve over time. Specifically, a spreadsheet-based weighted nonlinear analysis developed by Smith et al. (1998) was used to minimize the sum of the

squared weighted errors (SSWE).

$$SSWE = \sum_{i=1}^{n} \left[w_i \left(t_i^{obs} - t_i^{pred} \right) \right]^2 \tag{4.11}$$

where w_i is a weighting factor corresponding to the local slope of the substrate depletion curve, t_i^{obs} is the time of the i^{th} observation, and t_i^{pred} is the t value predicted by the model for the measured value.

4.7 Sensitivity analysis for parameter identifiability

Two approaches were used in this study to quantify the amount of correlation between q_{max} and K_S and ensure that the estimates were independent and reliable. First, sensitivity coefficients were calculated as the first derivatives of S with respect to either q_{max} or K_S, i.e., $\frac{dS}{dq_{\max}}$ and $\frac{dS}{dK_S}$ (Ellis et al. 1996; Grady et al. 1996; Robinson and Tiedje 1983) and used to determine the correlation coefficients (R^2) (Liu and Zachara, 2001). The relative standard deviation, $\frac{\sigma(\theta)}{\theta}$, where σ is the standard deviation of the replicate parameter estimates and θ is a Monod parameter, was used to assess the uncertainty associated with the estimated values. Finally, the linear interdependence of the sensitivity functions was quantified using the collinearity index, γ_K (Brun et al., 2002)

$$\gamma_K = \frac{1}{\sqrt{\min(EV(\tilde{S}^T \tilde{S}))}} \tag{4.12}$$

where $\tilde{S}$ is the normalized sensitivity coefficient matrix and EV is the eigenvalue of $\tilde{S}^T\tilde{S}$. γ_K approaches infinity as the degree of parameter dependence increases. On the contrary, if two parameters are completely independent, γ_K is equal to 1. In this study, the parameter estimates were considered identifiable if $\gamma_K \leq 15$, as recommended by Brun et al. (2002).

4.8 The measurement of cell yield

Y was estimated independently by measuring the increase in biomass and corresponding substrate consumption during the exponential growth phase according to equation 4.9. In order to maintain unrestricted culture growth, the initial PCE aqueous concentration was 20 times the initial biomass under the electron acceptor-limiting condition. For hydrogen kinetic study, the initial hydrogen concentration to initial biomass ratio was approximately 0.85 when both electron donor and biomass were expressed in terms of chemical oxygen demand (COD). Y measurements made during batch kinetic assays were performed in triplicate under the electron-acceptor limiting condition. Samples (1-mL) were obtained from each assay at 10, 26, 52, and 72 hrs for *Dhc. ethenogenes* and at 10, 20, 30 and 36 hrs for *Dhb. restrictus* and analyzed for protein and 16S rRNA gene copy numbers (following DNA extraction). The increase in biomass was estimated based on changes in either protein content or 16S rRNA gene copy numbers (measured via real-time qPCR).

4.9 The measurement of decay coefficient

The decay coefficient, k_d [T^{-1}], was measured independently following the procedures suggested by Cupples et al. (2003). Samples (3-mL) were withdrawn from the semi-continuous source cultures and maintained under non-growing conditions by withholding electron donor and electron acceptor. Under these conditions, the biomass undergoes decay and decreases in concentration over time. After 0, 1.5, 4.5, 8.5 and 11.5 days, duplicate 3-ml biomass samples were obtained from the non-growing cultures and transferred to batch bottles containing 58 ml of fresh medium, an electron acceptor (255 μM TCE for *Dhb. restrictus* and 415 μM *cis*-DCE for *Dhc. ethenogenes*) and excess electron donor (> 645 μM H_2). This initial rate of production of the dechlorination product (either $\frac{dM_{DCE}}{dt}$ or $\frac{dM_{VC}}{dt}$) was monitored for <10 h. The biomass concentration did not change significantly during this period, and thus should be the same as the concentration in the non-growing source culture at the time of sampling (X_t). Because the rate of dechlorination is propotional to X_t, k_d was estimated by fitting $\frac{dM_{DCE}}{dt}$ (for *Dhb. restrictus*) and $\frac{dM_{VC}}{dt}$ (for *Dhc. ethenogenes*) according to

$$\frac{dX}{dt} = -k_d X \tag{4.13}$$

$$\left(\frac{dM_{DCE(orVC)}}{dt}\right)_t = \left(\frac{dM_{DCE(orVC)}}{dt}\right)_0 e^{-k_d t} \tag{4.14}$$

where $\left(\frac{dM_{DCE(orVC)}}{dt}\right)_0$ is the dechlorination rate measured in the electron acceptor-free medium on day 0.

4.10 Determine of competitive inhibition coefficients

At low aqueous concentrations of chlorinated ethenes, dehalorespiration can be described using the Monod equation, as described above. However, at higher chlorinated ethene concentrations, self-inhibition and competitive inhibition effects may decrease the rate of substrate utilization. Therefore, various combinations of chlorinated ethenes were added to batch cultures to estimate the inhibition coefficients and describe these effects on dehalorespiration in *Dhc. ethenogenes* and *Dhb. restrictus*. The different pairs of target substrates and inhibitors, and their concentrations, are summarized in Table 4.2. Another series of experiments was conducted with single chlorinated ethenes to evaluate self inhibition effects, as summaried in Table 4.3.

The following procedure was used with both *Dhc. ethenogenes* and *Dhb. restrictus* when conducting the competitive and self inhibition experiments. Three ml of inoculum was transferred from a semi-continuous source culture to each 160-ml serum bottle containing 58 ml of fresh medium and excess hydrogen. X_0 was measured using the Bradford assay. Because it is difficult to reproducibly add neat chlorinated ethenes in the precise μL amounts needed to achieve the target concentrations in Table 4.2 or 4.3, the experiments were conducted using a set of 10 batch cultures, each of which contained the same electron

acceptor concentration but different concentrations of the inhibitor. K_I was estimated based on these batch cultures.

Competitive inhibition is described according to

$$\frac{dS_a}{dt} = -q_{\max} X \left(\frac{S_a}{K_S(1+\frac{S_I}{K_{CI}}) + S_a} \right) \tag{4.15}$$

where S_a [M_S L^{-3}] is the aqueous concentration of chlorinated ethene, and S_I [M_S L^{-3}] is the aqueous concentration of the chlorinated ethene inhibitor, and K_{CI} [M_S L^{-3}] is the competitive inhibition coefficient. Substrate depletion was monitored for 10 h and used to calculate dS_a/dt. During this relatively short time period, biomass did not increase significantly. Therefore, X could be treated as a constant and K_{CI} could be fitted to a linear form of Equation 4.16

$$\frac{q_{\max} S_a}{V_T} = S_a + K_S + \left(\frac{K_S}{K_{CI}} \right) S_I \tag{4.16}$$

where $V_T = dS_a/Xdt$ is the initial unit dechlorination rate [M_S M_X^{-1} T^{-1}], using previously obtained estimates of K_S and q_{max}.

In order to fit equation 4.16 to the substrate depletion data, appropriate estimates of q_{max} and K_S are needed. Fortunately, intrinsic q_{max} and K_S estimates were available from earlier experiments. To ensure that the intrinsic q_{max} and K_S parameter estimates could be applied, the inhibition kinetic experiments were conducted with an initial chlorinated ethene

concentration that was 20-fold in excess of the initial biomass concentration (on a COD basis), with one exception. In experiments involving VC, which does not sustain growth of *Dhc. ethenogenes*, the inhibitors were amended after all of the initial PCE had been completely transformed to VC.

Table 4.2 Initial conditions used in determination of competitive inhibition constants for *Dhc. ethenogenes* and *Dhb. restrictus*.

Organism	q_{max}[a]	K_S (μM)	Biomass (mg VSS/L)	Substrate	Approximate substrate conc. (μM)	Inhibitor	Inhibitor conc. (μM)
Dhc. ethenogenes	7.9	29	0.25	TCE	405	PCE	0-260
	13.2	33.6	0.24	cDCE	350	PCE	0-367
			0.18		416	TCE	0-196
	0.9	637	5.97	VC[b]	243	PCE	0-132
			4.39		314	TCE	0-100
			6.46		294	cDCE	0-328
Dhb. restrictus	29.8	1.3	0.19	TCE	492	PCE	0-326
	22.5	7.15	0.10	PCE	250	VC	0-67
	29.8	1.3	0.10	TCE	340	VC	0-45

[a]the unit of q_{max} = μmol/ mg VSS/

[b]VC does not serve as a growth substrate and is cometabolically transformed by *Dhc. ethenogenes*.

Table 4.3 Initial conditions used in the self-inhibition experiments with *Dhc. ethenogenes* and *Dhb. restrictus*

Organism	Self-inhibitor	Biomass conc. (mg VSS/L)	Inhibitor concentration (μM)
Dhc. ethenogenes	PCE	0.24	100-800
	TCE	0.53	50-1060
	cDCE	0.24	380-3135
Dhb. restrictus	PCE	0.31	210-924
	TCE	0.30	490-1140

4.11 Experimental approach for evaluating the effect of acetate availability on dechlorination rates and hydrogen thresholds

As noted in Section 4.3, the semi-continuous cultures of *Dhc. ethenogenes* and *Dhb. restrictus* were routinely maintained in media containing 5.0 mM acetate as the carbon source. To evaluate the effect of acetate on dechlorination rates, aliquots of the source culture were serially diluted to obtain an acetate concentration of less than 1.2 μM for *Dhc. ethenogenes* and lower than 0.45 μM for *Dhb. restrictus*. The experiments were conducted in duplicate. 60 μM PCE was provided as the electron acceptor for *Dhc. ethenogenes.* 200 μM PCE was provided for *Dhb. restrictus*. Both organisms were pressurized with 24.7 psi of 80% H_2/ 20% CO_2, to ensure excess H_2 was available as the electron donor. Initial biomass concentrations were 0.002 and 0.028 mg VSS/ L for *Dhc. ethenogenes* and *Dhb. restrictus*, based on qPCR analysis (described in Section 4.4.5). Acetate concentrations ranging from 5 mM to 2 μM were supplied to duplicate cultures. PCE consumption was monitored daily or every two days.

A separate set of experiments were conducted using duplicate cultures to assess whether different electron donor (H_2) thresholds occur if acetate is provided in excess or limiting amounts. The initial H_2 concentration was set at approximately 20 μM by sparging the headspace with 5% H_2/10% CO_2/85% N_2 (certified grade; Air Gas) with an initial acetate concentration of either 6.0 mM and 24 μM. Whenever all chlorinated ethene electron acceptors were consumed, 6 μL neat PCE (corresponding to an aqueous PCE

concentration of 380 μM) and 24 μM acetate were added to the assays to ensure excess electron acceptor and acetate were available. H_2 levels were monitored at least twice per week when dechlorination activity ceased.

4.12 Model development for estimating $K_{S,\ acetate}$ for *Dhb. restrictus* and *Dhc. ethenogenes*

As noted in Chapter 2, under non-inhibitory conditions, dehalorespiration of chlorinated ethenes is frequently described using a dual Monod equation (Equation 2.1) that accounts for the effects of electron donor and acceptor availability on the dechlorination rate (Bagley, 1998; Fennell and Gossett, 1998; Haston and McCarthy, 1999). However, as described below, experiments conducted in the current study demonstrate that the carbon source availability can also limit the dechlorination rate in some mixotrophs that utilize H_2 as the electron donor for dehalorespiration and an organic carbon source. In these cases, a multiple Monod equation that incorporates terms for the electron donor, electron acceptor, and carbon source is needed, according to:

$$\frac{dS_{PCE}}{dt} = -\left(\frac{q_{\max,PCE} X S_{PCE}}{K_{S,PCE} + S_{PCE}}\right)\left(\frac{S_{H_2} - S_{H_2,threshold}}{K_{S,H_2} + (S_{H_2} - S_{H_2,threshold})}\right)\left(\frac{S_{acetate}}{K_{S,acetate} + S_{acetate}}\right) \quad (4.17)$$

where Y is the true yield coefficient [$M_X\ M_S^{-1}$], and $K_{S,acetate}$ [$M_S\ L^{-3}$] and $S_{acetate}$ [$M_S\ L^{-3}$] are the acetate half-saturation coefficient and aqueous acetate concentration, respectively. $S_{H2,\ threshold}$ [$M_S\ L^{-3}$], is the H_2 threshold level, H_2 concentrations below this threshold cannot be substainally utilized by a given population. When the electron donor is provided in excess,

Equation 4.17 reduces to the following dual Monod equation (Equation 4.18)

$$\frac{dS_{PCE}}{dt} = -q_{\max} X \left(\frac{S_{PCE}}{K_{S,PCE} + S_{PCE}} \right) \left(\frac{S_{acetate}}{K_{S,acetate} + S_{acetate}} \right) \tag{4.18}$$

Microbial growth is described by Equation 4.9. Assuming acetate assimilation is stoichiometrically coupled to dehalorespiration, the rate of acetate utilization is described according to

$$Z \frac{dM_{PCE}}{dt} = \frac{dM_{acetate}}{dt} \tag{4.19}$$

where Z is a stoichiometric term that describes the mol of acetate consumed per mol of PCE respired (to VC in the case of *Dhc. ethenogenes* and *c*DCE in the case of *Dhb. restrictus*). The estimates of Y, q_{max}, and K_S used to fit $K_{S,acetate}$ are given in Section 5.1. The nonlinear least-squares optimization function, LSQNONLIN, was used with a fourth-order Runge Kutta method in Matlab (version 7.0.5) to fit $K_{S,acetate}$ by minimizing the sum of the squared errors (SSE) between the modeling predictions and experimental data. The Matlab code used to fit $K_{S,acetate}$ is given in Appendix A. SSE and the goodness of fit value (F) were used to quantify the model fit (DeVore and Peck, 1996).

4.13 Acetate assimilation experiments

As described below, PCE dechlorination by *Dhb. restrictus* appeared to be independent of the acetate concentration. Further, previous studies conducted with *Dhb. restrictus* have not demonstrated that acetate is necessary for dechlorination or incorporated

into the biomass during growth. Therefore, an experiment was conducted to evaluate whether acetate assimilation into biomass is coupled to dechlorination in *Dhb. restrictus* and *Dhc. ethenogenes*. Six replicate cultures were amended with 180 and 250 μM PCE and excess H_2 for *Dhb. restrictus* and *Dhc. ethenogenes*, respectively. A limiting amount of unlabeled acetate (24 μM) was added along with 1.0 μCi ^{14}C-acetate. Culture samples (0.5 mL) were filtered (0.2 μm, Millex-LG, 4 mm diameter, Fisher Scientific). ^{14}C-activity associated with biomass values were obtained by the counting the 0.5 mL filtered aqueous samples and 0.5 mL non-filtered aqueous samples. The initial experimental conditions are summarized in Table 4.4.

Table 4.4 Summary of experimental conditions used to evaluate effects of acetate availability on dechlorination rates, H_2 thresholds, and carbon assimilation by *Dhc. ethenogenes* and *Dhb. restrictus*

Experiment	Initial biomass (mg VSS/L)	Initial acetate levels	Initial hydrogen levels	Replication
Dechlorination rate	0.002[a]	1.2 μM-5 mM	> 600 μM[c]	2
	0.028[b]	0.45 μM-5 mM		
H_2 threshold	0.18[a]	24 μM and 6 mM	24 μM	2
	0.04[b]			
Acetate assimilation	0.25[a]	24 μM	> 600 μM[c]	6
	0.06[b]			

[a] *Dhc. ethenogenes*; [b] *Dhb. restrictus*; [c] Calculation described in the section 4.4.2 (under 24.7 psi, H_2 level corresponding to 3.3 mmol H_2; 18.8 μM corresponding to 60 μmol)

4.14 Experimental approach for the continuous-flow reactor experiments

The general experimental approach for the continuous-flow experiments was adapted based on the work done by Huang (2009), which along with current study was part of a larger NSF-funded project. The substrate interactions between *Dhc. ethenogenes* and *Dhb. restrictus* summarized in Table 4.5 were evaluated in two sets of experiments using the duplicate bioreactors described in Section 4.5. The experimental results and modeling simulations between dehalorespirers were compared to evaluate the validity of the mathematical model. The conditions used in the model simulations and experimental evaluations were representative of two commonly implemented bioremediation approaches: natural attenuation (electron donor limited conditions), and engineered bioremediation (electron donor is provided in excess). A PCE concentration of 14-15 μM was chosen to be similar to the range of contaminant concentrations at the Bachman Road Residential Wells Site (Lendvay et al., 2003) and other contaminated dry cleaning sites. In experiment 2, the electron donors hydrogen and acetate were provided in limiting amounts (~10 μM and ~8 μM, respectively), consistent with natural attenuation conditions.

Table 4.5 Experimental conditions used in the natural attenuation and engineered bioremediation scenarios

Experimental condition	Experiment number	Scenario	PCE conc. (μM)	Electron donor	Acetate conc. (μM)
Dhc. ethenogenes vs *Dhb. restrictus*	1	Engineered bioremediation	~15	600 μM H_2	5000
	2	Natural Attenuation	~15	~10 μM H_2	~8

4.15 Modeling approach

The model used to simulate the population interactions in the CSTRs builds on equations originally developed by Fennell and Gossett (1998) to describe competition among dehalorespiring bacteria and methanogens for hydrogen in batch cultures and modified by Becker (2006) to describe the competition for chlorinated ethenes and different electron donors between dehalorespiring populations in a continuous-flow system. In the current study, the multiple-step reductive dechlorination process was modeled using a dual or mutiple Monod model that incorporates inhibition effects that were shown to substantially impact dechlorination rate in batch cultures (as discussion in Section 5.2).

The equations used to describe dechlorination by *Dhc. ethenogenes* are as follows.

$$\frac{dS_{PCE}}{dt} = -\left(\frac{q_{\max,PCE} X S_{PCE}}{K_{S,PCE} + S_{PCE}}\right)\left(\frac{S_{H_2} - S_{H_2,threshold}}{K_{S,H_2} + (S_{H_2} - S_{H_2,threshold})}\right)\left(\frac{S_{acetate}}{K_{S,acetate} + S_{acetate}}\right) \quad (4.20)$$

$$\frac{dS_{TCE}}{dt}=\left(\frac{q_{\max,PCE}XS_{PCE}}{K_{S,PCE}+S_{PCE}}-\frac{q_{\max,TCE}XS_{TCE}}{K_{S,TCE}\left(1+\frac{S_{PCE}}{K_{CI,PCE/TCE}}\right)+S_{TCE}}\right)\left(\frac{S_{H_2}-S_{H_2,threshold}}{K_{S,H_2}+(S_{H_2}-S_{H_2,threshold})}\right)\left(\frac{S_{acetate}}{K_{S,acetate}+S_{acetate}}\right) \quad (4.21)$$

$$\frac{dS_{DCE}}{dt}=\left(\left(\frac{q_{\max,TCE}XS_{TCE}}{K_{S,TCE}\left(1+\frac{S_{PCE}}{K_{CI,PCE/TCE}}\right)+S_{TCE}}\right)-\left(\frac{q_{\max,DCE}XS_{DCE}}{K_{S,DCE}\left(1+\frac{S_{PCE}}{K_{CI,PCE/DCE}}+\frac{S_{TCE}}{K_{CI,TCE/DCE}}\right)+S_{DCE}}\right)\right)\times \quad (4.22)$$
$$\left(\frac{S_{H_2}-S_{H_2,threshold}}{K_{S,H_2}+(S_{H_2}-S_{H_2,threshold})}\right)\left(\frac{S_{acetate}}{K_{S,acetate}+S_{acetate}}\right)$$

$$\frac{dS_{VC}}{dt}=\left(\left(\frac{q_{\max,DCE}XS_{DCE}}{K_{S,DCE}\left(1+\frac{S_{PCE}}{K_{CI,PCE/DCE}}+\frac{S_{TCE}}{K_{CI,TCE/DCE}}\right)+S_{DCE}}\right)-\left(\frac{q_{\max,VC}XS_{VC}}{K_{S,VC}\left(1+\frac{S_{PCE}}{K_{CI,PCE/VC}}+\frac{S_{TCE}}{K_{CI,TCE/VC}}+\frac{S_{DCE}}{K_{CI,DCE/VC}}\right)+S_{VC}}\right)\right)\times \quad (4.23)$$
$$\left(\frac{S_{H_2}-S_{H_2,threshold}}{K_{S,H_2}+(S_{H_2}-S_{H_2,threshold})}\right)\left(\frac{S_{acetate}}{K_{S,acetate}+S_{acetate}}\right)$$

$$\frac{dS_{ETH}}{dt} = -\left(\frac{q_{\max,VC} X S_{VC}}{K_{S,VC}\left(1 + \frac{S_{PCE}}{K_{CI,PCE/VC}} + \frac{S_{TCE}}{K_{CI,TCE/VC}} + \frac{S_{DCE}}{K_{CI,DCE/VC}}\right) + S_{VC}} \right) \times \left(\frac{S_{H_2} - S_{H_2,threshold}}{K_{S,H_2} + (S_{H_2} - S_{H_2,threshold})} \right) \quad (4.24)$$

where S_{PCE}, S_{TCE}, S_{DCE}, S_{VC} and S_{ETH} are the aqueous concentrations [M_S L^{-3}] of PCE, TCE, cDCE, VC and ethene, respectively; $q_{max,PCE}$, $q_{\max,TCE}$, $q_{max,DCE}$, and $q_{\max,VC}$ are maximum specific substrate utilization rates [M_S M_X^{-1} T^{-1}] for PCE, TCE, cDCE, and VC, respectively; $K_{S,PCE}$, $K_{S,TCE}$, $K_{S,DCE}$, $K_{S,VC}$ and $K_{S,H2}$ are the half-saturation coefficients [Ms L^{-3}] for PCE, TCE, cDCE, VC, and H_2, respectively and where $K_{CI,inhibitor/electron\ acceptor}$ is the inhibition coefficient for a given inhibitor and electron acceptor (summarized in Table 5.5). As discussed in Chapter 5, dechlorination by *Dhb. restrictus* was not highly dependent on acetate availability. Therefore, the acetate terms in Equations 4.20—4.22 were not included in the PCE and TCE dechlorination models for *Dhb. restrictus* according to equation 4.25 and 4.26.

$$\frac{dS_{PCE}}{dt} = -\left(\frac{q_{\max,PCE} X S_{PCE}}{K_{S,PCE}\left(1 + \frac{S_{VC}}{K_{CI,VC/PCE}}\right) + S_{PCE}} \right) \left(\frac{S_{H_2} - S_{H_2,threshold}}{K_{S,H_2} + (S_{H_2} - S_{H_2,threshold})} \right) \quad (4.25)$$

$$\frac{dS_{TCE}}{dt} = \left(\left(\frac{q_{\max,PCE} X S_{PCE}}{K_{S,PCE}\left(1 + \frac{S_{VC}}{K_{CI,VC/PCE}}\right) + S_{PCE}} \right) - \left(\frac{q_{\max,TCE} X S_{TCE}}{K_{S,TCE}\left(1 + \frac{S_{PCE}}{K_{CI,PCE/TCE}} + \frac{S_{VC}}{K_{CI,VC/TCE}}\right) + S_{TCE}} \right) \right) \left(\frac{S_{H_2} - S_{H_2,threshold}}{K_{S,H_2} + (S_{H_2} - S_{H_2,threshold})} \right) \quad (4.26)$$

Growth of the dehalorespiring populations is described according to

$$\frac{dX}{dt} = \sum \left(\frac{q_{\max,CAHs} X Y S_{CAHs}}{K_{S,CAHs} + S_{CAHs}} \right) \left(\frac{S_{H_2} - S_{H_2,threshold}}{K_{S,H_2} + (S_{H_2} - S_{H_2,threshold})} \right) - k_d X \quad (4.27)$$

CAHs are chlorinated aliphatic hydrocarbons; and k_d [T^{-1}] is the decay coefficient. Because *Dhb. restrictus* is not capable of dechlorinating cDCE or VC, the biomass growth equation (4.27) only includes the PCE and TCE utilization and decay terms.

Hydrogen utilization was modeled based on electron acceptor utilization according to

$$\frac{dS_{H_2}}{dt} = -\frac{1}{fe} \sum \left(\frac{q_{\max,CAHs} X Y S_{CAHs}}{K_{S,CAHs} + S_{CAHs}} \right) \left(\frac{S_{H_2} - S_{H_2,threshold}}{K_{S,H_2} + (S_{H_2} - S_{H_2,threshold})} \right) \quad (4.28)$$

The model was constructed and implemented in STELLA Research 8.0 (High Performance Systems). A Runge-Kutta 4 integration method was used with a calculation time step of 0.125 h. The kinetic parameter inputs for *Dhc. ethenogenes* and *Dhb. restrictus* were obtained in this study, as described in Chapter 5.

Chapter 5 Result and discussion

5.1 Intrinsic and extant Monod kinetics and their implications for *Dehalobacter restrictus* and *Dehalococcoides ethenogenes*

5.1.1 Intrinsic electron donor kinetics

The single substrate depletion curves used to fit the intrinsic kinetic parameters for *Dhc. ethenogenes* and *Dhb. restrictus* under electron donor-limiting conditions are shown in Figure 5.1. The kinetic parameters fit to these data are summarized in Table 5.1 along with the electron acceptor kinetic parameter estimates. The magnitude of $S_{H2,threshold}$ reflects the ability of hydrogenotrophic organisms to utilize hydrogen at low concentrations. In systems where the substrate concentration may become quite low, e.g., batch cultures or continuous-flow systems with a very long SRT, $S_{H2,threshold}$ may affect the substrate utilization kinetics (Equation 2.1) of a population and thus its ability to compete for hydrogen.

As summarized in Table 5.2, several studies have reported $S_{H2,threshold}$ values of less than 2 nM for hydrogenotrophic dehalorespirers (Yang and McCarty, 1998; Fennell and Gossett, 1998; Smatlak et al., 1996). $S_{H2,threshold}$ values of 2-10 nM and < 23 nM were obtained in this study for *Dhc. ethenogenes* and *Dhb. restrictus*, respectively (Table 5.2). The relatively low $S_{H2,threshold}$ values of the dehalorespirers gives them a competitive advantage over other hydrogen-utilizing organisms, such as methanogens, which have higher $S_{H2,threshold}$ values, when hydrogen levels are low (Fennell and Gossett, 1998; Smatlak et al., 1996). Similarly, the $S_{H2,threshold}$ of *Dhb. restrictus* is higher than that of the other dehalorespirers, which may make it difficult for it to compete with *Dehalococcoides* strains when hydrogen is limiting.

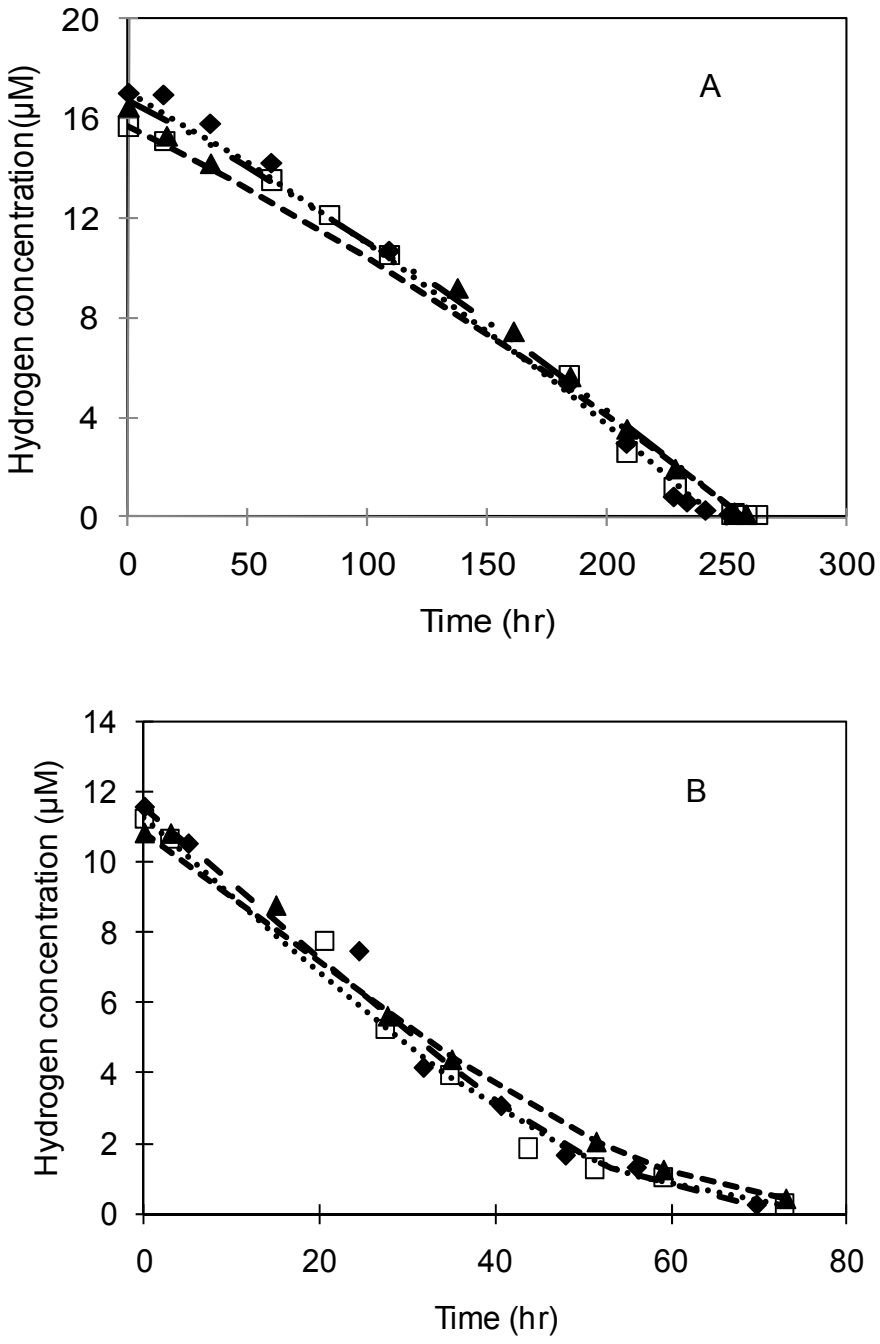

Figure 5.1 Electron donor depletion data used to fit $K_{S,donor}$ and $q_{max,donor}$ for hydrogen utilization by (A) *Dhc. ethenogenes* and (B) *Dhb. restrictus*. Data points represent experimental results for triplicate batch cultures. Dashed lines represent model predictions results for the individual triplicate batch cultures.

Table 5.1 Monod kinetic parameter estimates for *Dhc. ethenogenes*, *Dhb. restrictus* and several other chlorinated ethene-respiring cultures

Strain	*Dhc. ethenogenes* [a]	*Dhb. restrictus* [a]	Mixed culture containing *Dhc. ethenogenes*	Mixed culture PM containing *Dehalococcoides*-like microorganisms	*Dhc.* strain VS	*Dhb. restrictus*
Yield (mg VSS/μmol Cl^-)	0.0047 (0.0003)	0.0044 (0.0008)	0.00612	NA [b]	0.0022(0.0006)	NA
q_{max} (μmol/mg VSS/h)						
PCE	6.8 (0.5)	22.5 (0.5)	1.8	0.3 (0.04)		7.3
TCE	7.9 (0.6)	29.8 (0.7)	3	2.84 (0.39)		NA
cDCE	13.2 (0.9)		3	0.51 (0.04)	1.96	
VC	0.9 (0.0)		3	0.06 (0.01)	1.96	
H_2	12.8 (0.6)	56.4 (7.80)				NA
K_S (μM)						
PCE	21.5 (3.4)	7.2 (1.9)	0.54	3.9 (1.4)		NA
TCE	29.0 (9.2)	1.30 (0.3)	0.54	2.8 (0.3)		NA
cDCE	33.6 (7.1)		0.54	1.9 (0.50)	3.3 (2.2)	
VC	637 (14.9)		290	602 (7)	2.6 (1.9)	
H_2	0.03 (0.02)	3.3 (0.8)	0.1		0.007 (0.002)	NA
Reference	This study	This study	Fennell and Gossett, 1998	Yu et al., 2005	Cupples et al., 2003; 2004	Holliger et al., 1998

[a] Parameters values represent average of estimates fit to data obtained from triplicate cultures and values in parentheses represent 95% confidence interval; [b] Not available

Table 5.2 Hydrogen thresholds ($S_{H2,threshold}$) observed in hydrogenotrophic dehalorespiring populations using PCE as the electron acceptor

Organisms	$S_{H2,threshold}$ (nM)	Reference
Mixed culture containing *Dhc. ethenogene*	1.5	Fennell and Gossett, 1998
Benzoate-acclimated dehalogenating methanogenic mixed culture	2.2 ± 0.9	Yang and McCarty, 1998
Anaerobic enrichment culture	< 2	Smatlak et al. 1996
Dhc. ethenogenes	2-10	This study
Dhb. restrictus	<23	This study

As noted by Huang and Becker (2009), "most studies of chlorinated ethene dehalorespiration were generally conducted with excess levels of electron donors and therefore, estimates of q_{max} for electron donors were not generally determined. However, accurate estimates of q_{max} and K_s for electron donors were needed because these values may play an important role in determining the outcome of competition among dehalorespiring populations (Becker, 2006) or between dehalorespirers and other populations in continuous-flow systems. If these values are needed for modeling studies, they are generally calculated based on estimates of q_{max} for chlorinated ethenes and the fraction of electron donor equivalents that are used in energy production (f_e) (Bagley, 1998)". In this study, $q_{max,H2}$ values of 12.8 ± 0.6 and 56.4 ± 7.8 μmol/mg VSS/h were estimated for *Dhc. ethenogenes* and *Dhb. restrictus*, respectively (Table 5.1). The fitted $q_{max,H2}$ for *Dhb. restrictus* (56.7 μmol/mg VSS/h) compared fairly well to the calculated $q_{max,H2}$ value (60.8 μmol/mg VSS/h), which was obtained using the $q_{max,PCE}$ in Table 5.1 and the experimentally determined f_e value of 0.74 (Figure 5.2). However, the fitted $q_{max,H2}$ for *Dhc. ethenogenes* (12.8 μmol/mg VSS/h) was less than a half of the $q_{max,H2}$

value of 31.1 μmol /mg VSS/h calculated for *Dhc. ethenogenes* using the fitted $q_{max,PCE}$ (Table 5.1), and the experimentally determined f_e value of 0.87 (Figure 5.2). A previous study estimated that the f_e value for *Dhb. restrictus* was 0.73 (Löffler, et al., 1999), which was very similar to the value obtained in the current study. Previously reported f_e values for *Dhc. ethenogenes* range from 0.46 (Löffler et al., 1999) to 0.902 (Fennell, 1998). If f_e = 0.46 is used to calculate $q_{max,H2}$ for *Dhc. ethenogenes*, the resulting value (58.8 μmol/mg VSS/h) is even further off from the experimentally determined value. The high f_e values obtained in this study and by Fennell (1998) suggested that under some conditions reductive dechlorination may become uncoupled from growth in *Dhc. ethenogenes*. This is supported by molecular evidence (Johnson et al., 2008).

5.1.2 Intrinsic electron acceptor kinetics

The q_{max} and K_S values for the chlorinated ethenes obtained in this and earlier studies are reported in Table 5.1 and vary over more than an order of magnitude in different organisms. In particular, *Dehalococcoides* strains in pure and mixed cultures tend to exhibit substantially lower q_{max} and K_S values compared to the experimental results reported for the *Dhc. ethenogenes* and *Dhb. restrictus* in this study. For example, $q_{max,PCE}$ values of 6.8 and 22.5 μmol/mg VSS/h obtained in this study for *Dhc. ethenogenes* and *Dhb. restrictus*, respectively. Some qualitative observations about the conditions under which these populations are expected to be competitive can be made based on these parameter estimates. For example, at high PCE concentrations (which may develop near the contaminant source), *Dhb. restrictus* with its relatively higher $q_{max,PCE}$ may have an advantage over *Dhc. ethenogenes.* Under these conditions, it may be possible for *Dhc. ethenogenes* to grow on lesser chlorinated ethenes produced by *Dhb.*

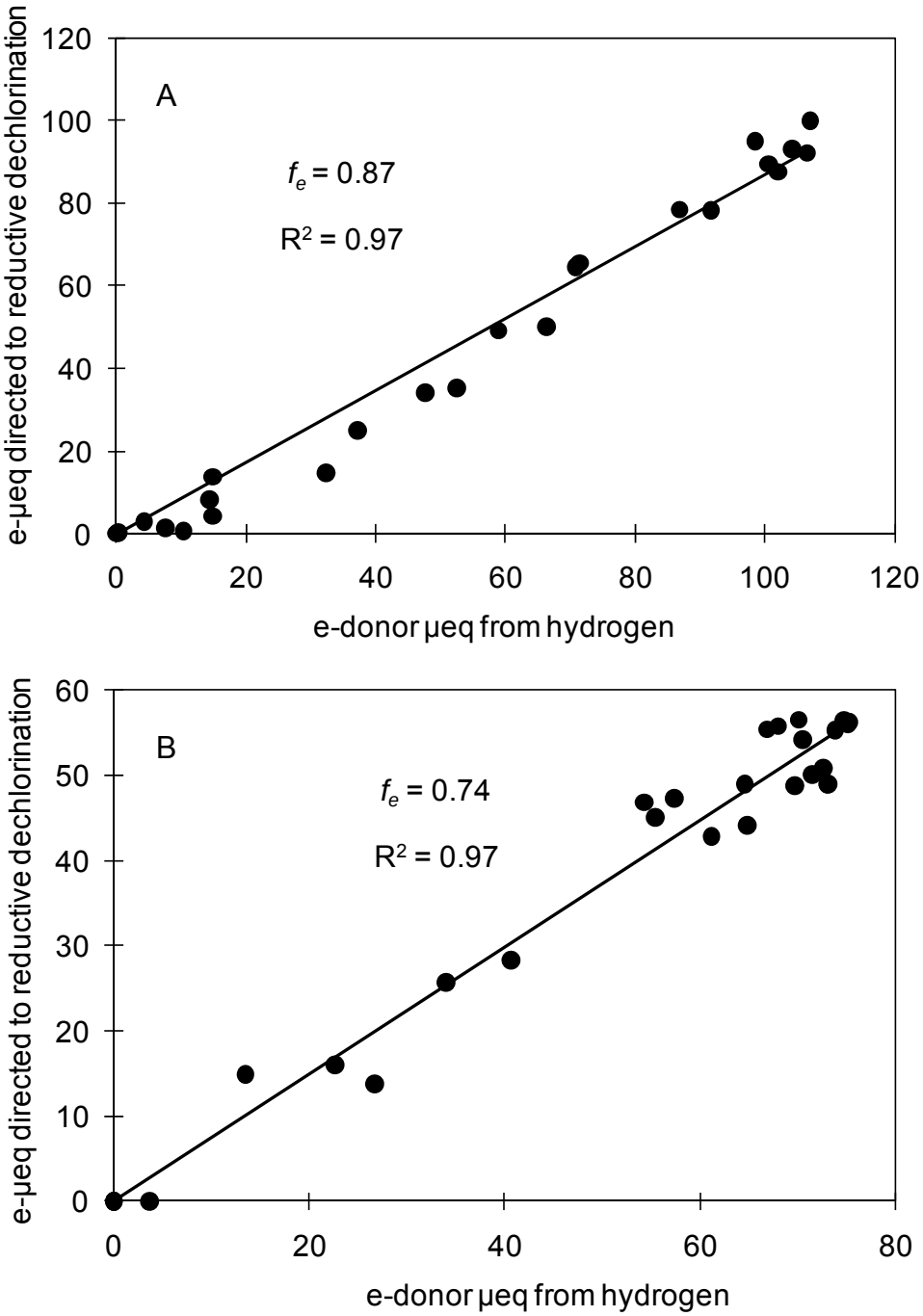

Figure 5.2 Determination of f_e values using hydrogen as electron donor for (A) *Dhc. ethenogenes*, and (B) *Dhb. restrictus*. Data points represent individual measurements in triplicate batch cultures. The f_e values were determined by linear regression analysis by plotting the amount of electron equivalents consumed by reductive dechlorination versus the amount of electron equivalents provided by the electron donor. f_e values were derived from the slopes of the regression lines.

restrictus, if adequate electron donor is available. The combination of *Dhc. ethenogenes* and *Dhb. restrictus* could thus lead to fast and complete detoxification of PCE.

However, compared with the other kinetic parameters reported in Table 5.1, the $q_{max,PCE}$ values estimated in this study for *Dhc. ethenogenes* and *Dhb. restrictus* from other studies were approximately one order of magnitude higher. Most likely, differences in the properties of the specific chlorinated ethene reductive dehalogenases influenced the values of the kinetic parameters for chlorinated ethene utilization reported for different dehalorespiers in Table 5.1. In addition, three interrelated factors—culture history (e.g., substrate availability), kinetic assay procedure and parameter correlation and identifiability—may have also caused some of the variability in the kinetic parameter estimates (Liu and Zachara, 2001; Grady, et al., 1996). For example, if the ratio of initial substrate to biomass concentration (S_0/X_0) used in previous studies did not truly allow unrestricted growth of the dehalorespirers to occur, it could explain at least in part, why lower q_{max} values were obtained in these studies.

Independent estimates of Y and k_d were also obtained in this study for *Dhc. ethenogenes* and *Dhb. restrictus* under electron acceptor-limiting conditions. The Y determined for *Dhc. ethenogenes* and *Dhb. restrictus* based on protein measurements, 0.0047 and 0.0044 mg VSS/μmol Cl^-, respectively, are of similar magnitude to those estimated using qPCR (0.0080 mg VSS/μmol Cl^- and 0.0062 mg VSS/μmol Cl^-, respectively). Few k_d values have been reported for dehalorespirers. Fennell and Gossett (1998) estimated that the k_d for dehalorespirers and other anaerobic microorganisms was 0.001 h^{-1}, and this value is often used in modeling studies (Becker 2006; Yu et al. 2005). The experimentally determined k_d for *Dhc. ethenogenes* (0.004 h^{-1}) in this study was very

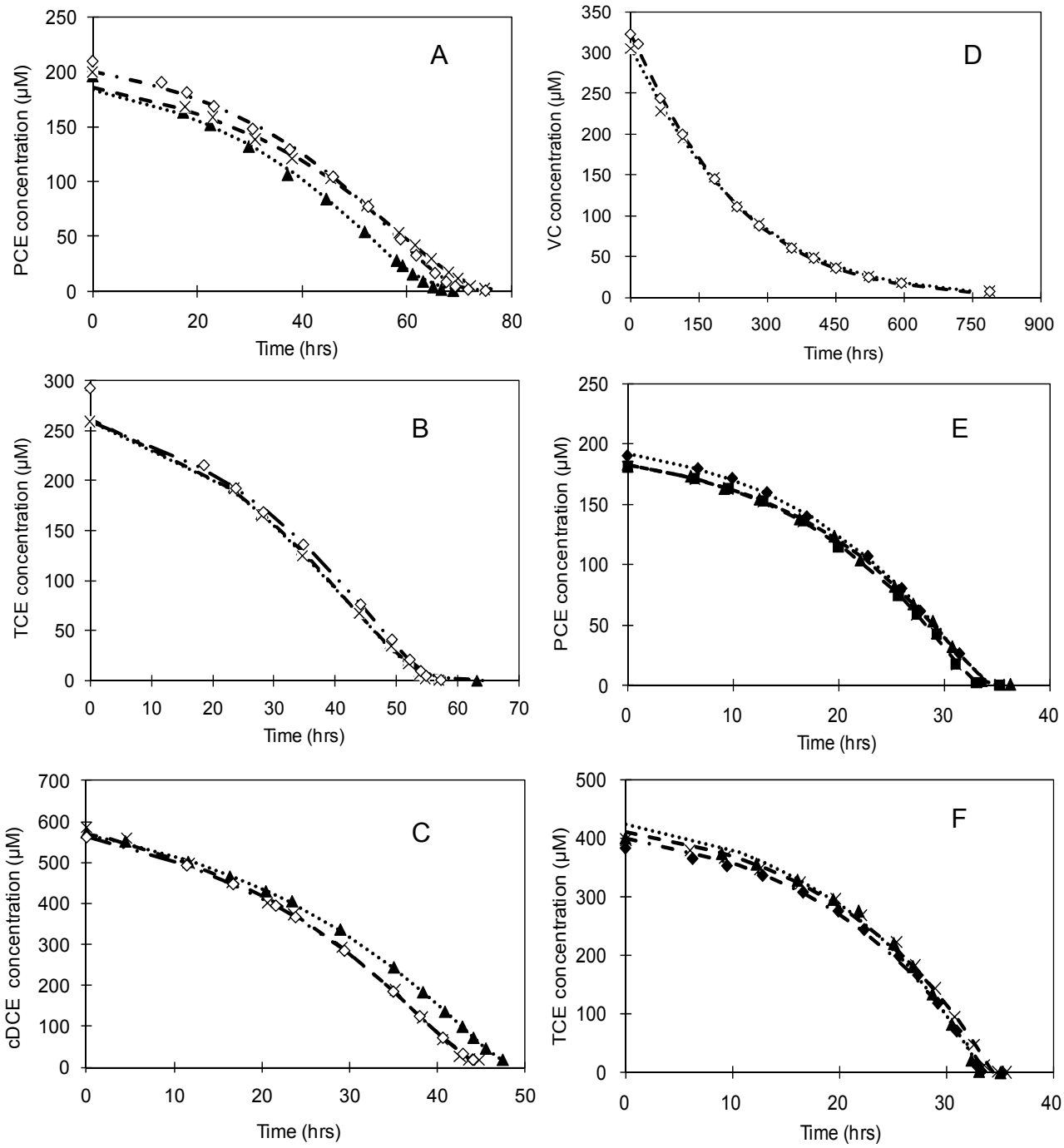

Figure 5.3 Electron acceptor depletion data used to fit K_S and q_{max} for *Dhc. ethenogenes* utilizing (A) PCE, (B) TCE, (C) cDCE, and (D) VC and for *Dhb. restrictus* utilizing (E) PCE and (F) TCE . Data points represent experimental results from triplicate (Panels A-C, E, and F) or duplicate (Panel D) batch cultures. Dashed lines represent model predictions

close to the value (0.00375 h^{-1}) (Cupples et al. 2003) for *Dehalococcoides* sp. strain VS under no-growth conditions in mixed cultures but both k_d estimates for *Dehalococcoides* strains are lower than the values obtained for *Dhb. restrictus* (0.017 h^{-1}). This high k_d suggests that *Dhb. restrictus* has to maintain a high gowth rate in order to maintain positive net growth and this might limit its competitiveness, particularly when substrate availiability is limited.

5.1.3 Parameter identifiability

The correlation coefficients (R^2) for the $q_{max,donor}$ and $K_{S,donor}$ estimates in individual assays involving *Dhc. ethenogenes* ranged from 0.79 to 0.84. R^2 ranged from 0.95 to 0.97 for *Dhb. restrictus*. While the R^2 values for *Dhb. restrictus* were quite high, they were in the same range as the values calculated in a study of the uncertainty in Monod kinetic parameter estimates conducted by Liu and Zachara (2001). In fact, the authors noted that it may be difficult to obtained $R^2 < 0.9$, which may limit the usefulness of this parameter when assessing the uniqueness of parameter estimates. Therefore, the collinearity index (γ_K) was also calculated for each set of parameter estimates (Table 5.3). The γ_K values calculated for the electron donor utilization kinetic parameter estimates ranged from 4.9 to 5.0 for *Dhc. ethenogenes* and from 9.9 to 13.1 for *Dhb. restrictus*. Previous studies have suggested that the maximum γ_K values for identifiable parameter estimates were less than 15 (Brockmann et al. 2008; Brun et al. 2002). Thus, the electron donor kinetic parameter estimates can be considered identifiable. Clearly, the R^2 and γ_K values for the *Dhc. ethenogenes* hydrogen utilization kinetic parameters were lower than those calculated for the *Dhb. restrictus* parameters. As described in greater detail below, this is because selecting initial conditions that result in a high S_0/K_S ratio (generally S_0/K_S

> 20) in batch kinetic assay is key to obtaining parameter estimates with a relatively low degree of correlation. The extremely low K_S value estimated for *Dhc. ethenogenes* virtually guaranteed that S_0/K_S was high, which in turn contributed to low parameter correlation. The R^2 values calculated for the kinetic parameters describing chlorinated ethene utilization ranged from 0.96 to 0.98 for *Dhc. ethenogenes*, and from 0.89 to 0.96 for *Dhb. restrictus*, respectively (Table 5.3). These R^2 values are higher than the values obtained for the hydrogen utilization kinetic parameters. Nevertheless, the γ_K values were generally less than 15, suggesting that in most cases, the estimates of q_{max} and K_S for chlorinated ethene utilization were identifiable. However, it is clear from the R^2 and γ_K values that $q_{max,VC}$ and $K_{S,VC}$ are highly correlated and poorly identifiable. Again, this can be understood by examining the magnitude of $K_{S,VC}$, which was very large because *Dhc. ethenogenes* transforms VC cometabolically. This caused S_0/K_S to be very small. As a result, independent estimates of $q_{max,VC}$ and $K_{S,VC}$ cannot be obtained. Instead, a lumped first-order coefficient (q_{max}/K_S) should be used to describe VC dechlorination by *Dhc. ethenogenes*.

Table 5.3 Collinearity index (γ_K) and correlation coefficient (R^2) values calculated for *Dhc. ethenogenes* and *Dhb. restrictus* kinetic parameter estimates

Strain	Electron acceptor /donor	R^2	γ_K
Dhc. ethenogenes	PCE	0.97-0.98	10.2-13.1
	TCE	0.96-0.98	11.0-15.1
	cDCE	0.96-0.97	9.4-11.5
	VC	0.996-0.998	26.7-35.4
	H_2	0.79-0.84	4.9-5.0
Dhb. restrictus	PCE	0.94-0.96	8.7-9.2
	TCE	0.89-0.90	6.2-6.7
	H_2	0.95-0.97	9.9-13.1

5.1.4 Extant kinetic parameter estimates

The corresponding substrate depletion curves obtained from the extant kinetic batch assays ($S_0/X_0 \leq 0.12$) are shown in Figure 5.4. Independent estimates of q_{max} and K_S were successfully fit to these curves, as summarized in Table 5.4. The S_0/K_S ratios ranged from 3.2 to 33.4. The R^2 for the $q_{max,acceptor}$ and $K_{S,acceptor}$ estimates in individual assays involving *Dhc. ethenogenes* ranged from 0.84 to 0.94. The R^2 values calculated for the *Dhb. restrictus* parameter estimates ranged from 0.84 to 0.94. The γ_K values calculated for these parameter estimates were below 10–15, indicating the parameter estimates are identifiable. It is important to note that because of the nature of extant kinetic parameters, the values reported in Table 5.4 are applicable only to *Dhc. ethenogenes* and *Dhb. restrictus* maintained at a 20-d SRT. The R^2 and γ_K values calculated for the parameter estimates in Table 5.4 are plotted as a function of S_0/K_S and S_0/X_0 in Figures 5.5 and 5.6, respectively.

Table 5.4 Extant kinetic parameter estimates for chlorinated ethene utilization at room temperature (23ºC) by *Dhc. ethenogenes* and *Dhb. restrictus* using cultures maintained at a 20-d SRT

	Electron acceptor	q_{max}[a] (μmol/mg VSS/h)	K_S[a] (μM)	Correlation coefficient (R^2)	Collinearity index(γ_K)
Dhc. ethenogenes	PCE	3.41 (0.16)	0.97 (0.14)	0.86 - 0.91	5.5-6.9
	TCE	3.44 (0.54)	2.25 (1.05)	0.84 - 0.94	5.6-9.4
	cDCE	6.59 (0.50)	4.61 (0.79)	0.90 - 0.91	7.1-7.6
Dhb. restrictus	PCE	12.77 (3.05)	4.91 (1.75)	0.90 - 0.94	7.3-9.3
	TCE	22.10 (1.26)	3.86 (0.19)	0.84 - 0.91	5.6-8.1

[a]Values in parentheses represent 95% confident interval of the estimates from the triplicate batch culture assays

Consistent with the previous numerical and experimental evaluations, higher S_0/K_S ratios were associated with lower correlation coefficients and lower collinearity index values, but S_0/X_0 ratios seemed to be independent of correlation and collinearity index values. The estimates of $q_{max,acceptor}$ obtained for *Dhc. ethenogenes* and *Dhb. restrictus* under extant conditions were 25 to 50% lower than the intrinsic kinetic values reported in Table 5.1. In addition, $K_{S,acceptor}$ values obtained under extant conditions for *Dhc. ethenogenes* was two orders of magnitude lower than the values obtained under intrinsic conditions. $K_{S,acceptor}$ values obtained for *Dhb. restrictus* under extant and intrinsic conditions varied less. The differences in the estimates obtained under intrinsic and extant conditions illustrate the importance of selecting appropriate initial conditions to obtain meaningful kinetic batch assays.

5.1.5 Conclusion and implication

Independent estimates of q_{max} and K_S describe that the intrinsic and extants under growth and non-growth conditions, respectively are successfully obtained for *Dhc. ethenogenes* and *Dhb. restrictus*. The values estimated under different growth conditions varied, as expected, and highlighted that care must be used when estimating and applying kinetic parameters in making modeling predictions. Calculation of the colinearity index (γ_K) and correlation coefficients (R^2) was used to quantitatively evaluate parameter independence. Because different q_{max} and K_S estimates are applicable under different growth conditions, it may be difficult to evaluate microbial competition when substrate availability and microbial growth condition vary with time in batch systems. Chemostats are better suited for this purpose because substrate and kinetic parameters are not variable at steady-state conditions.

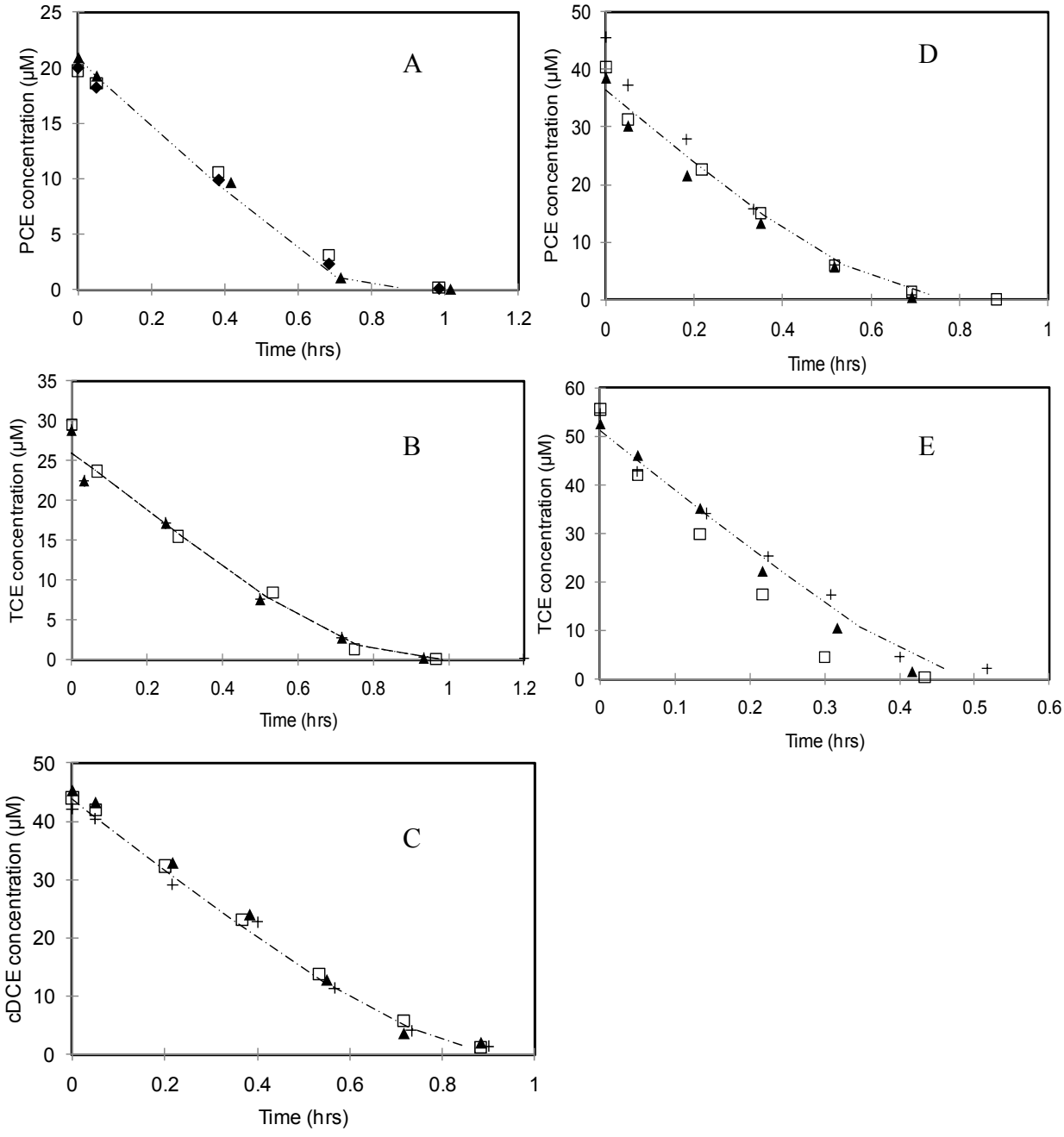

Figure 5.4 Extant kinetic substrate depletion curves for *Dhc. ethenogenes* using (A) PCE, (B) TCE, and (C) cDCE and for *Dhb. restrictus* using (D) PCE and (E) TCE as the electron acceptor. Assays were performed at room temperature (23ºC) using cultures that were maintained at a 20-d SRT, as described in the text. Symbols represent individual data points obtained in triplicate experiments. Dashed lines represent the model predictions using average parameter estimates.

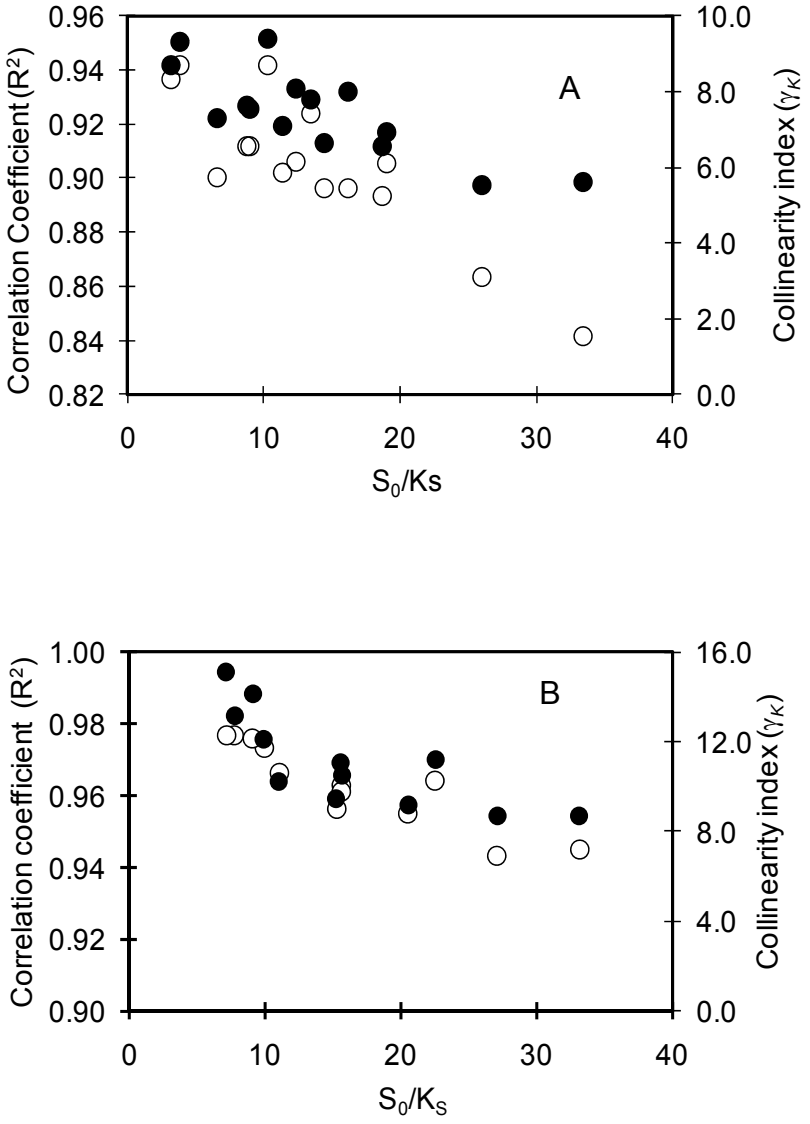

Figure 5.5 The effect of S_0/K_S on the correlation coefficients (hollow circles) and collinearity index values (dark circles) calculated for estimates of q_{max} and K_S. The data sets were generated by pooling data on PCE, TCE and cDCE dechlorination by *Dhc. ethenogenes* and data on PCE and TCE dechlorination by *Dhb. restrictus*. (A) Extant and (B) intrinsic kinetic parameter estimates.

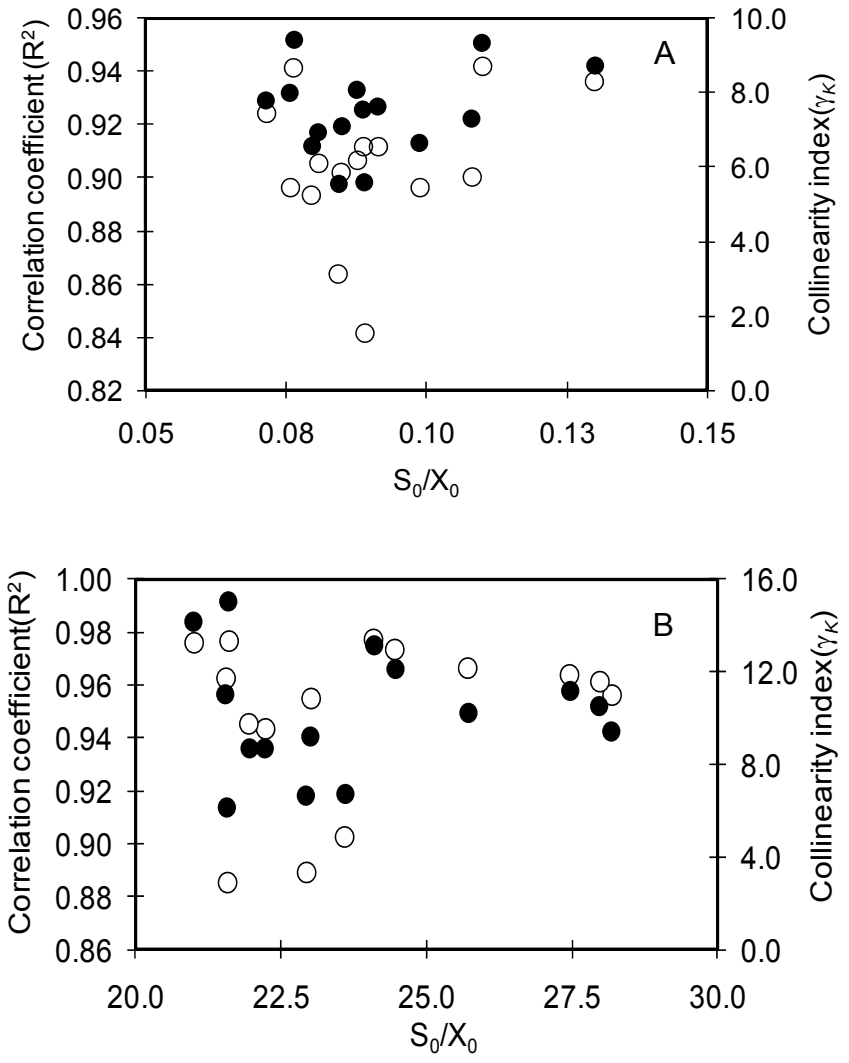

Figure 5.6 (A) The effect of S_0/X_0 on correlation coefficients (hollow circles) and collinearity index (dark circles) of the extant kinetic parameters (q_{max} and K_S) for PCE, TCE and cDCE dechlorination by *Dhc. ethenogenes* and for PCE and TCE dechlorination by *Dhb. restrictus* in batch cultures with different initial substrate-to-initial biomass ratios. (B) Correlation coefficients (hollow circles) and collinearity index values (dark circles) of the intrinsic kinetic parameters (q_{max} and K_S) for PCE, TCE and cDCE dechlorination by *Dhc. ethenogenes* and for PCE and TCE dechlorination by *Dhb. restrictus* in batch cultures with different initial substrate-to-initial biomass ratios.

5.2 Competitive and self inhibition effects on dechlorination by *Dhc. ethenogenes* and *Dhb. restrictus*

5.2.1 Competitive and self inhibition effect on dechlorination

Several sets of kinetic assays were conducted to evaluate whether the chlorinated ethenes were self-inhibitory substrates, that is, inhibited their own dechlorination at high substrate concentrations in *Dhc. ethenogenes* and *Dhb. restrictus.* In *Dhb. restrictus,* the initial PCE dechlorination rate decreased with increasing PCE concentrations ranging from 210 to 924 μM (concentrations that correspond to $16 \leq S_0/X_0 \leq 70$ on a COD basis; Figure 5.7A). At a PCE concentration of 924 μM, the PCE dechlorination rate was barely detectable. Interestingly, earlier studies indicated that PCE levels above 200 μM could not be dechlorinated by *Dhb. restrictus* (Holliger et al., 1998; 1993). However, initial TCE dechlorination rate was two-thirds that measured at lower TCE concentrations (Table 4.1) and did not appear to decrease with increasing TCE concentrations in the range of 494 to 1146 μM (concentrations that correspond to $17 \leq S_0/X_0 \leq 42$ on a COD basis; Figure 5.7B).

Similar trends were observed with *Dhc. ethenogenes*. At relatively low initial PCE concentrations (< 300 μM) the dechlorination rate was unaffected by the PCE concentration and was essentially equivalent to the intrinsic $q_{max,PCE}$ (Figure 5.8A). However, at higher PCE concentrations (340 to 800 μM), $q_{max,PCE}$ decreased with increasing PCE concentrations. At a PCE concentration of 800 μM, dechlorination was barely detectable. In contrast, self-inhibition of TCE (Figure 5.8B) and cDCE (Figure 5.8C) dechlorination by *Dhc. ethenogenes* was not observed, even at concentrations exceeding 1000 μM and 3000 μM, respectively.

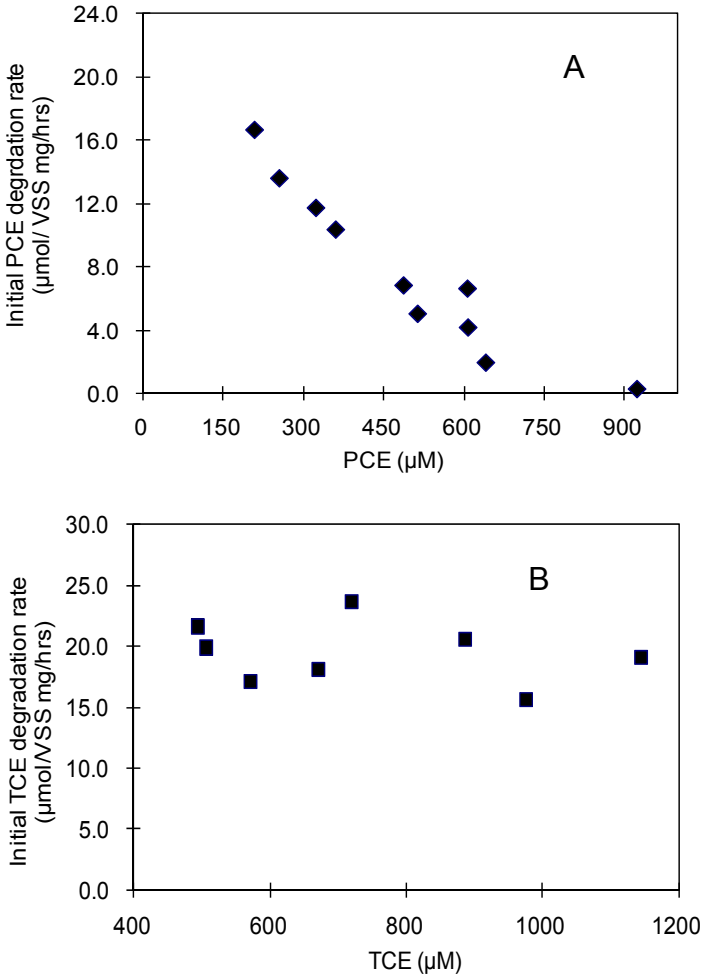

Figure 5.7 Initial rate of dechlorination of (A) PCE at different aqueous concentrations and (B) TCE at different aqueous concentration of TCE by *Dhb. restrictus.*

The effects of higher chlorinated ethenes on dechlorination of the less chlorinated ethenes followed a competitive inhibition pattern for both *Dhc. ethenogenes* and *Dhb. restrictus.* This means that the rate of dechlorination of one chlorinated ethene (the substrate) decreased as the initial concentration of a second chlorinated ethene (the inhibitor) increased. For example, in experiments involving *Dhb. restrictus*, the initial TCE dechlorination rate decreased with increasing PCE concentrations and PCE concentrations as low as 50 µM exhibited an effect, as shown in Figure 5.9. A K_{CI} value

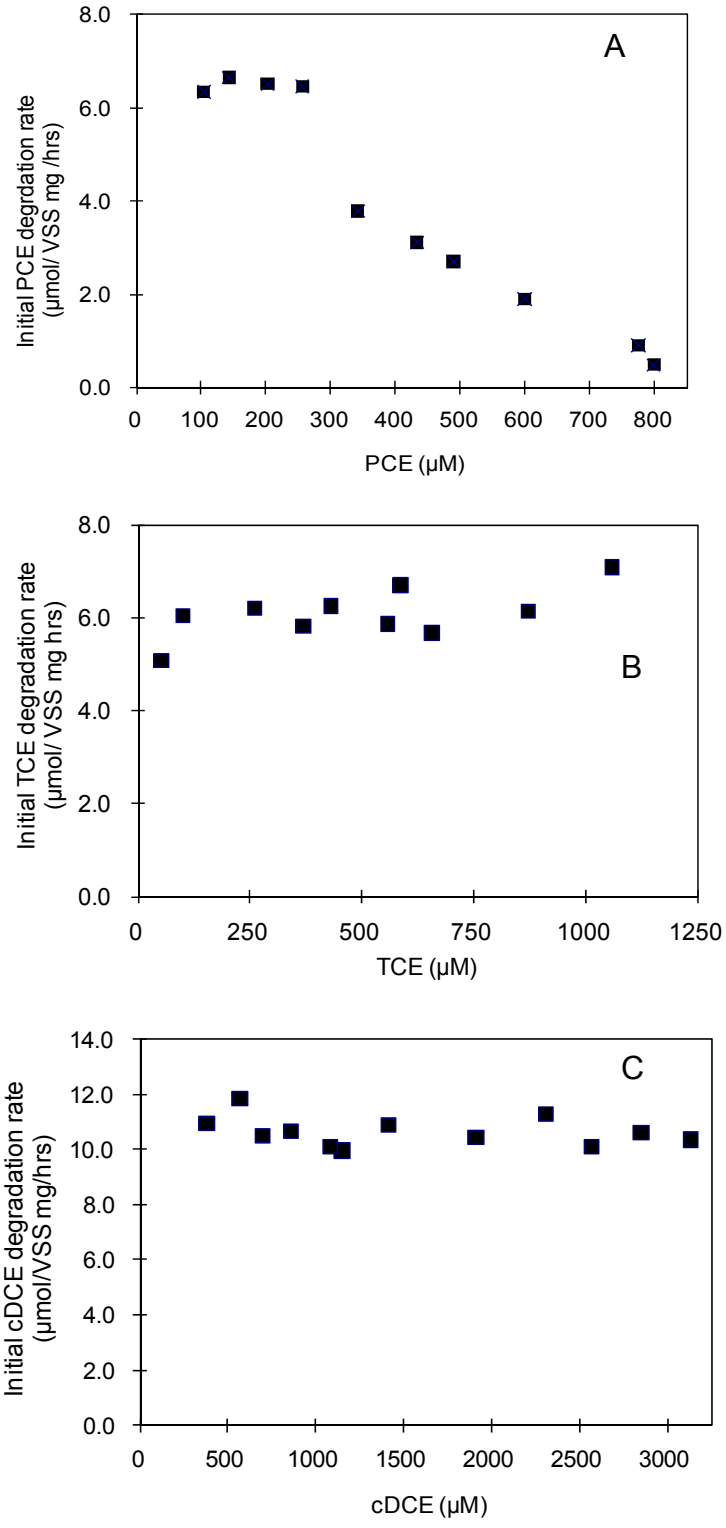

Figure 5.8 Initial dechlorination rate of (A) PCE in the presence of different aqueous concentrations of PCE; (B) TCE in the presence of different aqueous concentration of TCE; (C) cDCE in the presence of different aqueous concentration of cDCE by *Dhc. ethenogenes*

of 0.23 μM was obtained by fitting Equation 4.9 to these data using the intrinsic Monod kinetic parameters shown in Table 5.1. This K_{CI} value was more than an order of magnitude smaller than K_{CI} values obtained in the previous studies evaluating PCE inhibition of TCE dechlorination (Table 5.5), and suggests that PCE strongly inhibits TCE respiration by *Dhb. restrictus*. However, it is important to note that q_{max} is faster and K_S is lower for TCE compared with PCE utilization by *Dhb. restrictus*, and, as a result, TCE does not accumulate in *Dhb. restrictus* cultures growing on PCE. K_{CI} values of 3.74 and 0.56 μM for competitive inhibition between VC-to-PCE and VC-to-TCE (Figure 5.9) were also obtained in this study. The initial PCE dechlorination rate decreased slightly with increasing VC concentration. Compared with PCE depletion, the VC inhibition effect on TCE dechlorination was more noticeable. This finding is consistent with the persistence of VC during 1,1,1-trichloroethane and 1,1-dichloroethane dechlorination by *Dhb. restrictus* (Grostern et al., 2009).

Interestingly, after 48 hrs all of the PCE and most of the TCE amended was completely transformed to cDCE in the presence of VC. Only when the VC concentration exceeded 30 μM cDCE, TCE only partially transformed to cDCE. PCE concentrations of greater than 100 μM slightly inhibited the dechlorination of TCE and cDCE by *Dhc. ethenogenes* (Figure 5.10 A-B). The effects of PCE on VC dechlorination were more dramatic (Fig. 5.10 C). Even at concentrations of less than 10 μM PCE, VC dechlorination was sharply inhibited, and VC dechlorination was barely detectable during the first 5 h at higher than 30 μM PCE. The rates of cDCE dechlorination by *Dhc. ethenogenes* decreased slightly with increases in the TCE concentration up to

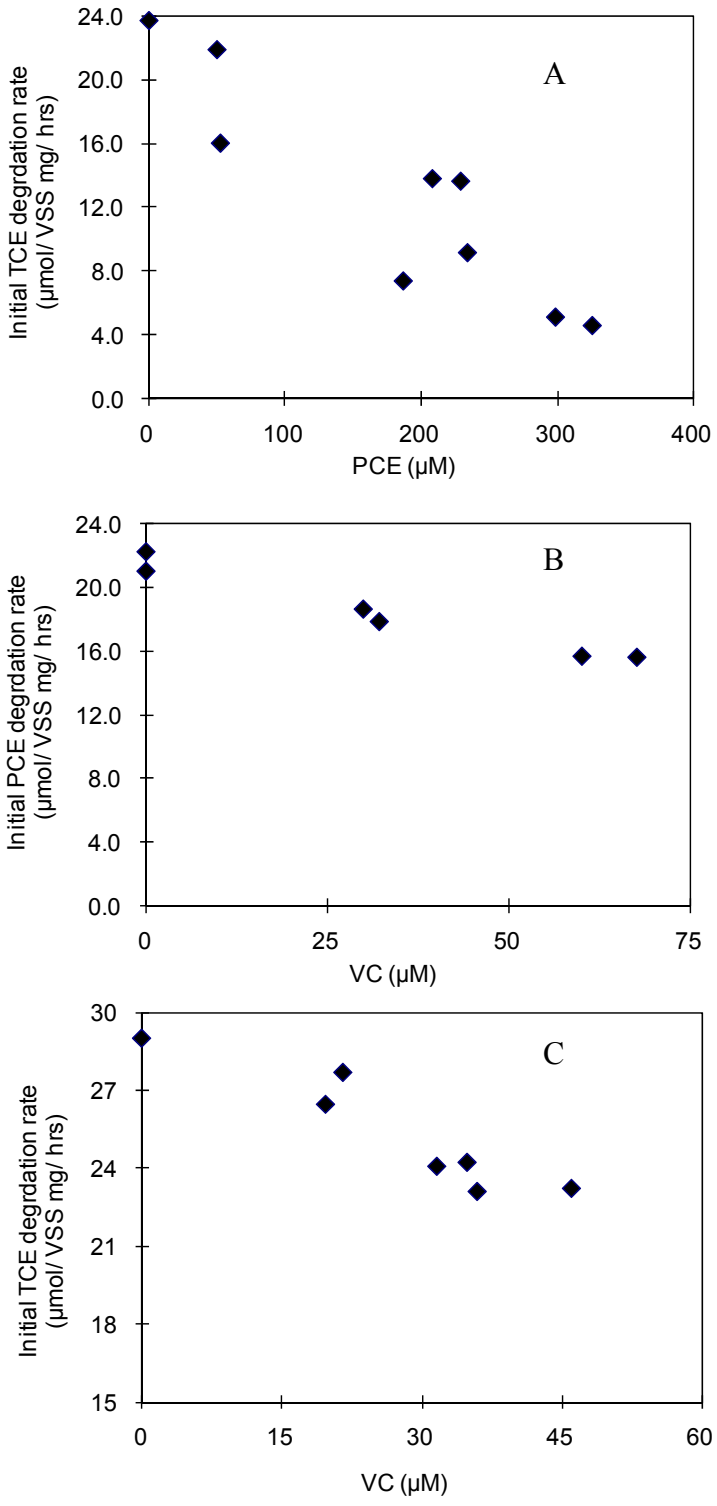

Figure 5.9 (A) Initial rates of dechlorination of TCE in the presence of different PCE concentrations; (B) PCE in the presence of different VC concentrations; and (C) TCE in the presence of different VC concentrations by *Dhb. restrictus*.

approximately 75 μM (Figure 5.10 D). Further increases in the TCE concentration had no apparent affect on the cDCE dechlorination rate. The rate of VC dechlorination by *Dhc. ethenogenes* also decreased substantially with increasing TCE or cDCE concentrations (Figure 5.10 E and F). VC dechlorination rates were negligible at TCE concentrations higher than 80 μM or cDCE concentrations higher than 170 μM during the first 5 h. K_{CI} values for each competitive inhibition effect were estimated, as summarized in Table 5.5. Previous studies that have evaluated the use of competitive inhibition models to describe dehalorespiration kinetics have generally assumed that K_{CI} equals K_S and did not independently estimate K_{CI} values (Yu et al., 2005; Cupples et al., 2004). Although modeling studies assuming K_{CI}=K_S generally fit the data well, it is not surprising that these assumed values are significantly different than the K_{CI} values determined experimentally in this study.

Table 5.5 Summary of K_{CI} estimates determined in this and previous studies involving dehalorespiration of chlorinated ethenes.

Inhibitor	Electron acceptor	*Dhc. ethenogenes*[1,2]	*Dhb. restrictus*[2]	*Dhc. sp.* strain VS[3]	Mixed culture containing *Dehalococcides*[4]
PCE	TCE	21.7	0.23		3.9
PCE	cDCE	55.1			
PCE	VC	9.6			
TCE	cDCE	10.7			2.8
TCE	VC	13			2.8
cDCE	VC	74.7		3.6	1.9
VC	cDCE			7.8	
VC	PCE		3.74		
VC	TCE		0.56		

[1] VC is transformed cometabolically by *Dhc. ethenogenes*; [2] This study; [3] Cupples et al., 2004. [4] Yu et al., 2005 and K_{CI} values were assumed to be equal to estimated K_S values.

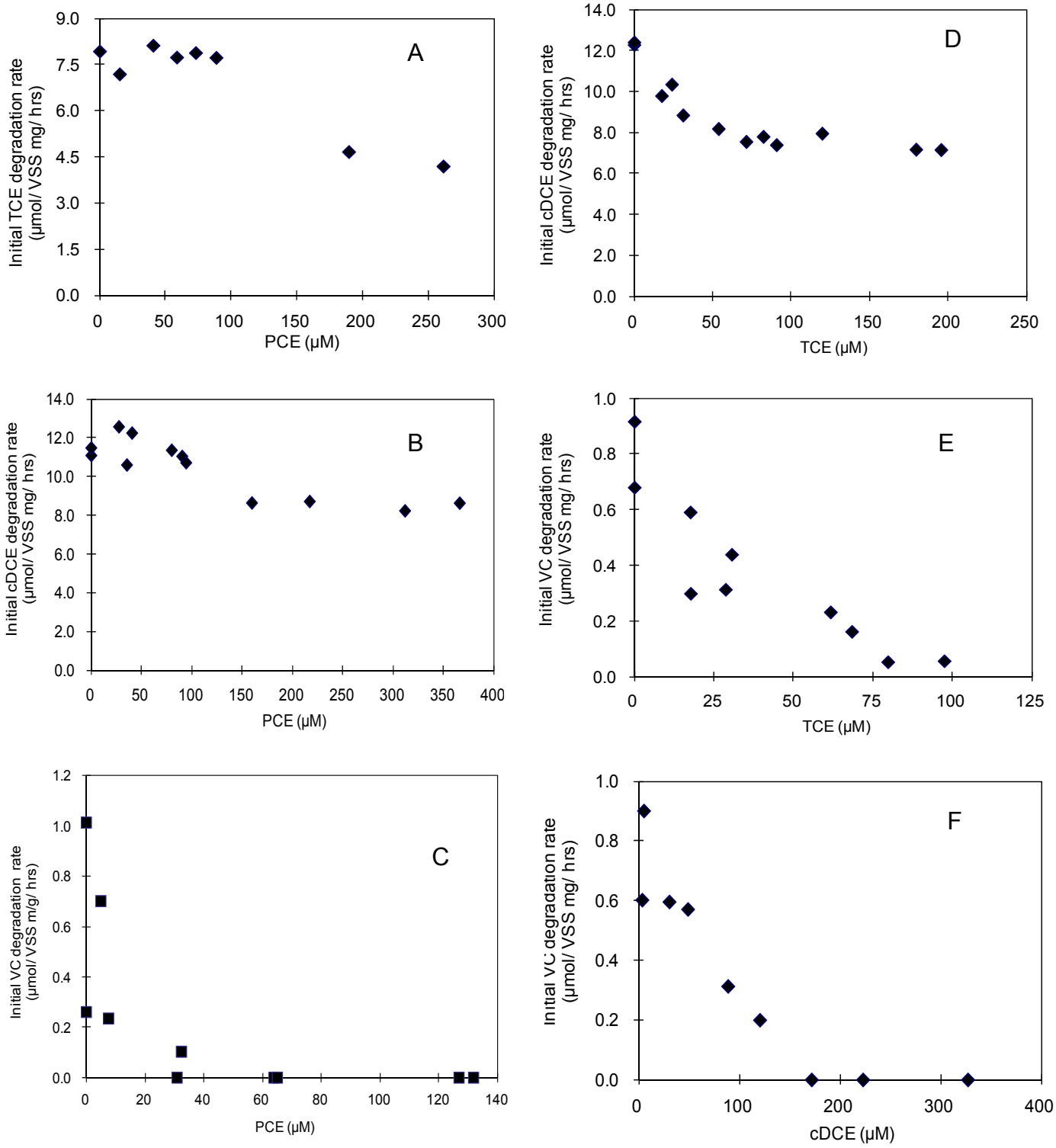

Figure 5.10 Initial dechlorination rates of (A) TCE in the presence of different PCE concentrations; (B) cDCE in the presence of different PCE concentrations; and (C) VC in the presence of different PCE concentrations; (D) cDCE in the presence of different TCE concentrations; (E) VC in the presence of different TCE concentrations; and (F) VC in the presence of different cDCE concentrations by *Dhc. ethenogenes*.

5.2.3 Conclusion and Implication

Competitive and self-inhibition effects on *Dhc. ethenogenes* and *Dhb. restrictus* were clearly observed in this study. In the competitive inhibition kinetics study, highly chlorinated ethenes negatively impacted dechlorination of the less chlorinated ethenes, which ultimately may slow down PCE detoxification. The inhibition effect of VC on PCE dechlorination by *Dhb. restrictus* could negate the competitive advantage it has due to its relatively fast PCE/TCE utilization rates when VC is present. This suggests that *Dhb. restrictus* would benefit from being cultured with a VC-respiring *Dehalococcoides* strains.

5.3 Carbon source effects on substrate utilization by *Dhc. ethenogenes* and *Dhb. restrictus*

5.3.1 Acetate availability effect on dechlorination

When hydrogen was provided in excess (> 0.6 mM H_2) and acetate was provided at initial concentrations ranging from 0.05 to 5 mM, *Dhc. ethenogenes* dechlorinated approximately 55 μM PCE within 12 days. However, dechlorination slowed substantially at an initial acetate concentration of 0.01 mM and stopped completely at 1.2 μM acetate (Figure 5.11A). These results are consistent with isotopomer and transcriptomic analyses, which showed that *Dhc. ethenogenes* assimilates CO_2 for the synthesis of cellular components but suggested that it is unable to grow autotrophically (Tang et al., 2009). In contrast, the initial acetate concentration did not have a clear impact on PCE dechlorination by *Dhb. restrictus*, which proceeded even at an initial acetate concentration of less than 0.45 μM (Figure 5.11B). This result was surpising because previous work indicated that provision of acetate as the carbon source, plus the amino acids arginine, histidine, and threonine, is required to sustain growth of *Dhb. restrictus* on hydrogen (the electron donor) and chlorinated ethene electron acceptors (Holliger et al., 1998). In the current study, peptone was provided as the source of amino acids. Peptone reportedly cannot replace acetate as the carbon source for *Dhb. restrictus* (Holliger et al., 1998). A β-hexachlorocyclohexane-dechlorinating culture that contains a *Dehalobacter* strain could grow on hydrogen without acetate (van Doesburg et al, 2005). However, a long lag period preceded dechlorination when acetate was not supplied, and the

Dehalobacter strain could carry out dechlorination only in co-culture with a *Sedimentbacter* strain that presumably provided it with essential growth factors.

In any case, the results shown in Figure 5.11 suggest that *Dhc. ethenogenes* and *Dhb. restrictus* respond very differently to acetate availability. These findings could have important implications for the implementation of bioremediation. If *Dhc. ethenogenes* is not able to effectively compete for acetate in the presence of acetotrophic dehalorespiring bacteria, e.g., *Desulfuromonas michiganensis*, *Geobacter lovleyi* and *Anaeromyxobacter dehalogenans* (Huang, 2009; Sung et al., 2006; He and Sanford, 2004), sulfate-reducing bacteria, or methanogens (Goevert and Conrad, 2008; Yang and McCarty, 1998), chlorinated ethene removal may be limited by the availability of acetate even where hydrogen is abundant. Although many studies have evaluated the importance of hydrogen thresholds in determining the competitiveness of hydrogenotrophic dehalorespiring bacteria, sulfate-reducing bacteria and methanogens (Kassenga et al., 2004; Luijten et al., 2004; Fennell and Gossett, 1998; Yang and McCarty, 1998), no prior studies have addressed the effects of acetate utilization and thresholds on the activity of hydrogenotrophic dehalorespiring bacteria. Importantly, these results demonstrate that the common engineered bioremediation approach of biosimulating *Dehalococcoides* populations by increasing the hydrogen supply may not be effective if acetate is deficient. On the other hand, increasing the hydrogen concentration could conceivably benefit *Dehalococcoides* populations not only by improving electron donor availability, but also by generating acetate through the activity of homoacetogens that synthesize acetate from hydrogen and carbon dioxide (He et al., 2002).

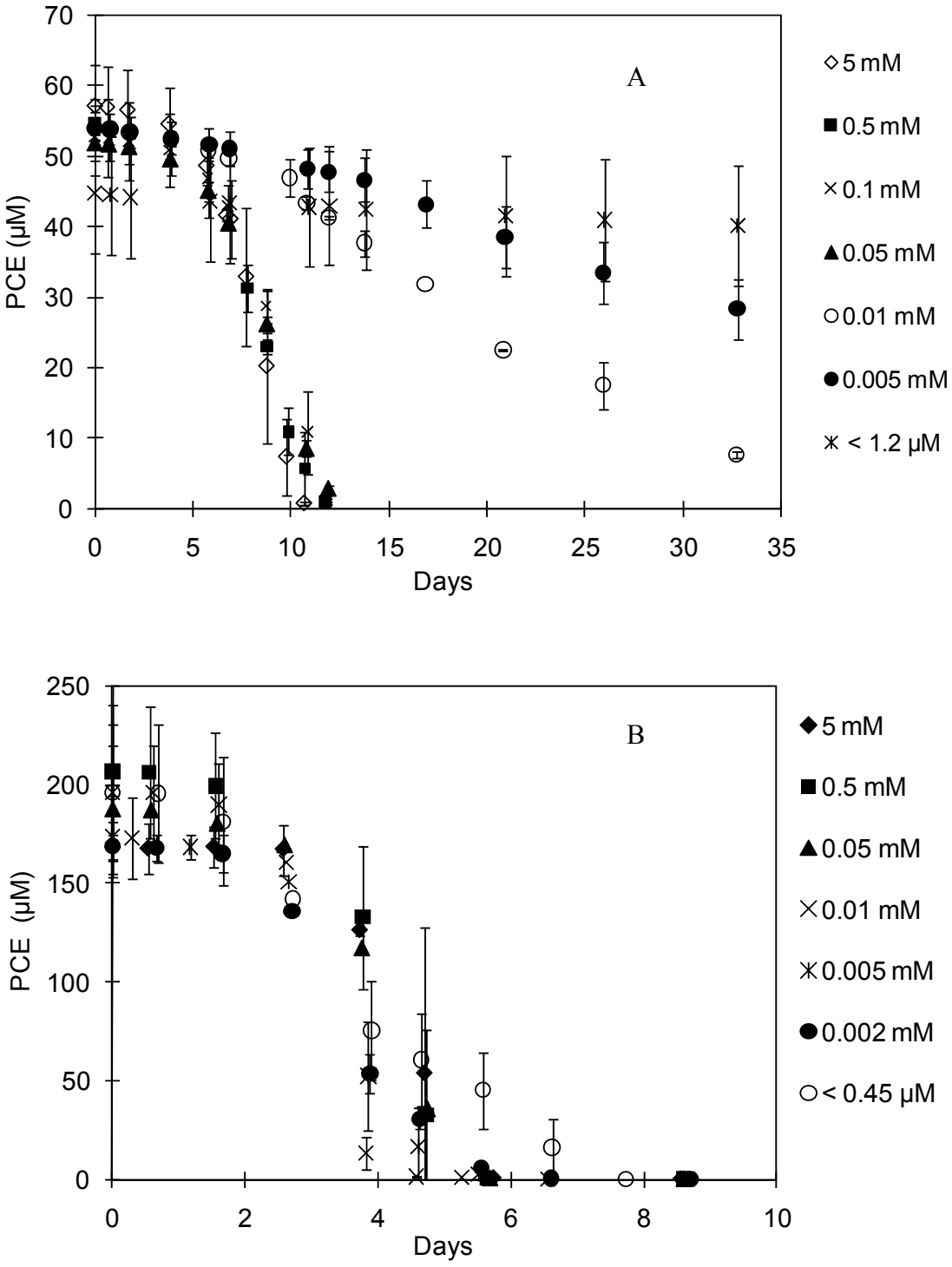

Figure 5.11 Effect of initial acetate concentrations from <0.45 to 5 mM on dechlorination by (A) *Dhc. ethenogenes* and (B) *Dhb. restrictus*. Error bars indicate the standard deviation about the average concentration for duplicate cultures.

The kinetic characteristics of a population, including the magnitude of $K_{s,\ acetate}$, are expected to play a key role in determining it ability to compete for acetate. The chlorinated ethene depletion curves obtained under acetate-limiting conditions (the three or four lowest acetate concentrations in Figure 5.11) were used to estimate $K_{S,\ acetate}$ and stoichiometric term Z for *Dhc. ethenogenes* and *Dhb. restrictus* by fitting Equation (4.18) to the chlorinated ethene data (Figure 5.11). The parameter estimates and goodness of fit values are summarized in Table 5.6.

The $K_{S,\ acetate}$ estimated for *Dhc. ethenogenes* and *Dhb. restrictus* are quite similar. However, the estimates of the stoichiometric term Z, which describe the amount of acetate consumed in relationship to chlorinated ethene utilization, differ by several orders of magnitude. The relatively high Z values estimated for *Dhc. ethenogenes* are consistent with its dependence on high acetate concentrations to sustain dechlorination. The very low values of Z estimated for *Dhb. restrictus* and the relatively poor fit of the model to the data (indicated by high SSE and low F values) support the idea that very little acetate was utilized during dechlorination under the conditions tested. It is possible that dechlorination was uncoupled from growth during the assays shown in Figures 5.11 and 5.12.

Table 5.6 Estimates of $K_{S,\ acetate}$ and Z and goodness of fit measures for *Dhc. ethenogenes* and *Dhb. restrictus*

	Dhc. ethenogenes			*Dhb. restrictus*			
Acetate (μM)	10	5	1.2	10	5	2	0.45
$K_{S,acetate}$ (μM)	1.59	2.82	1.52	2.06	2.34	1.09	0.19
Stoichiometric term (Z)	0.29	0.20	0.28	1.41×10^{-9}	5.70×10^{-9}	3.55×10^{-10}	2.30×10^{-3}
SSE (μM^2)	39.36	12.19	0.90	2701.4	1246.6	1061.8	898.89
F	246.48	330.15	91.73	59.37	126.33	130.31	222.28

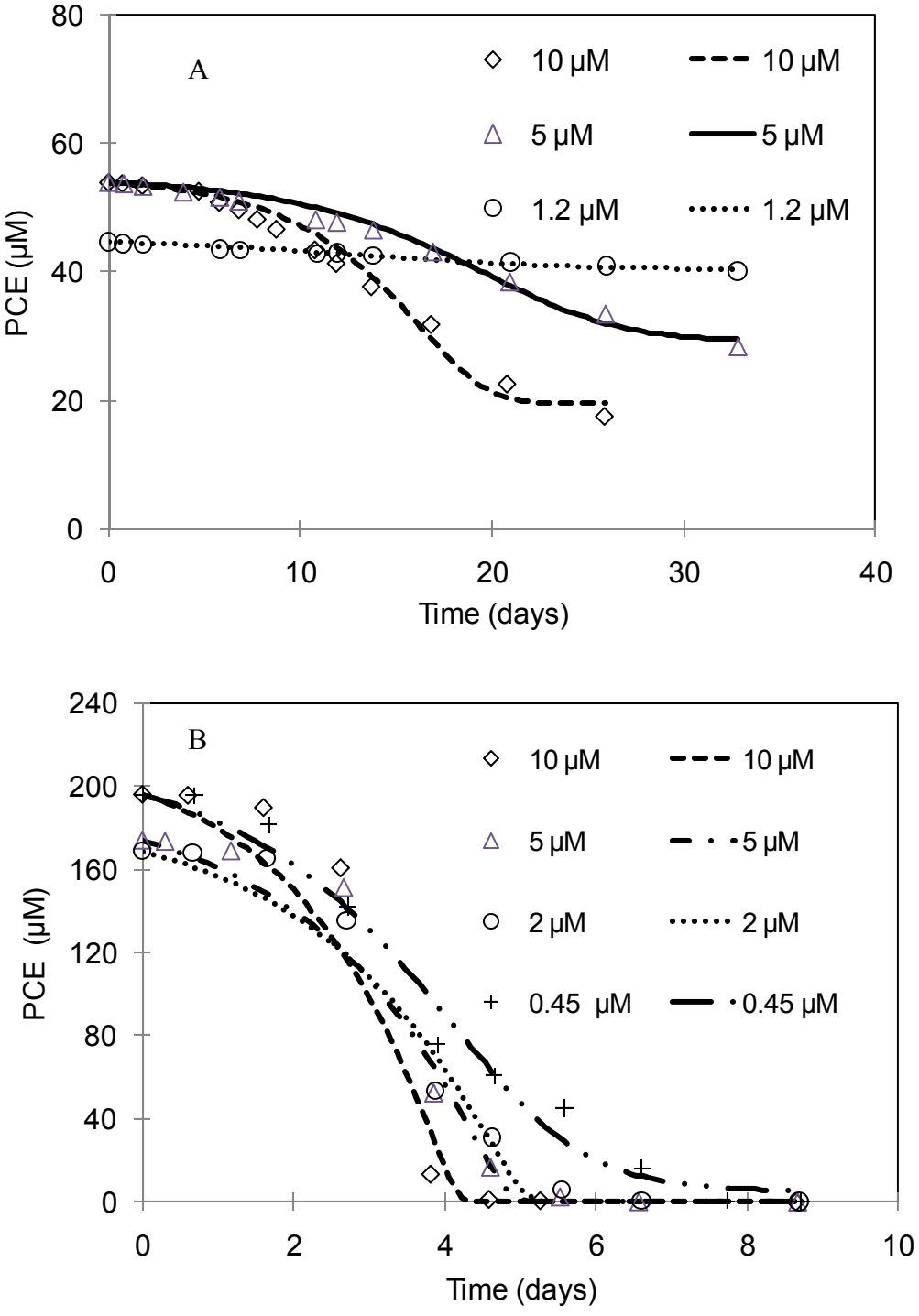

Figure 5.12 Model (Equation 4.18) fits used to estimate $K_{S,\text{ acetate}}$ and the stoichiometric coefficient Z for (A) *Dhc. ethenogenes* and (B) *Dhb. restrictus*. Data points represent the average concentrations shown in Figure 5.11. Lines represent the best model fits to the data.

5.3.2 Acetate utilization coupled with dehalorespiration

[^{14}C]Biomass increased concomitantly with the consumption of [^{14}C] acetate and dechlorination of PCE by *Dhc. ethenogenes* (Figure 5.13A), demonstrating that acetate is assimilated into the biomass of this organism. This result is consistent with the findings of other studies indicating that *Dhc. ethenogenes* requires acetate as a carbon source, e.g., Tang et al. (2009). Further, cDCE accumulated at low acetate concentrations (<0.8 μM) suggesting that dechlorination by *Dhc. ethenogenes* is not sustainable at low acetate concentrations.

Acetate (24 μM) was added to two of the *Dhc. ethenogenes* cultures at 160 hrs. Dechlorination of cDCE to VC in the acetate amended bottles proceeded very rapidly (Figure 5.14), confirming that dechlorination had been limited by acetate availability. In contrast, dechlorination of cDCE occurred much more slowly in the four bottles that did not receive additional acetate. Only 120 μM cDCE was transformed to VC between 160 and 550 hrs. This slow cDCE dechlorination process apparently was uncoupled from microbial growth, as has been previously observed for *Dhc. ethenogenes* (Johnson et al., 2008). In the current study, growth undoubtedly stopped due to the depletion of the carbon source acetate. However, other nutrient limitations and other mechanisms could cause dechlorination to become uncoupled from growth in other systems.

Assimilation of [^{14}C] acetate into biomass was also observed during dechlorination of PCE by *Dhb. restrictus* (Figure 5.13B). This was somewhat surprising because a previous experiment suggested that PCE dechlorination was not limited by low acetate concentrations (Figure 5.11B). Further, after 70 hrs, acetate levels were quite low (< 6 μM), yet a second dose of PCE (150 μM) was rapidly

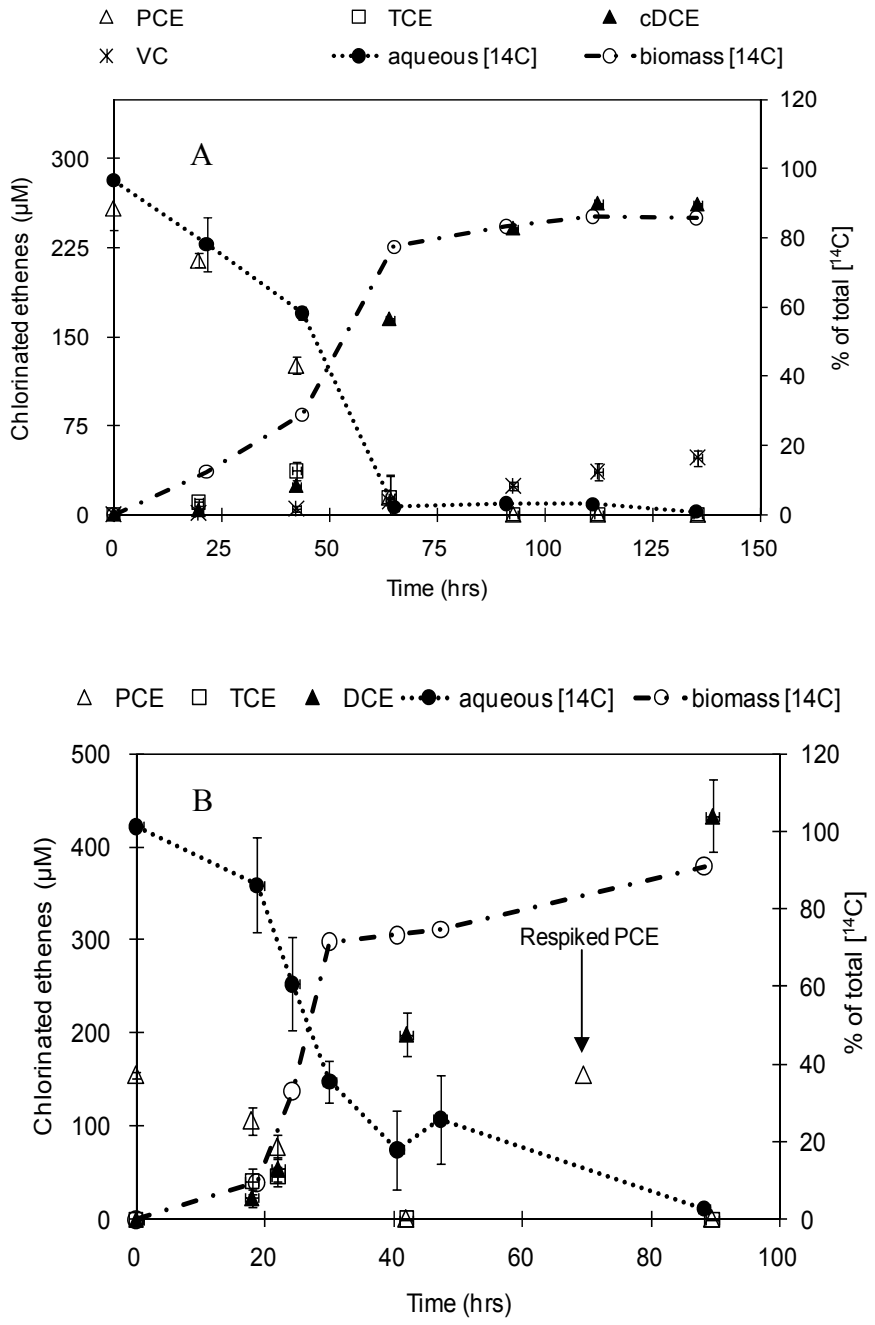

Figure 5.13 Assimilation of [^{14}C] acetate during PCE dechlorination by (A) *Dhc. ethenogenes* and (B) *Dhb. restrictus*. The cultures were initially provided with 3.3 mM H_2, 40 µmol (*Dhc. ethenogenes*) or 25 µmol (*Dhb. restrictus*) PCE, and 24 µM acetate. Chlorinated data points represent the average concentration in six (*Dhc. ethenogenes*) or five (*Dhb. restrictus*) replicates and error bars represent standard deviation. A second dose of PCE was added to *Dhb. restrictus* at 70 hrs.

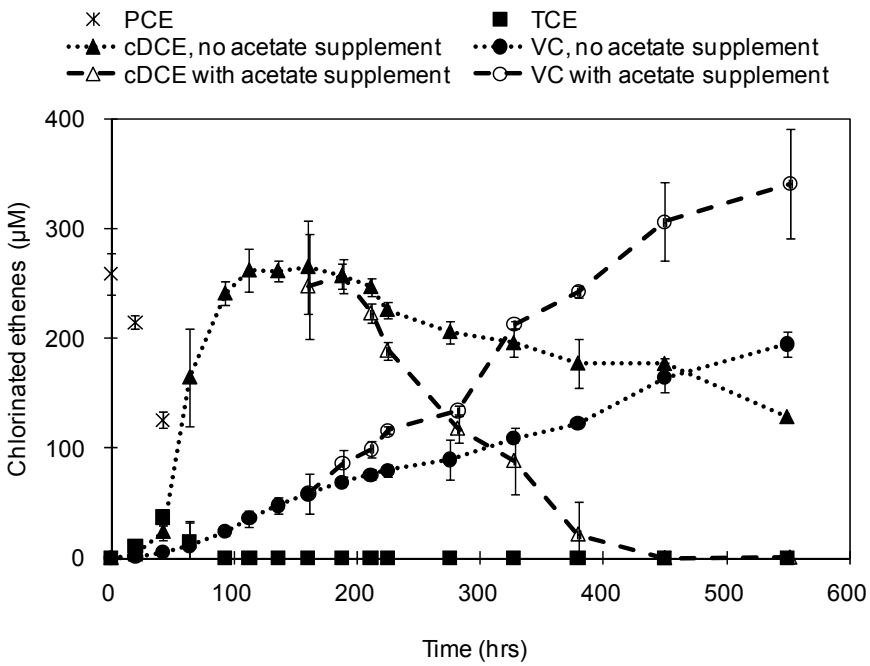

Figure 5.14 The effect of acetate on the long-term dechlorination of cDCE by acetate-limited *Dhc. ethenogenes* cultures. The first 130 hrs of data are shown in Figure 5.13A and were obtained using six replicates. At 160 hrs, acetate (24 µM) was added to two replicates. The other four replicates were not amended. The data points represent average concentrations in replicate cultures and the error bars represent standard deviation.

dechlorinated by *Dhb. restrictus* (Figure 5.13B). This finding also suggests that dechlorination by *Dhb. restrictus* does not require high acetate levels to sustain dechlorination, although acetate assimilation continued during dechlorination of the second PCE dose.

There are several potential explanations for the apparent discrepancies in how *Dhb. restrictus* responds to acetate. That is, dechlorination by *Dhb. restrictus* appears to be unafffected by acetate availability (Figure 5.11B); however, when acetate is available (at least at a concentration of ~24 µM), assimilation of acetate by *Dhb. restrictus* is observed (Figure 5.13B). One possible explanation is that acetate is in fact required for growth of *Dhb. restrictus*; however, dechlorination proceeded

uncoupled from growth when adequate acetate was not available. As described above, uncoupling of dechlorination and growth has been observed in *Dhc. ethenogenes* (Johnson et al., 2008; Tang et al., 2009) and other dehalorespiring strains. However, it seems likely that the rate of dechlorination that is uncoupled from growth would decrease over time and occur at a rate slower than a growth-linked process. Another related explanation is that *Dhb. restrictus* assimilate acetate without actually growing on this substrate. Total biomass measurements are needed to evaluate whether or not *Dhb. restrictus* grew concomitantly with acetate assimilation and PCE dechlorination, but were not obtained during the experiment shown in Figure 5.11B. Finally, it is possible that *Dhb. restrictus* has the potential to function as a mixtotroph by utilizing CO_2 and available acetate as carbon sources, and, when acetate is absent, *Dhb. restrictus* can grow using CO_2 plus key growth factors (provided by peptone in the current study). Such versatility in carbon metabolism has previously been observed. For example, environmental genomic analyses suggest that *Cenarchaeum symbiosum*, a marine crenarchaeote, can function as a strict autotroph or adopt a mixotrophic metabolism by using both carbon dioxide and organic carbon sources (Hallam et al., 2006).

Anaerobic bacteria frequently exhibit a threshold for an electron donor. A threshold is the minimum substrate concentration at which steady-state cellular growth can be maintained. Under many conditions, threshold concentrations appear to be thermodynamically controlled (Jackson and McInerney, 2002). Thus, if *Dhb. restrictus* can utilize different carbon sources, it is expected that it will exhibit different hydrogen thresholds for the different forms of carbon metabolism. Most

importantly, CO_2 is thermodynamically "expensive" as a carbon source because cells have to invest a large number of electrons to convert it to reduced cellular components (Rittmann and McCarty, 2001; McCarty, 1975). Thus, a relatively high hydrogen threshold is expected if *Dhb. restrictus* uses CO_2 as it primary carbon source. The hydrogen threshold for *Dhb. restrictus* growing on acetate as the carbon source is expected to be lower because acetate is more reduced compared with CO_2. Therefore, an experiment was conducted to evaluate the effect of different carbon sources on hydrogen thresholds in *Dhb. restrictus* as well as *Dhc. ethenogenes*.

Hydrogen concentrations were monitored until a threshold concentration was reached in cultures that were provided with high (6 mM) or low (24 μM) acetate levels. In *Dhc. ethenogenes*, the hydrogen thresholds did not appear to be affected by the dominant carbon source and ranged from 4 to 10 nM under all of the conditions tested (Figure 5.15A). Several steps were taken to ensure that these levels truly represent hydrogen thresholds and are not controlled directly by acetate availability. First, acetate (20 μM) was re-supplied to duplicate low acetate cultures at approximately 115 hrs. Hydrogen levels were not appreciably lower in the bottles that received this additional acetate dose compared to those that received a low acetate dose at time zero only. In addition, analysis of [^{14}C] acetate was performed at 750 hrs to confirm that acetate was not completely depleted in the low acetate cultures. Total acetate concentrations of 11.7 and 1.1 μM were detected in the bottles that were and were not re-supplied with acetate, respectively. The hydrogen thresholds measured in the current study are also of the same magnitude as those

estimated for *Dehalococcoides*-containing cultures in other studies (Fennell and Gossett, 1998; Yang and McCarty, 1998; Smatlak et al. 1996).

In contrast to *Dhc. ethenogenes*, very different hydrogen threshold levels, approximately 425 nM and 25 nM, were observed when *Dhb. restrictus* was supplied with low or high acetate doses, respectively (Figure 5.15B). Hydrogen levels did not decrease substantially when a second dose of acetate (20 μM) was supplied at 115 hrs and at 380 hrs, 18.7 and 1.5 μM acetate remained in the low acetate cultures that were and were not reamended with acetate, respectively, suggesting that the differences in the hydrogen levels observed were largely due to the dominant carbon source provided to *Dhb. restrictus*. Further, dechlorination in cultures that had reached a hydrogen threshold resumed when additional hydrogen was added (data not shown).

The hydrogen threshold measured for *Dhb. restrictus* with 6 mM acetate in this study was orders of magnitude higher than the thresholds measured for other dehalorespirers (Table 5.2). The results of the current study suggest that the concentration of the carbon source and, for organisms that have different forms of carbon metabolism, the nature of the carbon source, may affect the magnitude of measured hydrogen thresholds. Thus, hydrogen thresholds measured under different experimental conditions may not be directly comparable.

On the other hand, acetate thresholds have also been evaluated because of their potential role in determining the outcome of competition between acetate-oxidizing and other dehalorespiring bacteria (Huang and Becker, 2009; Supida, 2007; Hori et al., 2007; Sung et al., 2006; He and Sanford, 2004; Jetten al., 1992; Westermann et al., 1989). Acetate thresholds for mixotrophic dehalorespiring

bacteria, e.g., *Dhc. ethenogenes,* have not been well studied. However, the current study demonstrates that dehalorespiration by *Dhc. ethenogenes* is negatively impacted at 10 μM acetate. The acetate thresholds summarized in Table 5.7 for heterotrophic dehalorespiring bacteria and acetotrophic methanogens are generally less than 10 μM. Thus, *Dhc. ethenogenes* may not be able to compete effectively with these populations at low acetate concentrations, and this in turn may limit its ability to compete for chlorinated ethenes, despite its strong affinity for hydrogen.

Table 5.7 Acetate threshold levels observed in different microorganisms

Terminal electron accepting process	Organism	$S_{acetate,\ threshold}$ (nM)
Dehalorespiration / Fe(III) reduction[1]	*Anaeromyxobacter dehalogenans*	69 ± 4 /19 ± 8
Dehalorespiration[2]	*Geobacter lovleyi*	3
Fe(III) reduction[3]	*Geobacter metallireducens*	111
Dehalorespiration[4]	*Desulfuromonas michiganensis*	410
Methanogenesis[5]	*Methanothrix soehngenii*	7,000-69,000
Methanogenesis[6]	Aceticlastic methanogens	69-1,180

[1] He and Sanford (2004); [2] Sung et al., 2006; [3] Supida, 2007; [4] Huang and Becker, 2009; [5] Jetten et al., (1992); [6] Westermann et al., 1989.

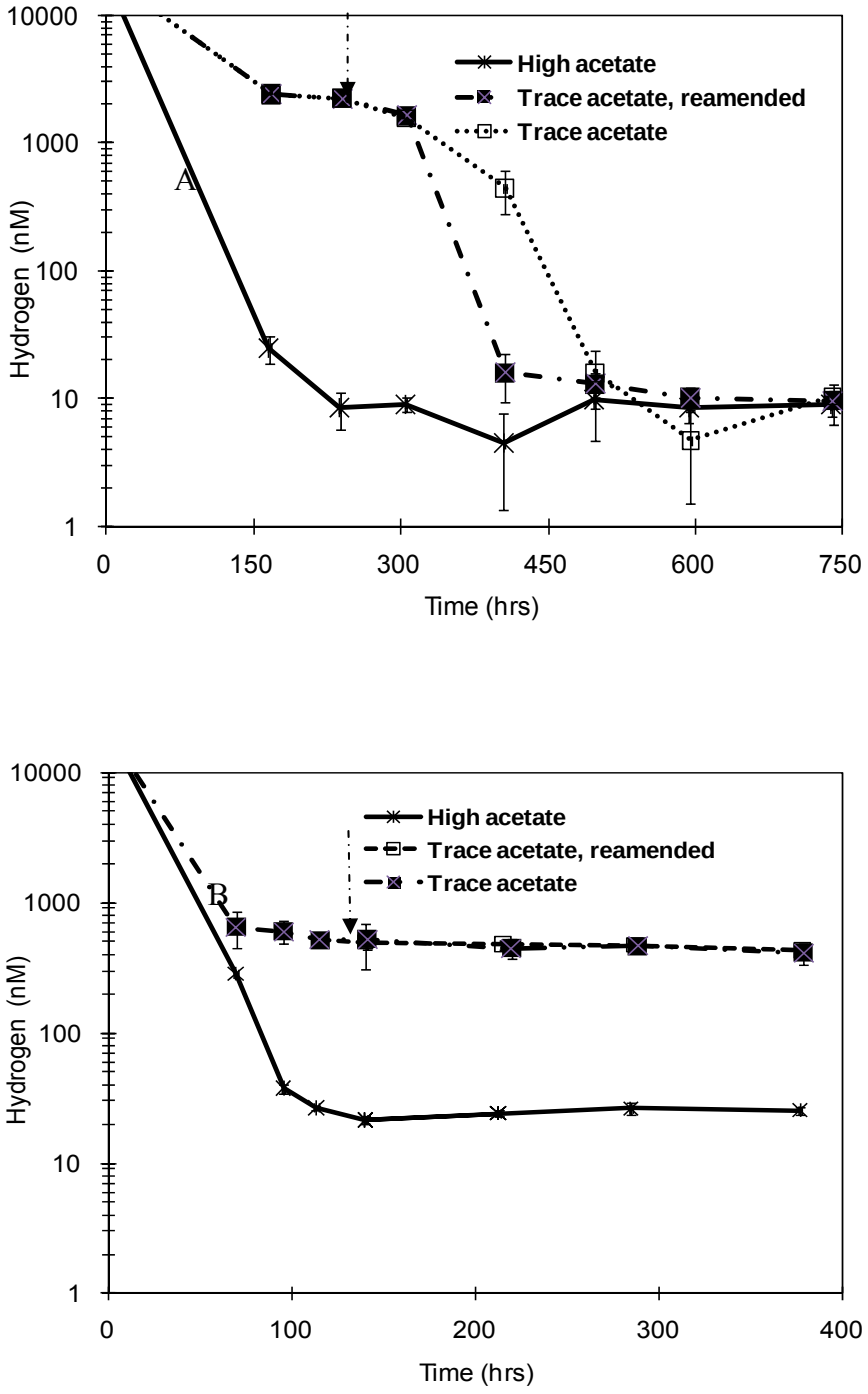

Figure 5.15 The effects of primary carbon source on hydrogen utilization and thresholds in (A) *Dhc. ethenogenes* and (B) *Dhb. restrictus* provided with excess PCE. Duplicate cultures obtained 6 mM acetate and four cultures received trace amounts of acetate (24 µM). Two of the low acetate cultures were reamended with 20 µM (indicated by the arrow).

5.3.3 Conclusions and Implications

The ability of dehalorespiring bacteria to compete for electron donors and electron acceptors has been a concern for some time. However, the importance of the availability of a carbon source for hydrogenotrophic dehalorespiring bacteria has not been well studied. The current study demonstrates that carbon source availability should not be neglected because of its potential effects on dehalorespiration kinetics and hydrogen thresholds. Without considering these carbon source effects, the ability of hydrogentrophic bacteria like *Dhc. ethenogenes* to compete for substrates and carry out dehalorespiration may be overestimated.

5.4 Experimental and mathematical evaluation of interactions between *Dehalococcoides ethenogenes* and *Dehalobacter restrictus*

The overall goal of this project was to integrate experimental and mathematical evaluations to improve our understanding of the substrate interactions among dehalorespiring bacteria so that this information can be applied to improve the implementation of bioremediation in the field. The interactions between *Dhc. ethenogenes* and *Dhb. restrictus* were experimentally evaluated under two sets of conditions in a CSTR inoculated with the two strains. The two sets of conditions corresponded to two common biomediation treatment scenarios—natural attenuation and an engineered bioremediation approach known as biostimulation. The application of biostimulation to bioremediate chlorinated ethene contamination involves increasing the supply of electron donors that are used to sustain the chlorinated ethene-respiring bacteria. Dehalorespiration by *Dhc. ethenogenes* was simulated using the multiple Monod model incorporating inhibition terms and acetate utilization (Equations 4.20—4.24), while PCE and TCE respiration by *Dhb. restrictus* was modeled using a dual Monod model that does not include an acetate uptake term but does incorporate chlorinated ethene inhibition terms (Equations 4.25 and 4.26). Biomass and hydrogen utilization by both organisms were modeled using Equations 4.27 and 4.28, respectively. The kinetic parameter inputs to the model were obtained as part of this study (Sections 5.1 and 5.3). The results of the experimental and modeling evaluations and their implications for bioremediation practice are discussed in this section.

5.4.1 Chlorinated ethene transformation by the co-culture under engineered bioremediation

In the engineered bioremediation scenario, excess electron donor (~600 μM H_2) and carbon source (5000 μM acetate) were provided to ensure that the electron acceptor (15 μM PCE) was limiting. As shown in Figure 5.16, the duplicate bioreactors performed similarly after reaching steady-state phase (> 5 days). The steady-state concentrations of PCE, TCE, and cDCE were all less than 1 μM. VC was the major product throughout the experiment, and the average aqueous VC concentration was 15 μM during the steady-state period. Ethene was not detected until day 20, but the ethene concentration never exceeded 0.9 μM. VC also accumulated in a similar experiment involving a co-culture of *Dhc. ethenogenes* and *Dsm. michiganensis* that was conducted as part of the larger study (Huang, 2009). VC accumulation in this earlier experiment was ascribed to the kinetics of VC transformation, which is a cometabolic process (Maymó-Gatell et al., 1999; 2001), and is much slower compared with the dechlorination of chlorinated ethenes that serve as growth substrates (Table 5.8).

During the steady-state period of bioreactor operation, biomass growth is restricted by substrate availability, and extant kinetic parameter estimates must be used to predict microbial activity. However, the chorinated ethene concentrations changed rapidly during the bioreactor start-up phase—the first few days of operation—before eventually leveling out and reaching a steady-state (Figure 5.16). As discussed by Huang (2009), the amount of substrate available is high relative to the amount of biomass during the startup period. Under these conditions, biomass growth is unrestricted and microbial activity is best described using intrinsic kinetic

Table 5.8 Model inputs for *Dhb. restrictus* and *Dhc. ethenogenes* used to simulate activity in the CSTRs under natural attenuation and engineered bioremediation conditions

		Dhb. restrictus	*Dhc. ethenogenes*
Y (mg VSS/μmol Cl^-)		0.0044 [a]	0.0047 [a]
Intrinsic	q_{max} (μmol/mg VSS h^{-1})		
	PCE	22.48	6.76
	TCE	29.77	7.93
	DCE		13.15
	VC		0.89 [b]
	K_S (μM)		
	PCE	7.15	21.45
	TCE	1.30	29.02
	cDCE		33.61
	VC		637 [b]
Extant	q_{max} (μmol/mg VSS h^{-1})		
	PCE	12.77	3.41
	TCE	22.10	3.44
	DCE		6.59
	VC		0.45 [c]
	K_S (μM)		
	PCE	4.91	0.97
	TCE	3.86	2.25
	DCE		4.61
	VC		28.8 [c]
Electron donors	K_S (μM)		
	Acetate		1.9 [d]
	H_2	3.30 [a]	0.03 [a]
	Threshold (μM)		
	H_2	0.5 [e]/0.027 [f]	0.006 [e, f]
	k_d (h^{-1})	0.001[g]	0.001[g]

[a] Values were estimated under intrinsic conditions; [b] Values were calculated based on extant kinetic estimated approach without growth term for cometabolism; [c] Values were calculated based on the ratio of $q_{max, VC}/q_{max, PCE}$ or $K_{S, VC}/K_{S, PCE}$ obtained under intrinsic conditions; [d] Values were based on batch experiments conducted under various acetate availiability (Section 5.3); [e] Values were based on batch experiments conducted under trace acetate (24 μM) for natural bioremediation (Section 5.3); [f] Values were based on batch experiments conducted under high acetate (6 mM) for engineered bioremediation (Section 5.3); [g] Value was adopted based on Fennell and Gossett, 1998.

parameters. Therefore, in the current study, the ability of the mathematical model to describe the experimental data using only extant kinetic parameter inputs (Figure 5.17A) and a combination of intrinsic and extant kinetic parameter inputs (Figure 5.17B) was compared. Intrinsic kinetic parameter inputs were used to simulate reactor performance from day 0 to day 2, because the PCE was almost completely dechlorinated to cDCE within this period, indicating that the S_0/X_0 ratio became relatively small and unrestricted microbial growth was not feasible after 2 days. Extant kinetic parameter inputs were used to simulate the remaining data. The combination of intrinsic and extant kinetic parameters captured the experimental data better during the start-up phase, especially the cDCE depletion curve.

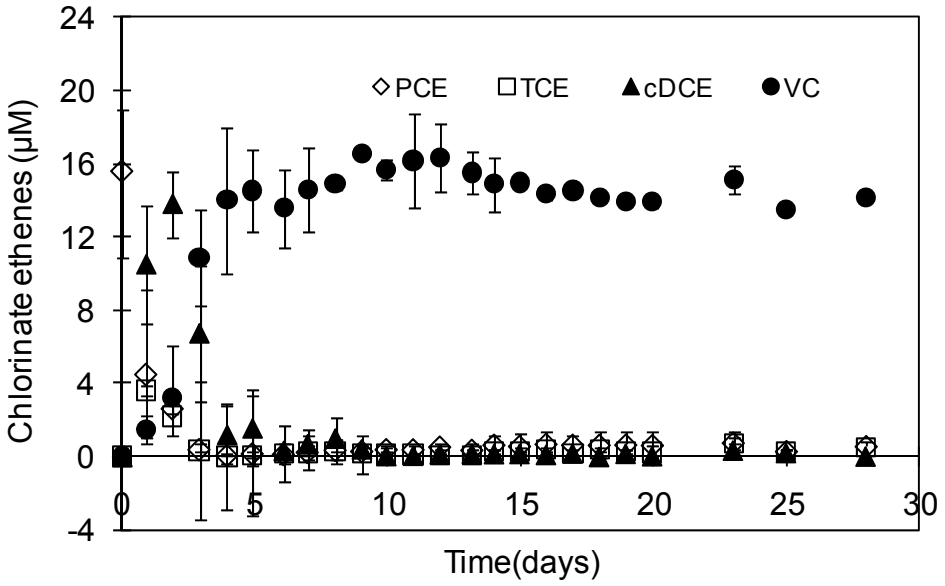

Figure 5.16 Duplicate chlorinated ethene concentrations under engineered bioremediation conditions in duplicate reactors containing a defined co-culture of *Dhc. ethenogenes* and *Dhb. restrictus*. The error bars represent the standard deviation of the concentrations in the duplicate reactors.

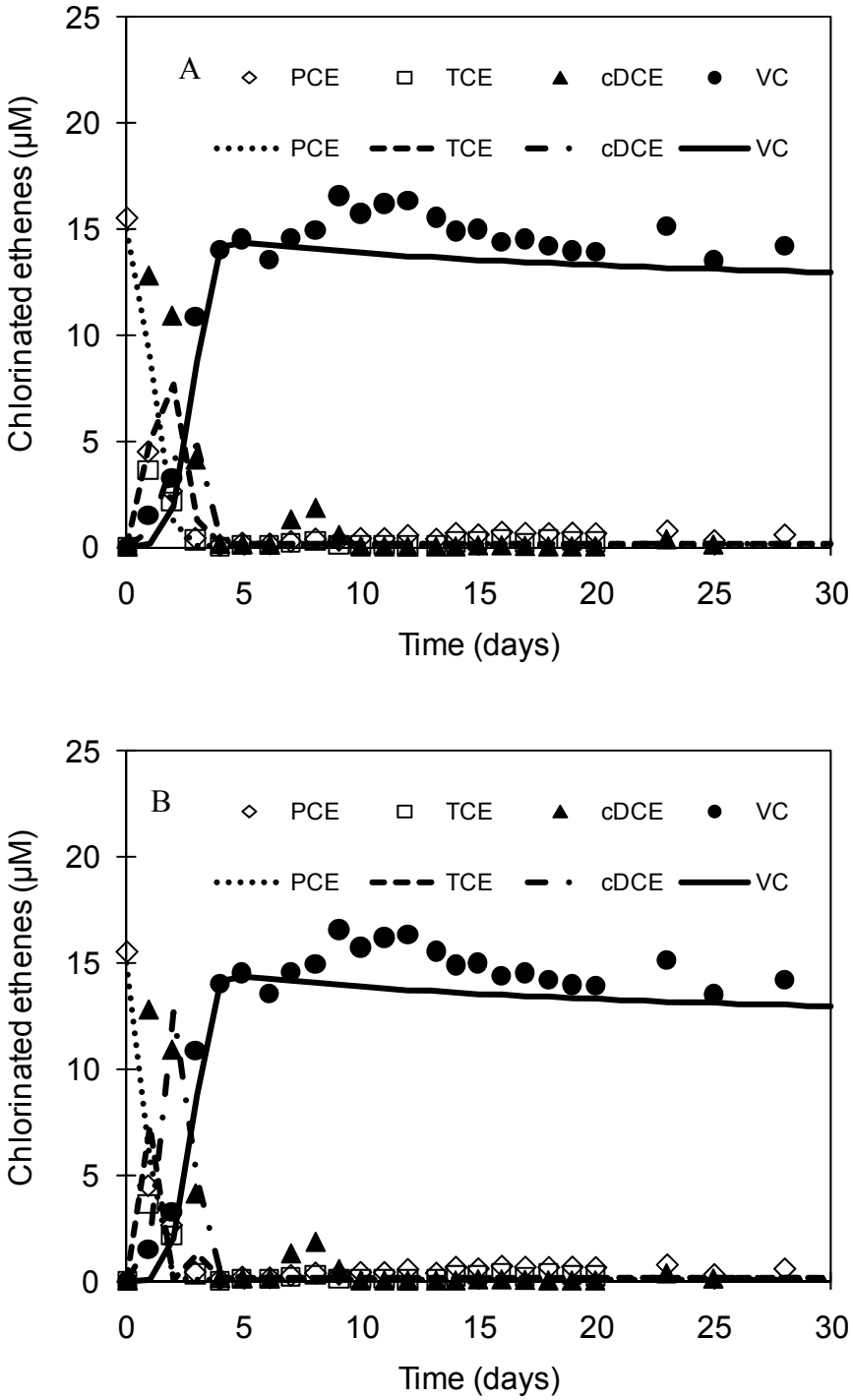

Figure 5.17 Comparison of model predictions (lines) and experimental results (points) of chlorinated ethene concentrations in the co-culture of *Dhc. ethenogenes* and *Dhb.restrictus* under engineered bioremediation conditions using (A) extant kinetic parameter inputs only; and (B) a combination of intrinsic kinetic parameter inputs for days 0-2 and extant kinetic parameters inputs for > 2 d.

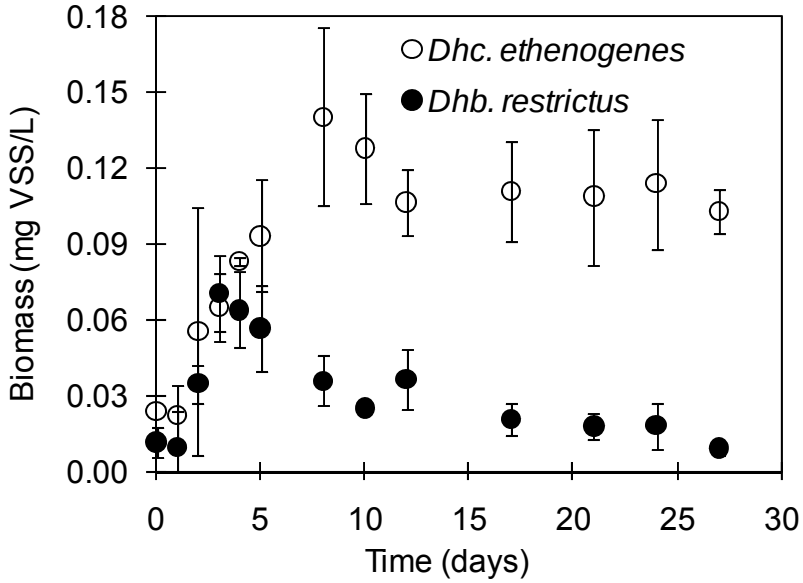

Figure 5.18 Biomass concentrations of *Dhc. ethenogenes* and *Dhb. restrictus* under engineered bioremediation conditions. Biomass concentrations were calculated based on gene copy numbers quantified with real-time PCR, assuming one 16S rRNA gene copy/cell and a cell mass of 1.6×10^{-14} g VSS/cell.

5.4.2 Biomass growth in the co-culture under engineered bioremediation conditions

The biomass concentrations of the two populations in the bioreactor were estimated based on 16S rRNA gene copy numbers (Figure 5.18). Both populations grew rapidly within the first 3 days. After day 3, *Dhc. ethenogenes* kept growing until it

leveled off on day 10 at a steady state concentration of approximately 0.11 mg VSS/L. In contrast, the concentration of *Dhb. restrictus* decreased at a relatively high rate between days 3 and 10 and then continued to decline more gradually for the remainder of the experiment. When compared to the chlorinated ethene levels, which did not change substantially after five days, the population shifts that occurred between days 5 and 10 demonstrate that the structure of dechlorinating cultures was

dynamic, even during periods of consistent chlorinated ethene removal. These results highlight one of the advantages of maintaining multiple dehalorespiring bacteria within a dechlorinating culture. If one population becomes inhibited or limited by substrate availability, dechlorination may be sustained by a population with different characteristics. In the engineered bioremediation experiment, it is likely that *Dhb. restrictus* grew rapidly on PCE and TCE, but *Dhc. ethenogenes* transformed increasing fractions of the PCE and TCE as the *Dhb. restrictus* population declined in the CSTRs.

The steady-state *Dhc. ethenogenes* biomass concentration was approximately four times greater compared with the levels of *Dhb. restrictus* biomass during this period. In contrast, the modeling results shown in Figure 5.19A predicted that the ratio of *Dhc. ethenogenes* to *Dhb. restrictus* biomass would range from approximately 1.1 to 1.8 from day 5 to day 30. These results suggested that the dual Monod model of dehalorespiration was not capturing some phenomenon that was limiting *Dhb. restrictus*' ability to carry out dehalorespiration. As described in Section 5.2, competitive inhibition constants were estimated for *Dhb. restrictus* and *Dhc. ethenogenes* as part of the current study. When the competitive inhibition terms were incorporated into the mathematical model, it provided a much better fit to the biomass data (Figure 5.19B) compared with the dual Monod model without competitive inhibition (Figure 5.19A). Presumably, inhibition of *Dhb. restrictus* was primarily due to VC, which accumulated to relatively high levels (15 μM) in the CSTRs. The steady-state concentrations of the other chlorinated ethenes were less than 1 μM, and the inhibition studies showed that dechlorination, especially of TCE,

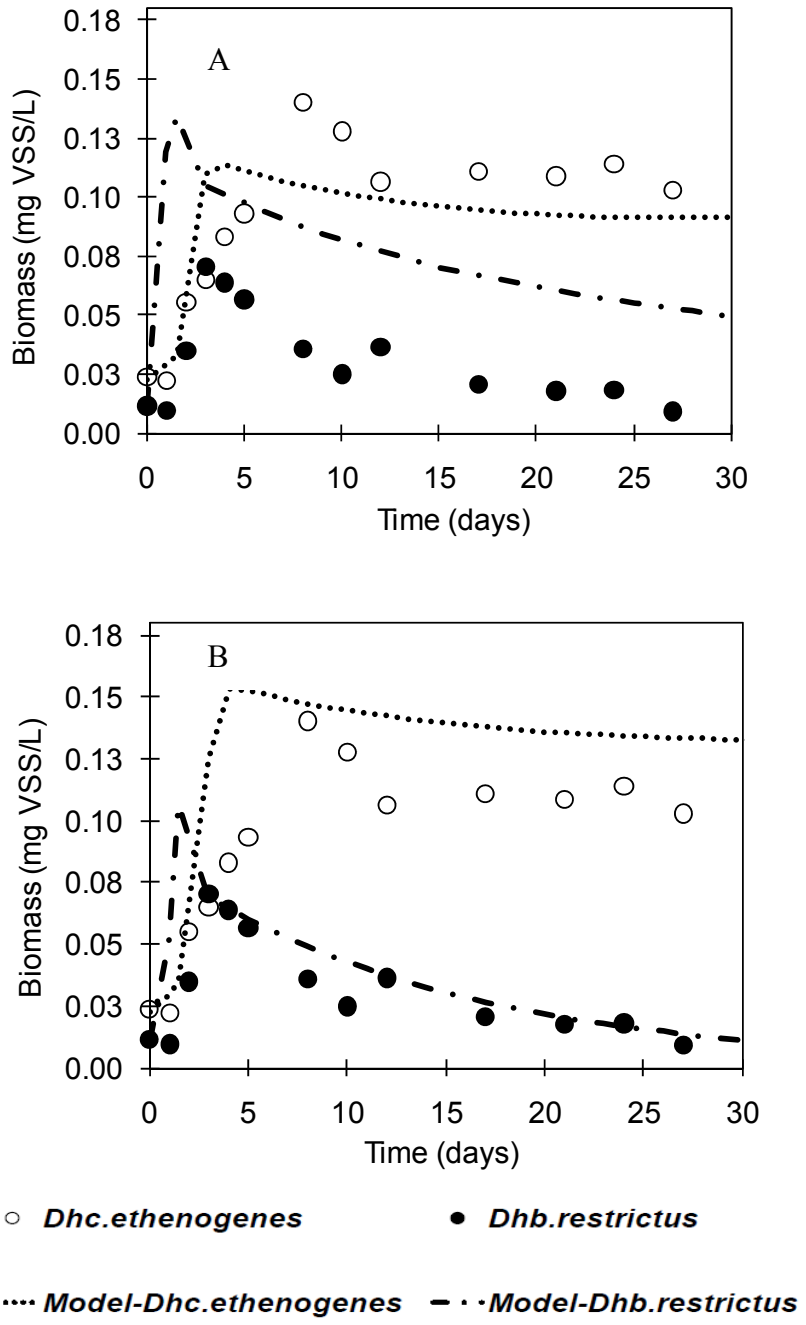

Figure 5.19 Comparison of predicted and measured biomass concentrations in a co-culture of *Dhc. ethenogenes* and *Dhb. restrictus* under engineered bioremediation conditions. (A) Concentrations predicted by a model that does not incorporate competitive inhibition terms. (B) Concentrations predicted using a model that does incorporate competitive terms. A combination of intrinsic (days 0-2) and extant (> 2 d) kinetic parameter inputs (Table 5. 8) were used in the model simulations.

was sensitive to VC. This finding could offer one explanation as to why *Dhb. restrictus* was out competed in a column that was inoculated with a culture that also contained a *Dehalococcoides* spp. and *Geobacter lovleyi* strain SZ (Amos et al., 2009). *Dhb. restrictus* was capable of faster substrate utilization rates but was very sensitive to the toxicity of VC according to the K_{CI} values estimated in this previous study. *Dhb. restrictus* has a number of desirable characteristics. It has relatively fast dechlorination kinetics and apparently has relatively low requirements for acetate. *Dehalobacter* strains are also desirable because of their ability to respire halogenated ethanes, which often occur as co-contaminants with chlorinated ethenes (Grostern et al., 2009; Grostern and Edwards, 2006a; Grostern and Edwards, 2006b). Thus, from the application standpoint, it would be beneficial to be able to sustain *Dhb. restrictus*, as well as *Dehalococcoides* strains, at sites where bioremediation is being implemented. Based on the results of the current study, it seems likely that this can be accomplished only if VC can be maintained at a low level, for example, by an organism that transforms VC metabolically at a relatively high rate that prevents VC from accumulating (e.g., *Dehalococcoides* strains BAV1, VS or GT (He et al., 2003 and Cupple et al., 2004; Sung et al., 2006).

5.4.3 Chlorinated ethene transformation by the co-culture under natural attenuation (low electron donor and carbon source) conditions

In the natural attenuation scenario, limiting amounts of H_2 (~10 μM) and acetate (~8 μM) were provided relative to the influent PCE concentration (15 μM) As shown in Figure 5.20, the duplicate bioreactors performed similarly. Initially, a modest drop in the PCE concentration was observed, and TCE, cDCE, and VC were produced concomitantly. However, after two days, the concentrations of all of the

chlorinated ethenes leveled off at the following concentrations: PCE, 12.5 μM; TCE, ~3 μM; cDCE, 1 μM; and VC, <0.1 μM.

5.4.4 Hydrogen and acetate consumption by the defined co-culture under natural attenuation conditions

As shown in Figure 5.21, the acetate level remained fairly constant (~8 μM) throughout the experiment, indicating that very little acetate was consumed by the two populations. The hydrogen level dropped rather quickly at the beginning of the

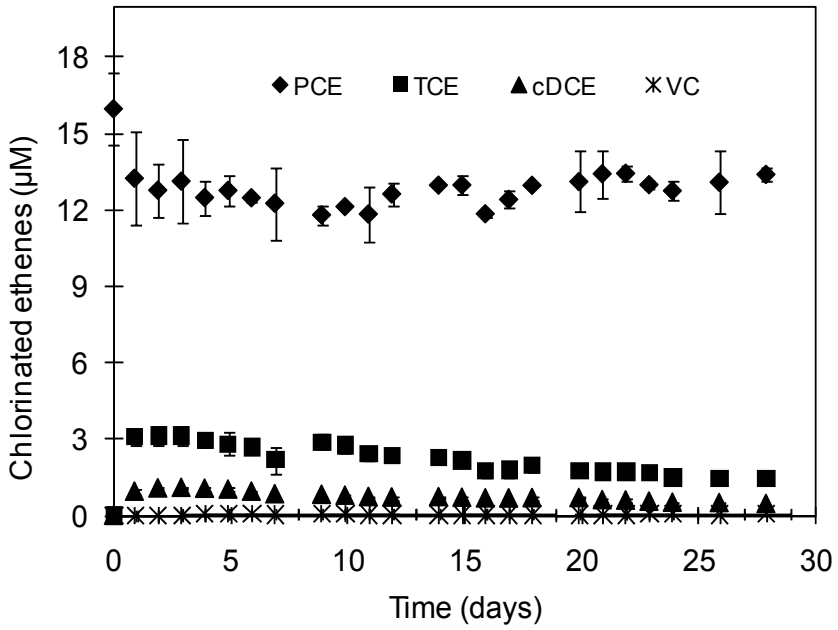

Figure 5.20 Duplicate chlorinated ethene concentrations under natural attenuation conditions in the CSTRs containing defined co-cultures of *Dhc. ethenogenes* and *Dhb. restrictus*. The error bars represent the standard deviation of the concentrations in samples from the duplicate reactors.

experiment—paralleling the initial decrease in PCE concentrations--and then leveled off at approximately 5.5 μM between days 3 and 12. After day 12, hydrogen increased slightly over time to 7.5 μM on day 28. According to CSTR theory, the effluent concentration of the limiting substrate is a function of the kinetic parameter values and reactor solids retention time (θ_x), according to

$$S = \frac{Ks(1+\theta_x k_d)}{\theta_x (Yq_{\max} - k_d) - 1} \tag{5.1}$$

Using the extant kinetic parameters summarized in Table 5.8 and Equation 5.1, the estimated effluent hydrogen levels for the individual cultures were 0.002 and 0.042 μM for *Dhc. ethenogenes* and *Dhb. restrictus*, respectively. Thus, the experimental hydrogen concentration was two to three orders of magnitude higher than predicted by the single Monod equation. The constant acetate levels and only 3-5 μM H_2 utilization throughout the experiment did not provide much insightful information that could be used to determine which population dominated.

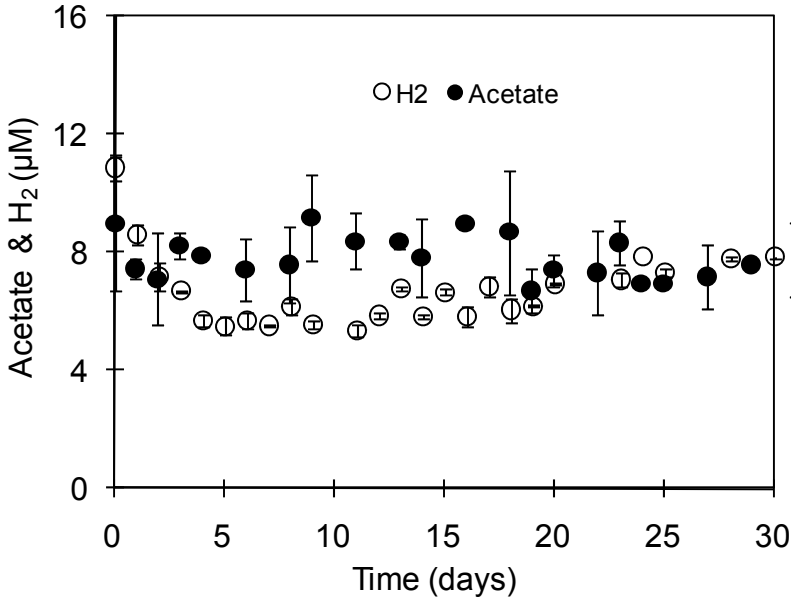

Figure 5.21 Duplicate H_2 and acetate concentrations under natural attenuation conditions in the CSTRs containing a defined co-culture of *Dhc. ethenogenes* and *Dhb. restrictus*. The error bars represent the standard deviation of the concentrations in samples from the duplicate reactors.

5.4.5 Biomass growth in the co-culture under natural attenuation conditions

The converted biomass concentrations of the two populations are shown in Figure 5.22. *Dhb. restrictus* grew rapidly in the very beginning of the experiment,

but its biomass concentration gradually dropped from 0.05 to 0.02 mgVSS /L during the experimental period. *Dhc. ethenogenes* did not have a sharp growth peak in the beginning of the experiment, and its biomass concentration was consistently below 0.01 mgVSS /L. Clearly, conditions in the CSTR were not conducive to growth of *Dhc. ethenogenes*, but it is also not clear whether long-term survival of *Dhb. restrictus* would be possible under these conditions.

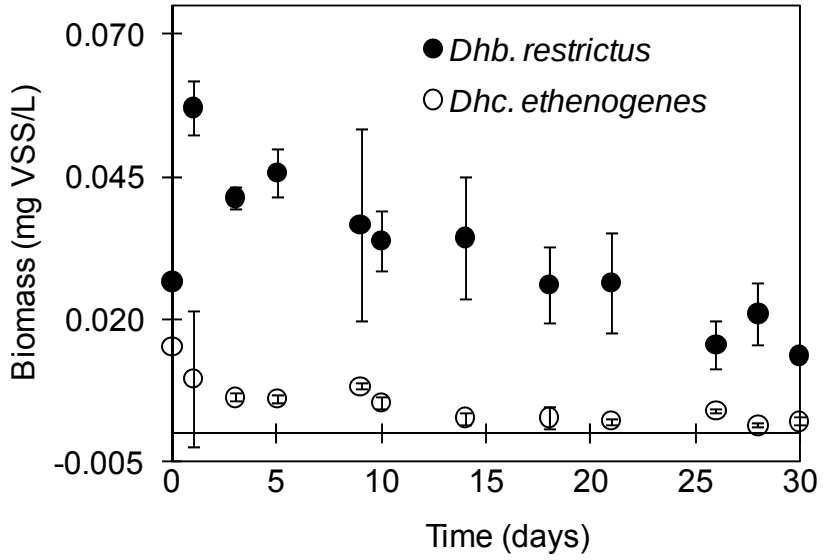

Figure 5.22 Biomass concentrations of *Dhc. ethenogenes* and *Dhb. restrictus* under natural attenuation conditions. Biomass concentrations were calculated based on gene copy numbers quantified with real-time PCR, assuming one 16S rRNA gene copy/cell and a cell mass of 1.6×10^{-14} g VSS/cell.

5.4.6 Comparison between experimental results and model predictions

The predicted chlorinated ethene, hydrogen, acetate, and biomass concentrations under natural attenuation conditions are shown in Figures 5.23–5.25. The model accurately predicted acetate concentrations and captured the general trends in the *Dhb. restrictus* biomass concentrations, i.e., an initial increase in the *Dhb.*

restrictus was followed by a gradual decrease. However, the model predicted a decrease in *Dhb. restrictus* concentration due to outcompetition by *Dhc. ethenogenes* for hydrogen, which clearly did not occur in the experiments. Obviously, the modeling predictions did not adequately capture some phenomenom that was occurring in the CSTRs, or one or more of the model inputs were inaccurate because the chlorinated ethene concentrations, energy source (hydrogen) consumption, and *Dhc. ethenogenes* biomass concentrations were not accurately predicted. In short, the model predicted that *Dhc. ethenogenes* would dominate in the CSTRs by growing much better than it actually did, resulting in hydrogren concentrations that approach the kinetically controlled substrate concentration (discussed above) and greater PCE dechlorination.

Dhc. ethenogenes clearly did dominate in the CSTRs under engineered bioremediation conditions. Thus, the poor performance of *Dhc. ethenogenes* under natural attenuation conditions must be due to the lower available hydrogen and/or acetate concentrations relative to the engineered bioremediation scenario. As noted in Section 5.3, *Dhc. ethenogenes* was very sensitive to acetate availability in batch cultures. PCE dechlorination by *Dhc. ethenogenes* slowed substantially at 10 μM acetate and was even slower at 5 μM acetate (Figure 5.11A). While a term describing acetate utilization by *Dhc. ethenogenes* was included in the model used to simulate the natural attenuation data, it is possible that this Monod-type term did not provide a good description of the response to *Dhc. ethenogenes* to acetate. For example, it is possible that a threshold concentration exists such that a steady-state population of *Dhc. ethenogenes* cannot be maintained at acetate concentrations below this

threshold. The acetate concentration in the CSTRs (8 μM) was within the range of acetate concentrations at which PCE dechlorination by *Dhc. ethenogenes* became severely inhibited (Figure 5.11A). The experimental data shown in Figure 5.11A were obtained under conditions of excess hydrogen. However, the low concentration of hydrogen in the CSTRs may have further limited *Dhc. ethenogenes*' ability to take up acetate due to thermodynamic constraints. Thus, it is quite plausible that the acetate concentration in the CSTRs was close to an acetate threshold for *Dhc. ethenogenes*.

Further, it is possible that electron donor and carbon source availability have interrelated effects on dehalorespiration that are not captured by the multiple Monod model used in this study, or that dual substrate limiting conditions cause additional unexpected impacts on the kinetic parameter estimates, that were not observed under the single substrate limiting conditions used in the batch kinetic assays. For example, the hydrogen threshold for *Dhb. restrictus* in cultures provided with low acetate levels was orders of magnitude higher compared with cultures that received high acetate doses (Figure 5.15B).

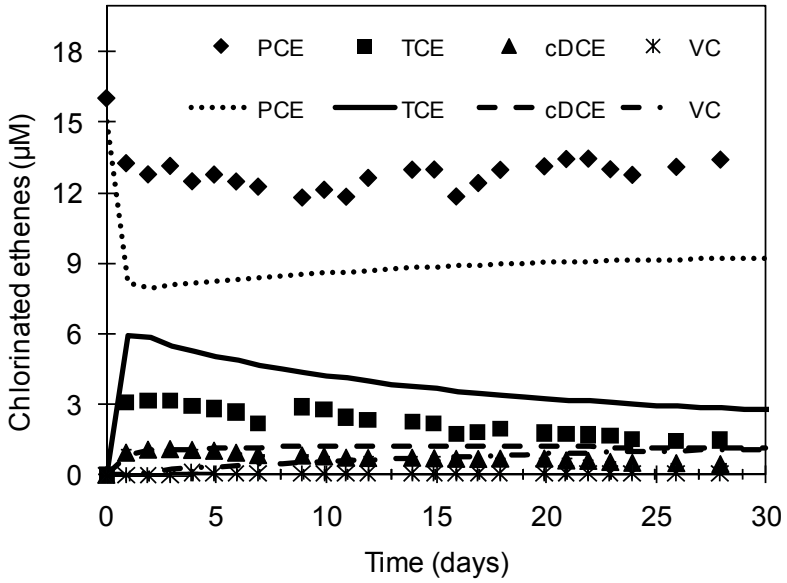

Figure 5.23 Comparison of model predictions (lines) and experimental measurements (points) of chlorinated ethene concentrations in the co-culture of *Dhc. ethenogenes* and *Dhb. restrictus* under natural attenuation conditions using using the kinetic parameters in Table 5.8. A combination of intrinsic (days 0-2) and extant (> 2 d) kinetic parameter inputs were used.

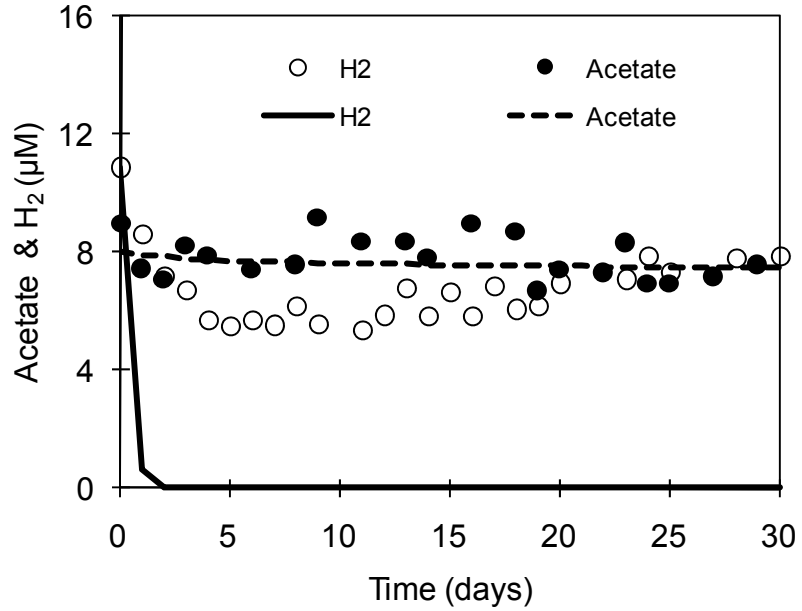

Figure 5.24 Comparison of model predictions (lines) and experimental measurements (points) of hydrogen and acetate concentrations in the co-culture of *Dhc. ethenogenes* and *Dhb. restrictus* under natural attenuation conditions using the kinetic parameters in Table 5.8. A combination of intrinsic (days 0-2) and extant (> 2 d) kinetic parameter inputs were used.

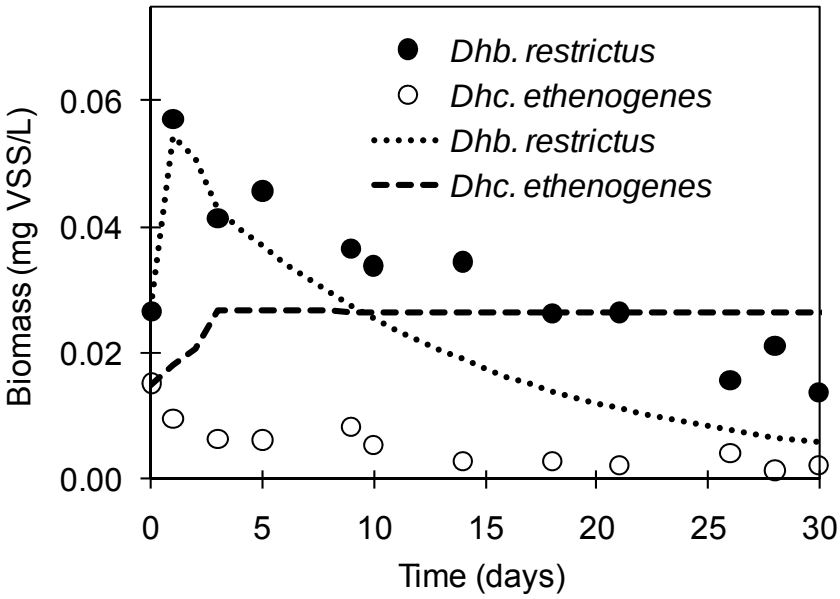

Figure 5.25 Comparison of model predictions (lines) and experimental results (points) of biomass concentrations in the co-culture of *Dhc. ethenogenes* and *Dhb. restrictus* under natural attenuation conditions using the kinetic parameters in Table 5.8. A combination of intrinsic (days 0-2) and extant (> 2 d) kinetic parameter inputs were used.

5.4.7 Conclusions and implications

Energy source (hydrogen) availability has long been a concern in terms of understanding the competition between dehalorespirers, but the effects of other factors including VC toxicity and carbon source availability, have not been well studied and are not generally addressed in conventional bioremediation practice. By incorporating the competitive inhibition terms in the model, (especially VC inhibition in *Dhb. restrictus*), the model predictions captured the experimental results much better than a Monod model without inhibition terms under engineered bioremediation conditions and demonstrated that *Dhb. restrictus* would be out competed by *Dhc. ethenogenes*. In contrast, due to limited hydrogen and acetate availability, *Dhb. restrictus* appears to have a competitive advantage over *Dhc. ethenogenes* under

natural attenuation conditions. The predominance of a PCE-to-cDCE dechlorinator over *Dehalococcoides* strains could explain why cDCE often accumulates at sites where engineered bioremediation approaches such as biostimulation or bioaugmentation have not been applied (Becker, 2006).

Most importantly, this study highlighted how acetate availability, which has previously been overlooked, can influence the outcome of microbial competition. Many heterotrophic dehalorespiring bacteria, e.g., *Desulfuromonas michiganensis* (Huang and Becker, 2009), *Anaeromyxobacter dehalogenans* (He and Sanford, 2004), *Geobacter lovleyi* strain SZ (Amos et al., 2009), aceticlastic methanogens, and acetate-oxidizing bacteria likely have much lower acetate thresholds (< 0.5 μM) than the acetate levels provided in the CSTRs. Thus, the presence of these populations may make it even more difficult for *Dehalococcoides* strains to compete for acetate. Thus a better understanding of the relationship between acetate availability and dehalorespiration in *Dehalococcoides* and *Dehalobacter* strains is needed to improve our ability to formulate a model of acetate utilization.

Chapter 6 Conclusions and recommendations

Substrate utilization kinetics for the hydrogenotrophic strains *Dhc. ethenogenes* and *Dhb. restrictus* were investigated under electron donor- and electron acceptor- limited conditions. Reliable estimates of q_{max} and K_S that describe intrinsic (unrestricted growth) and extant (non-growth) kinetics were successfully obtained under carefully selected initial conditions. The intrinsic and extant kinetic parameter values were different, as expected, and highlighted the importance of estimating and applying kinetic parameters under appropriate conditions.

Competitive and self-inhibition constants were estimated to describe the effects of chlorinated ethenes on dechlorination rates in *Dhc. ethenogenes* and *Dhb. restrictus*. Highly chlorinated ethenes competitively inhibited dechlorination of lesser chlorinated ethenes in *Dhc. ethenogenes* and *Dhb. restrictus*. In *Dhc. ethenogenes*, cometabolic transformation of VC was significantly inhibited by chlorinated ethenes that serve as growth substrates. Dechlorination of PCE and TCE by *Dhb. restrictus* was strongly inhibited by the presence of VC. The results of this inhibition study highlight that the presence of multiple chlorinated ethenes, which is likely to occur in contaminated groundwater aquifers, could result in substrate utilization rates and patterns that differ from those observed in biodegradation assays involving single substrates. Therefore, maintaining multiple dehalorespiring bacteria with different substrate ranges may be beneficial by minimizing these inhibition effects.

Experiments conducted with [^{14}C]-acetate confirmed that both *Dhc. ethenogenes* and *Dhb. restrictus* assimilate acetate. However, these organisms respond quite differently to low acetate concentrations, as reflected in their

dechlorination rates and hydrogen thresholds. Furture study should be conduted to evaluate whether *Dhb. restrictus* can be maintained without acetate (or < 1 μM acetate) over serial transfers and to confirm that peptone cannot serve as a carbon source for *Dhb. restrictus*. Howver, these preliminary studies suggest that *Dhb. restrictus* may tolerate low acetate concentrations much better than *Dhc. ethenogenes*. These findings suggest that it may be important to consider carbon source availability, including the effects of dehalorespiring and other populations on carbon source availability, when designing bioremediation strategies intended to stimulate *Dehalococcoides* strains.

The microbial interactions between *Dhc. ethenogenes* and *Dhb. restrictus* were investigated using CSTRs and mathematical models under engineered bioremediation and natural attenuation (low hydrogen and acetate concentration) conditions. The experimental results showed that *Dhc. ethenogenes* will dominate under engineered bioremediation conditions, and the modeling predictions suggested that the high levels of VC produced by *Dhc. ethenogenes* in this scenario inhibited the growth of *Dhb. restrictus*. On the contrary, *Dhb. restrictus* was dominant under natural attenuation conditions, apparently because its ability to tolerate low acetate concentrations gave it a competitive advantage over *Dhc. ethenogenes*. Under the engineered bioremediation scenario, significant ethene production was not observed in the CSTRs due to the slow rate of VC co-metabolism by *Dhc. ethenogenes*. These results highlight the need for VC-respiring *Dehalococcoides* strains, e.g., *Dehalococcides* strains BAV1 and VS (He et al., 2003; Cupples et al., 2004), in order to achieve complete detoxification of PCE in continuous-flow systems.

The modeling and experimental approach used in this study, especially the use of qPCR to quantify individual dehalorespirers in CSTRs, was effective and made it possible to evaluate the dynamics of dehalorespring bacteria in defined co-cultures under conditions relevant to bioremediation practice. Future studies should focus on improving our understanding of the relationship between carbon source availabilty and dehalorespiration in hydrogenotrophic populations and on improving our understanding of substrate interactions in more complex microbial consortia or communities. This may require the application of metagenomics to CSTRs or other continuous-flow reactors that can sustain complex microbial cultures.

Appendix A

H_2 depletion data used to fit K_S and q_{max} for (A) *Dhc. ethenogenes* and (B) *Dhb. restrictus*

(A) *Dhc. ethenogenes*

Time (hrs)	H_2 (μM)	Time (hrs)	H_2 (μM)	Time (hrs)	H_2 (μM)
0.0	17.0	0.0	15.7	0.0	16.5
14.5	17.0	15.2	15.1	16.0	15.3
34.0	15.8	59.7	13.5	34.3	14.2
59.5	14.2	83.8	12.1	137.4	9.2
108.7	10.7	108.8	10.5	160.8	7.4
183.8	5.3	183.8	5.7	184.5	5.6
207.8	2.9	208.0	2.6	208.2	3.5
227.5	0.8	228.2	1.2	228.3	1.9
233.1	0.6	252.3	0.1	253.0	0.1
240.8	0.2	258.0	0.1	258.0	0.1
250.7	0.1	262.7	0.1		

(B) *Dhb. restrictus*

Time (hrs)	H_2 (μM)	Time (hrs)	H_2 (μM)	Time (hrs)	H_2 (μM)
0.0	11.6	0.0	11.2	0.0	10.8
5.0	10.5	3.0	10.7	3.0	10.8
24.4	7.5	20.5	7.8	15.0	8.8
31.7	4.1	27.5	5.3	27.7	5.6
40.6	3.1	34.8	3.9	35.0	4.4
47.9	1.7	43.7	1.9	51.5	2.0
56.0	1.3	51.2	1.3	59.2	1.2
69.7	0.2	59.1	1.1	73.1	0.4
		72.8	0.3		

Appendix B

Chlorinated ethenes depletion data (intrinsic kinetics and VC kinetics) used to fit K_S and q_{max} for *Dhc. ethenogenes*

Time (hrs)	PCE (μM)	Time (hrs)	PCE (μM)	Time (hrs)	PCE (μM)
0.0	196.5	0.0	199.5	0.0	209.7
17.3	163.4	17.6	168.0	18.0	181.2
22.5	152.1	22.8	158.7	23.2	168.6
29.9	132.3	31.0	138.5	30.6	148.1
37.3	106.6	38.0	121.1	37.7	129.3
44.7	84.5	45.4	103.1	46.0	104.5
52.0	54.6	52.3	78.8	52.7	77.3
58.1	28.5	58.5	53.2	58.8	47.7
59.3	23.8	61.5	41.7	61.8	33.0
61.2	16.0	64.6	29.4	65.4	16.8
63.2	9.5	67.9	17.4	67.6	8.8
65.1	4.3	69.7	11.8	69.3	4.7
66.7	2.1	72.1	5.1	71.8	1.9
68.9	1.1	74.8	1.9	75.1	0.8

Time (hrs)	TCE (μM)	Time (hrs)	TCE (μM)	Time (hrs)	TCE (μM)
0.0	293.7	0.0	259.0	0.0	292.1
23.3	191.8	23.6	192.4	18.6	215.1
27.8	164.8	28.1	165.2	23.8	192.0
34.3	129.3	34.6	124.8	28.3	168.2
43.7	66.4	43.9	67.4	34.9	135.8
48.8	35.6	49.1	34.5	44.2	76.0
51.8	18.8	52.0	16.6	49.3	40.7
53.5	7.6	53.8	6.0	52.3	20.6
54.4	3.5	54.7	2.1	54.0	9.3
56.8	0.4	57.0	0.3	54.9	4.5
63.2	0.2			57.3	0.3

Time (hrs)	cDCE (μM)	Time (hrs)	cDCE (μM)	Time (hrs)	cDCE (μM)
0.0	573.4	0.0	585.0	0.0	562.4
4.4	551.3	4.6	559.9	11.4	493.5
11.6	501.3	11.8	497.7	16.7	447.6
16.3	465.5	16.6	450.6	21.6	395.2
20.4	429.9	20.7	401.9	23.9	367.1
23.4	405.5	23.6	373.7	29.4	285.2
28.9	336.8	29.2	292.0	35.0	185.4
35.0	244.6	35.3	188.8	38.0	125.3
38.3	184.0	38.3	121.6	40.7	72.8
40.8	136.4	40.7	67.9	43.0	33.5
42.8	99.9	42.6	25.6	44.1	19.5
44.1	72.8	43.7	18.8	44.1	18.8
45.5	46.9	44.8	17.9		
47.4	19.4				

Time (hrs)	VC (μM)	Time (hrs)	VC (μM)
0.0	304.8	0.0	322.5
65.3	227.9	17.2	310.5
114.1	195.7	65.3	243.8
184.3	146.8	114.1	199.6
233.5	111.4	184.6	144.6
282.0	90.8	233.6	110.5
353.3	60.0	282.0	87.1
401.7	48.5	353.3	59.9
450.5	37.2	401.3	47.4
522.3	26.2	450.5	35.1
593.9	18.2	522.2	23.9
787.6	7.6	593.8	16.8
		787.5	6.5

Appendix C

Chlorinated ethenes depletion data (intrinsic kinetics) used to fit K_S and q_{max} for *Dhb. restrictus*

Time (hrs)	PCE (μM)	Time (hrs)	PCE (μM)	Time (hrs)	PCE (μM)
0.0	183.5	0.0	181.2	0.0	189.9
6.0	173.7	6.3	171.1	6.7	179.4
9.2	163.3	9.5	163.3	9.9	171.3
12.5	154.5	12.8	152.6	13.2	159.5
16.3	138.0	16.6	136.0	17.0	139.6
19.6	123.7	20.0	115.0	22.7	106.9
22.1	103.9	25.6	75.0	26.0	80.4
25.3	82.0	27.4	58.8	27.7	61.6
27.0	67.3	29.3	42.7	31.4	26.5
28.9	53.0	31.1	17.5	33.5	3.2
30.8	31.8	33.0	2.6		
33.6	3.5	35.2	0.4		
36.2	0.4				

Time (hrs)	TCE (μM)	Time (hrs)	TCE (μM)	Time (hrs)	TCE (μM)
0.0	401.1	0.0	397.2	0.0	383.0
9.0	374.6	6.0	378.1	6.3	365.3
12.2	356.3	9.2	366.7	9.5	352.9
16.1	328.8	12.6	347.5	12.8	336.4
19.4	296.0	16.3	323.7	16.6	307.9
21.8	276.2	19.7	295.6	19.9	275.8
25.1	220.6	22.1	267.9	22.3	244.1
26.9	181.4	25.3	222.1	25.6	199.2
28.7	134.7	27.1	182.4	27.4	166.5
30.5	82.9	29.0	143.1	29.2	118.7
32.3	21.7	30.8	94.8	31.0	71.3
33.0	2.5	32.5	46.7	32.8	13.5
35.1	0.2	33.5	11.6	33.3	2.8
		34.8	0.4	35.3	0.2
		35.6	0.2		

Appendix D

Chlorinated ethenes depletion data (extant kinetics) used to fit K_S and q_{max} for *Dhc. ethenogenes*

Time (mins)	PCE (μM)	Time (mins)	PCE (μM)	Time (mins)	PCE (μM)
0	20.0	0	19.7	0	20.9
3	18.3	3	18.6	3	19.3
23	9.9	23	10.6	25	9.7
41	2.3	41	3.1	43	1.1
59	0.1	59	0.1	61	0.1

Time (mins)	TCE (μM)	Time (mins)	TCE (μM)	Time (mins)	TCE (μM)
0	27.4	0	29.5	0	28.8
5	23.3	4	23.7	2	22.5
19	8.7	17	15.5	15	17.2
32	1.6	32	8.5	30	7.6
45	0.2	45	1.3	43	2.8
59	0.0	58	0.1	56	0.3
				72	0.1

Time (mins)	cDCE (μM)	Time (mins)	cDCE (μM)	Time (mins)	cDCE (μM)
0	44.0	0	45.4	0	42.1
3	42.0	3	43.3	3	40.4
12	32.3	13	32.9	13	29.2
22	23.2	23	24.1	24	22.7
32	13.8	33	12.9	34	11.4
43	5.8	43	3.7	44	4.1
53	1.2	53	2.1	54	1.4

Appendix E

Chlorinated ethenes depletion data (extant kinetics) used to fit K_S and q_{max} for *Dhb. restrictus*

Time (mins)	PCE (μM)	Time (mins)	PCE (μM)	Time (mins)	PCE (μM)
0	40.4	0	38.6	0	45.5
3	31.2	3	30.2	3	37.3
13	22.6	11	21.6	11	27.8
21	15.0	21	13.3	20	15.7
31	6.0	31	5.7	31	6.1
42	1.4	42	0.4	42	0.8
53	0.1				

Time (mins)	TCE (μM)	Time (mins)	TCE (μM)	Time (mins)	TCE (μM)
0	55.6	0	53	0	54.8
3	42.0	3	46	3	42.9
8	29.9	8	35	8	34.1
13	17.5	13	22	14	25.2
18	4.6	19	11	18	17.4
26	0.4	25	2	24	4.6
				31	2.2

Appendix F

Effect of initial acetate concentrations from <0.45 to 5 mM on dechlorination by (A) *Dhc. ethenogenes* and (B) *Dhb. restrictus*

(A) *Dhc. ethenogenes*

5 mM			0.5 mM			0.1 mM		
Days	PCE (μM)	STDEV	Days	PCE (μM)	STDEV	Days	PCE (μM)	STDEV
0	57.1	5.9	0	54.7	2.4	0	52.7	5.5
1	56.9	5.9	1	56.2	N.A	1	52.5	5.5
2	56.5	5.7	2	55.8	N.A	2	52.2	5.6
4	54.5	5.1	4	53.9	N.A	4	50.8	5.2
6	48.6	2.7	5	52.0	N.A	6	46.9	5.6
7	41.6	0.8	6	47.6	N.A	7	43.0	3.0
7	41.1	5.5	7	42.7	N.A	9	28.7	2.3
8	32.9	9.8	8	31.3	3.4	11	10.9	5.9
9	20.2	11.0	9	23.0	1.0	12	1.3	0.2
10	7.3	5.3	10	11.0	3.3			
11	0.7	0.2	11	5.7	5.2			
			12	1.1	0.5			

0.05 mM			0.01 mM			0.005 mM		
Days	PCE (μM)	STDEV	Days	PCE (μM)	STDEV	Days	PCE (μM)	STDEV
0	51.7	2.3	0	53.9	0.8	0	54.0	2.3
1	51.6	2.3	1	53.7	0.8	1	53.8	2.3
2	51.2	2.2	2	53.4	0.8	2	53.4	2.2
4	49.5	2.2	4	52.4	1.0	4	52.5	2.3
6	45.0	1.4	6	50.8	1.0	6	51.7	2.3
7	40.4	0.4	7	49.7	1.0	7	51.1	2.4
9	26.2	1.1	10	46.9	2.6	11	48.2	2.8
11	8.6	1.1	11	43.4	1.0	12	47.8	2.9
12	3.0	0.4	12	41.3	0.2	14	46.6	3.1
			14	37.7	1.8	17	43.2	3.3
			17	31.8	0.0	21	38.5	4.4
			21	22.5	0.0	26	33.5	4.4
			26	17.5	3.3	33	28.4	4.3
			33	7.6	0.5			

< 1.2 µM		
Days	PCE (µM)	STDEV
0	44.7	8.6
1	44.4	8.5
2	44.2	8.7
6	43.6	8.4
7	43.4	8.6
11	42.8	8.3
12	42.9	8.4
14	42.4	8.4
21	41.6	8.5
26	41.0	8.6
33	40.1	8.5

(B) *Dhb. restrictus*

5 mM			0.5 mM			0.05 mM		
Days	PCE (µM)	STDEV	Days	PCE (µM)	STDEV	Days	PCE (µM)	STDEV
0.0	168.1	12.8	0	206.6	34.1	0	187.8	23.3
0.5	167.5	12.8	1	206.3	33.7	1	187.2	23.3
1.5	168.4	10.6	2	199.4	26.8	2	180.4	20.3
2.6	167.1	12.7	4	132.8	36.0	3	169.6	N.A.
3.7	126.2	2.3	5	32.5	43.1	4	117.3	37.6
4.7	54.0	73.9	6	0.9	0.3	5	35.7	48.0
5.7	1.0	0.3	9	0.4	0.0	6	0.7	0.1
8.6	0.4	0.1				9	0.3	0.0

0.01 mM			0.005 mM			0.002 mM		
Days	PCE (µM)	STDEV	Days	PCE (µM)	STDEV	Days	PCE (µM)	STDEV
0	196.2	24.0	0	173.7	20.6	0	168.7	6.3
1	195.7	24.3	0	173.1	20.6	1	168.1	6.3
2	189.8	20.6	1	168.5	6.1	2	165.2	9.3
3	160.9	N.A.	3	150.9	N.A.	3	135.7	N.A.
4	13.7	8.3	4	52.4	27.9	4	53.7	10.2
5	1.6	0.2	5	16.9	19.3	5	31.0	5.1
5	1.0	0.1	6	2.6	2.5	6	6.2	0.6
9	0.3	0.0	7	0.3	0.0	7	0.6	0.1
			9	0.2	0.0	9	0.3	0.0

<0.45 μM		
Days	PCE (μM)	STDEV
0	196.2	34.6
1	195.6	34.6
2	181.3	32.5
3	142.0	N.A.
4	75.6	24.8
5	60.8	23.6
6	45.3	19.3
7	16.4	14.3
8	0.5	0.1
9	0.3	0.0

Appendix G

The Matlab codes used to fit $K_{S,\ acetate}$ for *Dhc. ethenogenes* and *Dhb. restrictus*

(A) *Dhc. ethenogenes*

```
function dPCEdt = zigzag(t, PCE)
% model PCE with time-interpolated values of Acetate
global qmax Kspce Ksace Y
global X0 PCE0 ACE0
global stoic
% interpolate acceptor concentrations from data
X = X0 + Y/6.502 * max((PCE0 - PCE),0);
ACE = max(ACE0 - stoic * (PCE0-PCE),0);
% calculate PCE dechlorination rate
dPCEdt = - qmax * X * (PCE /(Kspce + PCE)) *(ACE / (Ksace + ACE));

global t_fit PCE_data1
global weights
global qmax Kspce Ksace Y
global X0 PCE0 ACE0
format compact
T_PCE = ...
    [0.00   53.90
0.72    53.73
1.76    53.41
4.71    52.55
5.78    50.82
6.81    49.66
7.76    48.18
8.76    46.64
10.77   43.42
11.89   41.31
13.72   37.70
16.84   31.82
20.81   22.54
25.90   17.51]

t_fit = T_PCE(:,1);
PCE_data1 = T_PCE(:,2);

%-------------------------------------------------------------------
---------
qmax=162.24
Y=0.014
ACE0=10
PCE0=PCE_data1(1)
X0=0.002
Kspce=21.45
Ksaceguess=1.5
stoicguess = 0.185
% set weights for optimization
%weights = 1./Xstd_fit;
weights = ones(size(t_fit)); % un-comment to set weights to 1
% Optimize
```

```
options = optimset('LargeScale', 'on');
[parms, sse, residuals] = ...
    lsqnonlin('PCE_AC_reg_fit_error',[Ksaceguess stoicguess],[0
0],[Inf Inf],options);%error function:give vector of
errors:model(param)-data(vector)

%
% Show Results

Ksace = parms(1)
stoic = parms(2)
sse

% Calculate F-values


    tsamp  = t_fit;   % tsamp is the measured time
    Ssamp  = PCE_data1;     % Ssamp is the measured PCE
concentration
    options = odeset('RelTol',1e-6,'AbsTol',1e-9);

    [times, model_values] =
ode23s('zigzag',tsamp,[Ssamp(1)],options);
                                    %zigzag',t_fit,[PCE0],options
                                         % Solve the equation for
predicted PCE concentrations
    S_all_pred= model_values(:,1);
    S_all_samp= Ssamp;


dev=S_all_samp-mean(S_all_samp);            % deviations - measure
of spread
SST=sum(dev.^2);                             % total variation to be
accounted for
resid=S_all_samp-S_all_pred;                % residuals - measure of
mismatch
SSE = sum(resid.^2);                        % variation NOT
accounted for
Rsq=1-SSE/SST;                              % percent of error
explained
SSR=SST-SSE;                                % the "ANOVA identity"
dfr=2;                                      % order of the
polynomial
dfe=length(S_all_samp)-1-dfr;                         % degrees of
freedom for error
MSE=SSE/dfe;                                % mean-square error of
residuals
MSR=SSR/dfr;                                % mean-square error for
regression
f=MSR/MSE;                                  % f-statistic for
regression
f

%-------------------------------------------------------------------
-----
```

```
% plot data and results
%-------------------------------------------------------------------
-----
% 1- Protein: X(t)
%--------------------
results = [];
figure
plot(t_fit,PCE_data1,'+')
hold on
% Calculate and plot model predictions
options = odeset('RelTol',1e-6,'AbsTol',1e-9);
tm = linspace(0,t_fit(end),101);
%[times, model_values] = ode23s('PCE_AC_reg_model',tm,PCE0,options);
[times, model_values] = ode23s('zigzag',tm,PCE0,options);
plot(times,model_values,'k')
hold off
% add axis titles, etc...
xlabel('Time (day)')
ylabel('PCE (\muM)')
axis([ 0 40 0 60])
ACE =ACE0 - stoic * (PCE0 - model_values);
results = [results times model_values ACE];
save 'results_Dhc10.txt' results -ASCII


global t_fit PCE_data1
global weights
global qmax Kspce Ksace Y
global X0 PCE0 ACE0
format compact
T_PCE = ...
    [0.0    54.0
0.8 53.8
1.8 53.4
3.9 52.5
5.8 51.7
6.8 51.1
10.8 48.2
11.9 47.8
13.8 46.6
16.9 43.2
20.9 38.5
25.9 33.5
32.8 28.4]

t_fit = T_PCE(:,1);
PCE_data1 = T_PCE(:,2);

%-------------------------------------------------------------------
---------
qmax=162.24
Y=0.014
ACE0=5
PCE0=PCE_data1(1)
X0=0.002
Kspce=21.45
```

```
Ksaceguess=1.5
stoicguess = 0.185
% set weights for optimization
%weights = 1./Xstd_fit;
weights = ones(size(t_fit)); % un-comment to set weights to 1
% Optimize
options = optimset('LargeScale', 'on');
[parms, sse, residuals] = ...
    lsqnonlin('PCE_AC_reg_fit_error',[Ksaceguess stoicguess],[0
0],[Inf Inf],options);
% Show Results

Ksace = parms(1)
stoic = parms(2)

sse
% Calculate F-values


    tsamp  = t_fit;   % tsamp is the measured time
    Ssamp  = PCE_data1;     % Ssamp is the measured PCE
concentration
    options = odeset('RelTol',1e-6,'AbsTol',1e-9);

    [times, model_values] =
ode23s('zigzag',tsamp,[Ssamp(1)],options);
                                  %zigzag',t_fit,[PCE0],options
                                       % Solve the equation for
predicted PCE concentrations
    S_all_pred= model_values(:,1);
    S_all_samp= Ssamp;


dev=S_all_samp-mean(S_all_samp);            % deviations - measure
of spread
SST=sum(dev.^2);                             % total variation to be
accounted for
resid=S_all_samp-S_all_pred;                % residuals - measure of
mismatch
SSE = sum(resid.^2);                        % variation NOT
accounted for
Rsq=1-SSE/SST;                              % percent of error
explained
SSR=SST-SSE;                                % the "ANOVA identity"
dfr=2;                                      % order of the
polynomial
dfe=length(S_all_samp)-1-dfr;                         % degrees of
freedom for error
MSE=SSE/dfe;                                % mean-square error of
residuals
MSR=SSR/dfr;                                % mean-square error for
regression
f=MSR/MSE;                                  % f-statistic for
regression
f
```

```
%-----------------------------------------------------------------------
-----
% plot data and results
%-----------------------------------------------------------------------
-----
% 1- Protein: X(t)
%--------------------
results = [];
figure
plot(t_fit,PCE_data1,'+')
hold on
% Calculate and plot model predictions
options = odeset('RelTol',1e-6,'AbsTol',1e-9);
tm = linspace(0,t_fit(end),101);
%[times, model_values] = ode23s('PCE_AC_reg_model',tm,PCE0,options);
[times, model_values] = ode23s('zigzag',tm,PCE0,options);
plot(times,model_values,'k')
hold off
% add axis titles, etc...
xlabel('Time (day)')
ylabel('PCE (\muM)')
axis([ 0 40 0 60])

results = [results times model_values];

save 'results_Dhc05.txt' results -ASCII


global t_fit PCE_data1
global weights
global qmax Kspce Ksace Y
global X0 PCE0 ACE0
format compact
T_PCE = ...
    [0.00   44.70
0.77    44.44
1.82    44.18
5.84    43.58
6.86    43.37
10.89   42.81
11.94   42.93
13.79   42.45
20.94   41.57
25.98   40.98
32.78   40.08]

t_fit = T_PCE(:,1);
PCE_data1 = T_PCE(:,2);

%-----------------------------------------------------------------------
---------
qmax=162.24
Y=0.014
ACE0=1.2
```

```
PCE0=PCE_data1(1)
X0=0.002
Kspce=21.45
Ksaceguess=1.5
stoicguess = 0.185
% set weights for optimization
%weights = 1./Xstd_fit;
weights = ones(size(t_fit)); % un-comment to set weights to 1
% Optimize
options = optimset('LargeScale', 'on');
[parms, sse, residuals] = ...
    lsqnonlin('PCE_AC_reg_fit_error',[Ksaceguess stoicguess],[0
0],[Inf Inf],options);
% Show Results

Ksace = parms(1)
stoic = parms(2)

sse
% Calculate F-values


    tsamp  = t_fit;   % tsamp is the measured time
    Ssamp  = PCE_data1;     % Ssamp is the measured PCE
concentration
    options = odeset('RelTol',1e-6,'AbsTol',1e-9);

    [times, model_values] =
ode23s('zigzag',tsamp,[Ssamp(1)],options);
                                %zigzag',t_fit,[PCE0],options
                                     % Solve the equation for
predicted PCE concentrations
    S_all_pred= model_values(:,1);
    S_all_samp= Ssamp;


dev=S_all_samp-mean(S_all_samp);            % deviations - measure
of spread
SST=sum(dev.^2);                             % total variation to be
accounted for
resid=S_all_samp-S_all_pred;                % residuals - measure of
mismatch
SSE = sum(resid.^2);                        % variation NOT
accounted for
Rsq=1-SSE/SST;                              % percent of error
explained
SSR=SST-SSE;                                % the "ANOVA identity"
dfr=2;                                      % order of the
polynomial
dfe=length(S_all_samp)-1-dfr;                         % degrees of
freedom for error
MSE=SSE/dfe;                                % mean-square error of
residuals
MSR=SSR/dfr;                                % mean-square error for
regression
```

```
f=MSR/MSE;                                  % f-statistic for
regression
f

%-------------------------------------------------------------------
-----
% plot data and results
%-------------------------------------------------------------------
-----
% 1- Protein: X(t)
%--------------------
results = [];
figure
plot(t_fit,PCE_data1,'+')
hold on
% Calculate and plot model predictions
options = odeset('RelTol',1e-6,'AbsTol',1e-9);
tm = linspace(0,t_fit(end),101);
%[times, model_values] = ode23s('PCE_AC_reg_model',tm,PCE0,options);
[times, model_values] = ode23s('zigzag',tm,PCE0,options);
plot(times,model_values,'k')
hold off
% add axis titles, etc...
xlabel('Time (day)')
ylabel('PCE (\muM)')
axis([ 0 40 0 60])

results = [results times model_values];

save 'results_Dhc01.txt' results -ASCII
```

(B) *Dhb. restrictus*

```
function dPCEdt = zigzag(t, PCE)
% model PCE with time-interpolated values of Acetate
global qmax Kspce Ksace Y
global X0 PCE0 ACE0
global stoic
% interpolate donor and acceptor concentrations from data
X = X0 + Y/6.502 * max((PCE0 - PCE),0);
ACE = max(ACE0 - stoic * (PCE0-PCE),0);


% Fit Dhb carbon kinetic model to experimental data
%-------------------------------------------------------------------
-------
global t_fit PCE_data1
global weights
global qmax Kspce Ksace Y
global X0 PCE0 ACE0
format compact
T_PCE = ...
    [0.00   196.20
0.60    195.74
1.60    189.80
```

```
2.62    160.88
3.81    13.70
4.58    1.59
5.26    1.00
8.64    0.32
]

t_fit = T_PCE(:,1);
PCE_data1 = T_PCE(:,2);

%-----------------------------------------------------------------------
---------
qmax=539.52
Y=0.0087
ACE0=10
PCE0=PCE_data1(1)
X0=0.0286
Kspce=7.2
Ksaceguess=2
stoicguess = 0.2
% set weights for optimization
%weights = 1./Xstd_fit;
weights = ones(size(t_fit)); % un-comment to set weights to 1
% Optimize
options = optimset('LargeScale', 'on');
[parms, sse, residuals] = ...
    lsqnonlin('PCE_AC_reg_fit_error',[Ksaceguess stoicguess],[0
0],[Inf Inf],options);
% Show Results

Ksace = parms(1)
stoic = parms(2)

sse
% Calculate F-values


    tsamp  = t_fit;   % tsamp is the measured time
    Ssamp  = PCE_data1;     % Ssamp is the measured PCE
concentration
    options = odeset('RelTol',1e-6,'AbsTol',1e-9);

    [times, model_values] =
ode23s('zigzag',tsamp,[Ssamp(1)],options);
                                    %zigzag',t_fit,[PCE0],options
                                         % Solve the equation for
predicted PCE concentrations
    S_all_pred= model_values(:,1);
    S_all_samp= Ssamp;


dev=S_all_samp-mean(S_all_samp);            % deviations - measure
of spread
SST=sum(dev.^2);                             % total variation to be
accounted for
```

```
resid=S_all_samp-S_all_pred;                % residuals - measure of
mismatch
SSE = sum(resid.^2);                        % variation NOT
accounted for
Rsq=1-SSE/SST;                              % percent of error
explained
SSR=SST-SSE;                                % the "ANOVA identity"
dfr=2;                                      % order of the
polynomial
dfe=length(S_all_samp)-1-dfr;                       % degrees of
freedom for error
MSE=SSE/dfe;                                % mean-square error of
residuals
MSR=SSR/dfr;                                % mean-square error for
regression
f=MSR/MSE;                                  % f-statistic for
regression
f
%-----------------------------------------------------------------------
-----
% plot data and results
%-----------------------------------------------------------------------
-----
% 1- Protein: X(t)
%--------------------
results = [];
figure
plot(t_fit,PCE_data1,'+')
hold on
% Calculate and plot model predictions
options = odeset('RelTol',1e-6,'AbsTol',1e-9);
tm = linspace(0,t_fit(end),101);
%[times, model_values] = ode23s('PCE_AC_reg_model',tm,PCE0,options);
[times, model_values] = ode23s('zigzag',tm,PCE0,options);
plot(times,model_values,'k')
hold off
% add axis titles, etc...
xlabel('Time (day)')
ylabel('PCE (\muM)')
axis([ 0 10 0 260])
results = [results times model_values];

save 'results_Dhb10.txt' results -ASCII

% Fit Dhb carbon kinetic model to experimental data
%-----------------------------------------------------------------------
-------
global t_fit PCE_data1
global weights
global qmax Kspce Ksace Y
global X0 PCE0 ACE0
format compact
T_PCE = ...
    [0.00   173.72
0.30    173.11
1.17    168.54
```

```
2.66    150.95
3.85    52.42
4.60    16.88
5.52    2.62
6.56    0.31
8.66    0.18
 ]

t_fit = T_PCE(:,1);
PCE_data1 = T_PCE(:,2);

%-------------------------------------------------------------------
---------
qmax=539.52
Y=0.0088
ACE0=5
PCE0=PCE_data1(1)
X0=0.0286
Kspce=7.2
Ksaceguess=2
stoicguess = 0.2
% set weights for optimization
%weights = 1./Xstd_fit;
weights = ones(size(t_fit)); % un-comment to set weights to 1
% Optimize
options = optimset('LargeScale', 'on');
[parms, sse, residuals] = ...
    lsqnonlin('PCE_AC_reg_fit_error',[Ksaceguess stoicguess],[0
0],[Inf Inf],options);
% Show Results

Ksace = parms(1)
stoic = parms(2)

sse
% Calculate F-values


    tsamp  = t_fit;   % tsamp is the measured time
    Ssamp  = PCE_data1;     % Ssamp is the measured PCE
concentration
    options = odeset('RelTol',1e-6,'AbsTol',1e-9);

    [times, model_values] =
ode23s('zigzag',tsamp,[Ssamp(1)],options);
                                    %zigzag',t_fit,[PCE0],options
                                         % Solve the equation for
predicted PCE concentrations
    S_all_pred= model_values(:,1);
    S_all_samp= Ssamp;


dev=S_all_samp-mean(S_all_samp);            % deviations - measure
of spread
```

```
SST=sum(dev.^2);                                % total variation to be
accounted for
resid=S_all_samp-S_all_pred;                    % residuals - measure of
mismatch
SSE = sum(resid.^2);                            % variation NOT
accounted for
Rsq=1-SSE/SST;                                  % percent of error
explained
SSR=SST-SSE;                                    % the "ANOVA identity"
dfr=2;                                          % order of the
polynomial
dfe=length(S_all_samp)-1-dfr;                           % degrees of
freedom for error
MSE=SSE/dfe;                                    % mean-square error of
residuals
MSR=SSR/dfr;                                    % mean-square error for
regression
f=MSR/MSE;                                      % f-statistic for
regression
f
%-----------------------------------------------------------------------
-----
% plot data and results
%-----------------------------------------------------------------------
-----
% 1- Protein: X(t)
%--------------------
results = [];
figure
plot(t_fit,PCE_data1,'+')
hold on
% Calculate and plot model predictions
options = odeset('RelTol',1e-6,'AbsTol',1e-9);
tm = linspace(0,t_fit(end),101);
%[times, model_values] = ode23s('PCE_AC_reg_model',tm,PCE0,options);
[times, model_values] = ode23s('zigzag',tm,PCE0,options);
plot(times,model_values,'k')
hold off
% add axis titles, etc...
xlabel('Time (day)')
ylabel('PCE (\muM)')
axis([ 0 10 0 260])
results = [results times model_values];

save 'results_Dhb05.txt' results -ASCII


% calculate PCE dechlorination rate
dPCEdt = - qmax * X * (PCE /(Kspce + PCE)) *(ACE / (Ksace + ACE));

% Fit Dhb carbon kinetic model to experimental data
%-----------------------------------------------------------------------
-------
global t_fit PCE_data1
global weights
global qmax Kspce Ksace Y
```

```
global X0 PCE0 ACE0
format compact
T_PCE = ...
    [0.00   168.69
0.66    168.13
1.65    165.21
2.70    135.74
3.88    53.75
4.63    30.97
5.55    6.23
6.60    0.56
8.68    0.33
]

t_fit = T_PCE(:,1);
PCE_data1 = T_PCE(:,2);

%-----------------------------------------------------------------------
---------
qmax=539.52
Y=0.0088
ACE0=2
PCE0=PCE_data1(1)
X0=0.0286
Kspce=7.2
Ksaceguess=2
stoicguess = 0.2
% set weights for optimization
%weights = 1./Xstd_fit;
weights = ones(size(t_fit)); % un-comment to set weights to 1
% Optimize
options = optimset('LargeScale', 'on');
[parms, sse, residuals] = ...
    lsqnonlin('PCE_AC_reg_fit_error',[Ksaceguess stoicguess],[0
0],[Inf Inf],options);
% Show Results

Ksace = parms(1)
stoic = parms(2)

sse
% Calculate F-values


    tsamp  = t_fit;   % tsamp is the measured time
    Ssamp  = PCE_data1;     % Ssamp is the measured PCE
concentration
    options = odeset('RelTol',1e-6,'AbsTol',1e-9);

    [times, model_values] =
ode23s('zigzag',tsamp,[Ssamp(1)],options);
                                  %zigzag',t_fit,[PCE0],options
                                       % Solve the equation for
predicted PCE concentrations
    S_all_pred= model_values(:,1);
```

```
    S_all_samp= Ssamp;


dev=S_all_samp-mean(S_all_samp);            % deviations - measure
of spread
SST=sum(dev.^2);                             % total variation to be
accounted for
resid=S_all_samp-S_all_pred;                % residuals - measure of
mismatch
SSE = sum(resid.^2);                        % variation NOT
accounted for
Rsq=1-SSE/SST;                              % percent of error
explained
SSR=SST-SSE;                                % the "ANOVA identity"
dfr=2;                                      % order of the
polynomial
dfe=length(S_all_samp)-1-dfr;                        % degrees of
freedom for error
MSE=SSE/dfe;                                % mean-square error of
residuals
MSR=SSR/dfr;                                % mean-square error for
regression
f=MSR/MSE;                                  % f-statistic for
regression
f

%-------------------------------------------------------------------------
-----
% plot data and results
%-------------------------------------------------------------------------
-----
% 1- Protein: X(t)
%--------------------
results = [];
figure
plot(t_fit,PCE_data1,'+')
hold on
% Calculate and plot model predictions
options = odeset('RelTol',1e-6,'AbsTol',1e-9);
tm = linspace(0,t_fit(end),101);
%[times, model_values] = ode23s('PCE_AC_reg_model',tm,PCE0,options);
[times, model_values] = ode23s('zigzag',tm,PCE0,options);
plot(times,model_values,'k')
hold off
% add axis titles, etc...
xlabel('Time (day)')
ylabel('PCE (\muM)')
axis([ 0 10 0 260])
results = [results times model_values];

save 'results_Dhb02.txt' results -ASCII

% Fit Dhb carbon kinetic model to experimental data
%-------------------------------------------------------------------------
-------
global t_fit PCE_data1
```

```
global weights
global qmax Kspce Ksace Y
global X0 PCE0 ACE0
format compact
T_PCE = ...
    [0.00   196.21
0.69    195.58
1.67    181.34
2.71    142.01
3.90    75.61
4.65    60.84
5.58    45.31
6.61    16.39
7.73    0.47
8.71    0.33
]

t_fit = T_PCE(:,1);
PCE_data1 = T_PCE(:,2);

%-----------------------------------------------------------------------
---------
qmax=539.52
Y=0.0088
ACE0=0.45
PCE0=PCE_data1(1)
X0=0.0286
Kspce=7.2
Ksaceguess=8
stoicguess = 0.2
% set weights for optimization
%weights = 1./Xstd_fit;
weights = ones(size(t_fit)); % un-comment to set weights to 1
% Optimize
options = optimset('LargeScale', 'on');
[parms, sse, residuals] = ...
    lsqnonlin('PCE_AC_reg_fit_error',[Ksaceguess stoicguess],[0
0],[Inf Inf],options);
% Show Results

Ksace = parms(1)
stoic = parms(2)

sse
% Calculate F-values


    tsamp  = t_fit;   % tsamp is the measured time
    Ssamp  = PCE_data1;     % Ssamp is the measured PCE
concentration
    options = odeset('RelTol',1e-6,'AbsTol',1e-9);

    [times, model_values] =
ode23s('zigzag',tsamp,[Ssamp(1)],options);
                                    %zigzag',t_fit,[PCE0],options
```

```
                                        % Solve the equation for
predicted PCE concentrations
    S_all_pred= model_values(:,1);
    S_all_samp= Ssamp;


dev=S_all_samp-mean(S_all_samp);            % deviations - measure
of spread
SST=sum(dev.^2);                             % total variation to be
accounted for
resid=S_all_samp-S_all_pred;                % residuals - measure of
mismatch
SSE = sum(resid.^2);                        % variation NOT
accounted for
Rsq=1-SSE/SST;                              % percent of error
explained
SSR=SST-SSE;                                % the "ANOVA identity"
dfr=2;                                      % order of the
polynomial
dfe=length(S_all_samp)-1-dfr;                        % degrees of
freedom for error
MSE=SSE/dfe;                                % mean-square error of
residuals
MSR=SSR/dfr;                                % mean-square error for
regression
f=MSR/MSE;                                  % f-statistic for
regression
f
%-------------------------------------------------------------------
-----
% plot data and results
%-------------------------------------------------------------------
-----
% 1- Protein: X(t)
%--------------------
results = [];
figure
plot(t_fit,PCE_data1,'+')
hold on
% Calculate and plot model predictions
options = odeset('RelTol',1e-6,'AbsTol',1e-9);
tm = linspace(0,t_fit(end),101);
%[times, model_values] = ode23s('PCE_AC_reg_model',tm,PCE0,options);
[times, model_values] = ode23s('zigzag',tm,PCE0,options);
plot(times,model_values,'k')
hold off
% add axis titles, etc...
xlabel('Time (day)')
ylabel('PCE (\muM)')
axis([ 0 10 0 260])
results = [results times model_values];

save 'results_Dhb0045.txt' results -ASCII
```

Appendix H

Assimilation of [^{14}C] acetate during PCE dechlorination by (A) *Dhc. ethenogenes* and (B) *Dhb. restrictus*

(A) *Dhc. ethenogenes*

Time (hrs)	Aqueous [^{14}C]	STDEV	% of total [^{14}C] in biomass
0	96.6	0.0	0.0
22	78.2	7.7	12.4
44	58.2	1.8	28.9
65	2.2	0.7	77.4
91	3.1	0.8	83.2
111	3.0	1.0	86.2
135	0.8	0.7	85.8

(B) *Dhb. restrictus*

Time (hrs)	Aqueous [^{14}C]	STDEV	% of total [^{14}C] in biomass
0	101.3	0.0	0.0
19	86.2	12.3	9.5
24	60.7	12.0	33.0
30	35.6	5.3	71.5
41	17.9	10.0	73.3
47	25.8	11.3	74.7
88	2.7	1.0	91.0

Appendix I

The effect of acetate on the long-term dechlorination of cDCE by acetate-limited *Dhc. ethenogenes* cultures (Figure 5.14)

Time (hrs)	VC	VC (STDEV)	cDCE	cDCE (STDEV)	TCE	TCE (STDEV)	PCE	PCE (STDEV)
0	0.0	0.0	0.0	0.0	0.0	0.0	258.5	19.2
20	1.2	0.7	3.4	0.9	10.6	2.8	214.5	5.9
42	5.2	2.1	24.0	7.2	37.0	7.8	125.8	7.3
64	11.1	2.1	164.6	44.1	14.6	19.2	14.5	18.1
93	24.0	3.7	241.0	10.6	0.0	0.0	0.2	0.1
112	36.3	7.4	262.1	18.9	0.0	0.0	0.2	0.0
135	47.9	6.9	262.1	18.5	0.0	0.0	0.1	0.1
161	58.8	18.4	247.5	47.6	0.0	0.0	0.1	0.1
188	86.0	12.1	257.1	15.2	0.0	0.0	0.2	0.0
212	99.2	7.7	223.0	9.3	0.0	0.0	0.1	0.1
225	116.4	3.5	189.0	8.3	0.0	0.0	0.0	0.0
282	134.1	5.0	117.9	12.2	0.0	0.0	0.0	0.0
328	212.5	3.7	88.5	30.5	0.0	0.0	0.0	0.0
380	242.6	4.8	21.5	29.5	0.0	0.0	0.0	0.0
450	306.1	35.6	0.0	0.0	0.0	0.0	0.0	0.0
551	340.8	49.5	0.4	0.1	0.0	0.0	0.0	0.0

Appendix J

The effects of primary carbon source on hydrogen utilization and thresholds by (A) *Dhc. ethenogenes* and (B) *Dhb. restrictus*

(A) *Dhc. ethenogenes*

	High acetate		Trace acetate		Trace acetate, reamended	
Days	H_2 (μM)	STDEV	H_2 (μM)	STDEV	H_2 (μM)	STDEV
0	20450.0	830.0	20450.0	830.0	20450.0	830.0
166	24.9	5.9	2396.3	163.4	2414.8	84.3
238	8.5	2.7	2237.9	30.1	2222.3	176.0
305	9.1	1.1	1556.2	12.5	1653.0	42.4
405	4.5	3.1	447.6	170.3	15.9	6.5
497	9.9	5.3	16.0	7.6	13.1	3.0
593	8.5	2.1	4.7	3.2	10.2	2.0
738	9.0	1.8	10.4	1.1	9.6	3.3

(B) *Dhb. restrictus*

	High acetate		Trace acetate		Trace acetate, reamended	
Days	H_2 (μM)	STDEV	H_2 (μM)	STDEV	H_2 (μM)	STDEV
0	20450.0	830.0	20450.0	830.0	20450.0	830.0
69	285.4	85.0	650.2	199.8	650.2	199.8
95	37.5	3.2	601.3	116.2	601.3	116.2
115	26.7	1.3	516.7	38.0	516.7	38.0
141	21.5	1.6	521.2	83.0	497.2	187.5
219	24.1	1.1	445.9	75.7	478.7	38.3
288	26.4	2.6	464.4	33.3	471.3	46.4
378	25.4	1.8	409.4	72.3	430.1	11.2

Appendix K

Chlorinated ethene transformation by the co-culture under engineered bioremediation

Days	VC	STDEV	cDCE	STDEV	TCE	STDEV	PCE	STDEV
0	0.00	0.00	0.00	0.00	0.00	0.00	15.54	3.42
1	1.49	0.78	10.52	3.24	3.62	3.02	4.50	4.64
2	3.25	0.04	13.82	1.80	2.17	3.07	2.64	3.46
3	10.88	2.63	6.75	3.73	0.34	0.48	0.42	0.30
4	14.01	3.99	1.21	1.54	0.00	0.00	0.09	0.13
5	14.53	2.25	1.56	2.06	0.08	0.11	0.19	0.03
6	13.58	2.14	0.33	0.34	0.13	0.04	0.15	0.02
7	14.57	2.32	0.69	0.83	0.22	0.13	0.26	0.29
8	14.94	0.33	1.00	1.17	0.28	0.22	0.38	0.52
9	16.55	0.07	0.42	0.17	0.13	0.14	0.31	0.18
10	15.71	0.54	0.05	0.07	0.10	0.17	0.41	0.14
11	16.19	2.59	0.07	0.09	0.10	0.14	0.40	0.23
12	16.35	1.87	0.15	0.22	0.07	0.10	0.55	0.17
13	15.54	1.11	0.18	0.25	0.08	0.12	0.38	0.30
14	14.89	1.48	0.16	0.23	0.26	0.15	0.65	0.44
15	14.98	0.12	0.16	0.15	0.30	0.14	0.58	0.63
16	14.39	0.35	0.11	0.08	0.38	0.02	0.70	0.61
17	14.52	0.20	0.19	0.24	0.20	0.28	0.66	0.50
18	14.18	0.21	0.00	0.00	0.37	0.08	0.64	0.77
19	13.97	0.22	0.17	0.25	0.28	0.15	0.66	0.72
20	13.91	0.27	0.04	0.06	0.24	0.21	0.64	0.71
23	15.12	0.77	0.35	0.02	0.71	0.70	0.77	0.56
25	13.51	0.04	0.22	0.19	0.25	0.35	0.31	0.05
28	14.18	0.28	0.03	0.00	0.47	0.05	0.58	0.29

Appendix L

Biomass growth in the co-culture under engineered bioremediation conditions

Days	*Dhc ethenogenes*		*Dhb restrictus*	
	average (mg VSS/L)	STDEV	average (mg VSS/L)	STDEV
0	0.024	0.000	0.012	0.006
1	0.022	0.012	0.010	0.014
2	0.055	0.049	0.035	0.007
3	0.065	0.013	0.070	0.015
4	0.083	0.001	0.064	0.015
5	0.093	0.022	0.057	0.017
8	0.140	0.035	0.036	0.010
10	0.128	0.022	0.025	0.002
12	0.106	0.013	0.036	0.012
17	0.111	0.020	0.021	0.006
21	0.109	0.027	0.018	0.005
24	0.114	0.026	0.018	0.009
27	0.103	0.009	0.009	0.003

Appendix M

Chlorinated ethene transformation by the co-culture under natural attenuation

Days	VC	STDEV	cDCE	STDEV	TCE	STDEV	PCE	STDEV
0	0.00	0.00	0.00	0.00	0.00	0.00	16.00	1.41
1	0.00	0.00	0.94	0.13	3.10	0.30	13.25	1.85
2	0.00	0.00	1.07	0.03	3.15	0.38	12.78	1.07
3	0.00	0.00	1.09	0.05	3.15	0.36	13.13	1.64
4	0.10	0.01	1.06	0.07	2.93	0.23	12.48	0.67
5	0.07	0.01	1.03	0.07	2.83	0.45	12.77	0.58
6	0.07	0.02	0.94	0.04	2.69	0.13	12.47	0.17
7	0.06	0.00	0.84	0.00	2.20	0.53	12.26	1.44
9	0.06	0.01	0.82	0.03	2.90	0.29	11.80	0.34
10	0.06	0.00	0.79	0.02	2.77	0.32	12.12	0.06
11	0.05	0.00	0.73	0.04	2.45	0.29	11.83	1.08
12	0.06	0.01	0.72	0.08	2.35	0.02	12.63	0.46
14	0.06	0.01	0.73	0.04	2.28	0.02	12.97	0.02
15	0.05	0.00	0.71	0.07	2.19	0.19	12.98	0.36
16	0.05	0.00	0.68	0.02	1.76	0.24	11.84	0.11
17	0.05	0.00	0.68	0.01	1.81	0.28	12.41	0.33
20	0.04	0.01	0.69	0.03	1.79	0.06	13.12	1.20
21	0.05	0.00	0.61	0.10	1.72	0.03	13.43	0.93
22	0.06	0.01	0.60	0.06	1.72	0.02	13.44	0.30
23	0.07	0.01	0.55	0.01	1.68	0.01	12.99	0.13
24	0.07	0.00	0.51	0.02	1.50	0.05	12.75	0.35
26	0.05	0.01	0.50	0.02	1.44	0.03	13.09	1.24
28	0.07	0.00	0.46	0.03	1.48	0.11	12.44	1.13

Appendix N

Biomass growth in the co-culture under natural attenuation conditions

Days	*Dhc. ethenogenes*		*Dhb. restrictus*	
	average (mg VSS/L)	STDEV	average (mg VSS/L)	STDEV
0	0.015	0.001	0.027	0.018
1	0.010	0.012	0.057	0.005
3	0.006	0.001	0.041	0.002
5	0.006	0.001	0.046	0.004
9	0.008	0.000	0.037	0.017
10	0.006	0.001	0.034	0.005
14	0.003	0.001	0.034	0.011
18	0.003	0.002	0.026	0.007
21	0.002	0.001	0.026	0.009
26	0.004	0.000	0.016	0.004
28	0.001	0.000	0.021	0.005
30	0.002	0.001	0.014	0.001

Appendix O

Acetate and H_2 consumption by the defined co-culture under natural attenuation conditions

	Acetate			H_2	
Days	average (μM)	STDEV	Days	average (μM)	STDEV
0	8.99	2.29	0	10.88	0.42
1	7.46	0.35	1	8.59	0.34
2	7.09	1.56	2	7.19	0.51
3	8.25	0.42	3	6.70	0.03
4	7.90	1.41	4	5.71	0.19
6	7.45	1.05	5	5.50	0.31
8	7.60	1.26	6	5.71	0.26
9	9.18	1.46	7	5.53	0.04
11	8.38	0.96	8	6.17	0.25
13	8.39	0.24	9	5.55	0.13
14	7.82	1.29	11	5.36	0.23
16	8.99	0.06	12	5.87	0.13
18	8.69	2.08	13	6.79	0.07
19	6.71	0.77	14	5.84	0.05
20	7.40	0.52	15	6.66	0.11
22	7.33	1.40	16	5.82	0.35
23	8.33	0.73	17	6.85	0.35
24	6.97	0.00	18	6.06	0.40
25	6.93	0.11	19	6.19	0.04
27	7.18	1.10	20	6.95	0.04
29	7.59	0.07	21	5.98	0.23
			23	7.09	0.26
			24	7.88	0.00
			25	7.34	0.12
			28	7.78	0.08
			30	7.89	0.08

References

Adrian, L., Szewzyk, U., Wecke, J., Gorisch, H. 2000. Bacterial dehalorespiration with chlorinated benzenes. *Nature.* 408: 580-3.

Azizian, M. F., Behrens, S., Sabalowsky, A., Dolan, M. E., Spormann, A. M., Semprini, L. 2008. Continuous-flow column study of reductive dehalogenation of PCE upon bioaugmentation with the Evanite enrichment culture. *J. Contam. Hydrol*. 100: 11-21.

Bagley, D. M. 1998. Systematic Approach for modeling tetrachloroethene biodegradation. *J. Environ. Eng*. 124: 1076-1086.

Becker, J. G. 2006. A Modeling study and implications of competition between *Dehalococcoides ethenogenes* and other tetrachloroethene- respiring bacteria. *Environ. Sci. Technol.* 40: 4473-4480.

Bradley, P. M. 2003. History and ecology of chloroethene biodegradation: a review. *Bioremediation J.* 7: 81–109.

Brockmann, D., Rosenwinkel, K. H., Morgenroth, E. 2008. Practical identifiability of biokinetic parameters of a model describing two-step nitrification in biofilms *Biotechnol. Bioeng*. 101: 497-514.

Brun, R., Kühni, M., Siegrist, H., Gujer, W., Reicher, P. 2002. Practical identifiability of ASM2d parameters-systematic selection and tuning of parameter subsets. *Wat. Res*. 36: 4113-4127.

CERCLA Overview. U.S. Environmental Protection Agency (EPA). 2005.

Christ, J.A., Ramsburg, C. A., Abriola, L. M., Pennell, K. D., Löffler, F. E. 2005. Coupling aggressive mass removal with microbial reductive dechlorination for remediation of DNAPL source zones: a review and assessment. *Environ. Health Perspect*. 113: 465–477.

Coleman, N. V., Mattes, T. E., Gossett, J. M., Spain, J. C. 2002. Biodegradation of cis-dichloroethene as the sole carbon source by a ß-Proteobacterium. *Appl. Environ. Microbiol.* 68: 2726-2730.

Cupples, A. M, Spormann, A. M., McCarty, P. L. 2003. Growth of a *Dehalococcoides*-like microorganism on vinyl chloride and cis-dichloroethene as electron acceptors as determined by competitive PCR. *Appl. Environ. Microbiol*. 69: 953- 959.

Cupples, A. M, Spormann, A. M., McCarty, P. L. 2004. Vinyl chloride and *cis*-dichloroethene dechlorination kinetics and microorganism growth under substrate limiting conditions. *Environ. Sci. Technol*. 38: 1102– 1107.

De Wever, H., Cole, J. R., Fettig, M. R., Hogan, D. A., Tiedje, J. R. 2000. Reductive dehalogenation of trichloroacetic acid by *Trichlorobacter thiogenes* gen. nov., sp. nov. *Appl. Environ. Microbiol.* 66: 2297-2301.

de Wildeman, S., Diekert, G., Van Langenhove, H., Verstraete, W. H. 2003. Stereoselective microbial dehalorespiration with vicinal dichlorinated alkanes. *Appl. Environ. Microbiol*. 69: 5643-5647.

deWeerd, K. A., Mandelco, L., Tanner, R. S., Woese, C. R., Suflita, J. M. 1990. *Desulfomonile tiedjei* gen. nov. and sp. nov., a novel anaerobic, dehalogenating, sulfate-reducing bacterium. *Arch. Microbiol*.154: 23-30.

DSMZ, German Collection of Microorganisms and Cell Cultures. 2010. Medium 732. **(**http://www.dsmz.de/microorganisms/medium/pdf/DSMZ_Medium732.pdf**)**

Drzyzga, O., Gottschal, J. C. 2002. Tetrachloroethene Dehalorespiration and Growth of *Desulfitobacterium frappieri* TCE1 in Strict Dependence on the Activity of *Desulfovibrio fructosivorans. Appl. Environ. Microbiol*. 68: 642-649.

Duhamel, M., Edwards, E. A. 2006. Microbial composition of chlorinated ethenedegrading cultures dominated by *Dehalococcoides*. *FEMS Microbiol. Ecol.* 58: 538-549.

Ellis, T. G., Barbeau, D.S., Smets, B. F., Grady, C. P. L., Jr. 1996. Respirometric technique for determination of extant kinetic parameters describing biodegradation. *Water Environ. Res*. 68: 917-926.

Fennell, D. E., Carroll, A. B., Gossett, J.M., Zinder, S.H. 2001. Assessment of indigenous reductive dechlorinating potential at a TCE-contaminated site using microcosms, polymerase chain reaction analysis, and site data. *Environ. Sci*. *Technol*. 32: 1830-1839.

Fennell, D. E., Gossett, J. M. 1999. Comment on "Enrichment of high-rate PCE dechlorination and comparative study of lactate, methanol, and hydrogen as electron donors to sustain activity". *Environ. Sci. Technol* 33:2681-2682.

Fennell, D. E., Gossett, J. M. 1998. Modeling the production of and competition for hydrogen in a dechlorinating culture. *Environ. Sci. Technol*. 32: 2450-2460.

Fennell, D. E. 1998. Comparison of alternate hydrogen donors for anaerobic reductive dechlorination. Ph.D. Dissertation, Cornell Univeristy.

Jetten, M. S M., Stams, A. J. M., Zehnder, A. J. B. 1990. Acetate threshold values and acetate activating enzymes in methanogenic bacteria. *FEMS Microbiol. Ecol*. 73: 339–344.

Freedman, D.L., Gossett, J. M. 1989. Biological reductive dechlorination of tetrachloroethylene and trichloroethylene to ethylene under methanogenic conditions. *Appl. Environ. Microbiol*. 55: 2144-2151.

Furukawa, K. 2003. 'Super bugs' for bioremediation. *Trends Biotechnol.* 21: 187–90.

Grostern, A., Chan, W. W., Edwards, E. 2009. A1,1,1-trichloroethane and 1,1-dichloroethane reductive dechlorination kinetics and co-contaminant effects in a *Dehalobacter*-containing mixed culture. *Environ. Sci. Technol*. 43: 6799-6807.

Grostern, A., Edwards, E. A. 2006a. Growth of *Dehalobacter* and *Dehalococcoides* spp. during Degradation of Chlorinated Ethanes. *Appl. Environ. Microbiol*. 72: 428-436.

Grostern, A., Edwards, E. A. 2006b. A 1,1,1-trichloroethane-degrading anaerobic mixed microbial culture enhances biotransformation of mixtures of chlorinated ethenes and ethanes. *Appl. Environ. Microbiol* .72: 7849-7856.

Gerritse, J., Drzyzga, O., Kloetstra, G., Keijmel, M., Wiersum, L. P., Hutson, R., Collins, M. D., Gottschal, J. C. 1999. Influence of different electron donors and accepters on dehalorespiration of tetrachloroethene by *Desulfitobacterium frappieri* TCE1. *Appl. Environ. Microbiol.* 65: 5212-5221.

Gerritse, J., Renard, V., Gomes, T. M. P., Lawson, P. A., Collins, M. D., Gottschal, J. C. 1996. *Desulfitobacterium* sp. strain PCE1, an anaerobic bacterium that can grow by reductive dechlorination of tetrachloroethene or ortho-chlorinated phenols. *Arch. Microbiol*. 165: 132-140.

Goevert, D., Conrad, R. 2008. Carbon isotope fractionation by sulfate-reducing bacteria using different pathways for the oxidation of acetate. *Environ. Sci. Technol.* 42: 7813–7817.

Gossett, J. M. 1987. Measurement of Henry's Law Constant for C1 and C2 chlorinated hydrocarbons. *Environ. Sci.Technol*. 21: 202-208.

Gossett, J.M., Zinder, S.H. 1997. Microbiological aspects relevant to natural attenuation of chlorinated ethenes. *Proceedings of the US EPA Symposium in Natural Attenuation of Chlorinated Organics in Ground Water*. Dallas, Texas. EPA /540/R-97/504: 12-15.

Grady, C. P. L., Jr, Smets, B. F., Barbeau, D. S. 1996. Variability in kinetic parameter

estimates: A review of possible causes and a proposed terminology. *Wat. Res*. 30: 742-748.

Grady, C. P. L., Jr., 1985 Biodegradation: Its measurement and microbiological basis. *Biotechnol. Bioeng. 27*: 660-674.

Hallam, S. J., T. J. Mincer, C. Schleper, C. M. Preston, K. Roberts, P. M. Richardson, E. F. DeLong. 2006. Pathways of carbon assimilation and ammonia oxidation suggested by environmental genomic analyses of marine *Crenarchaeota*. *PLOS Biology*. 4: 0520-0536.

Haston, Z. C., McCarty, P. L. 1999. Chlorinated ethene half-velocity coefficients (*Ks*) for reductive dehalogenation. *Environ. Sci.Technol*. 33: 223-226.

He, J., Holmes, V. F., Lee, P. K., Alvarez-Cohen, L. 2007. Influence of vitamin B_{12} and cocultures on the growth of *Dehalococcoides* isolates in defined medium. *Appl. Environ. Microbiol.* 73: 2847-2853.

He, J., Ritalahti, K. M., Yang, K. L., Koenigsberg, S. S, Löffler, F. E. 2003. Detoxification of vinyl chloride to ethene coupled to growth of an anaerobic bacterium. *Nature.* 424: 62-65.

He, J., Sung, Y., Dollhopf, M. E., Fathepure, B.Z., Tiedje, J. M., Löffler, F. E. 2002. Acetate versus hydrogen as direct electron donors to stimulate the microbial reductive dechlorination process at chloroethene-contaminated sites. *Environ. Sci. Technol.* 36:3945–3952.

He, Q., Sanford, R. A. 2004. Acetate threshold Concentrations suggest varying energy requirements during anaerobic respiration by *Anaeromyxobacter dehalogenans*. *Appl. Environ. Microbiol*. 70: 6940-6943.

Horri, T., Noll, M., Igarashi, Y., Friedrich, M. W., Conrad, R. 2007. Identification of Acetate-Assimilating Microorganisms under Methanogenic Conditions in Anoxic Rice Field Soil by Comparative Stable Isotope Probing of RNA. *Appl. Environ. Microbiol*. 73: 101-109.

Huang, Deyang. 2009. The Kinetics of two heterotrophic tetrachloroethene-respiring populations and their effects on the substrate interactions with Dehalococcoides strains. Ph. D. Dissertation. University of Maryland.

Huang, D.Y., Becker, J. G. 2009. Determination of intrinsic Monod kinetic parameters for two heterotrophic tetrachloroethene (PCE)-respiring strains and insight into their application. *Biotechnol. Bioeng.* 104: 301-311.

Holliger, C., Wohlfarth, G., Diekert, G. 1999. Reductive dechlorination in the energy metabolism of anaerobic bacteria. *FEMS Microbiol. Rev.* 22: 383–98

Holliger, C., Hahn, D., H., Ludwig, W., Schumacher, B., Tindall, F., Vazquez, N. W., Zehnder, A. J. B. 1998. *Dehalobacter restrictus* gen. nov. and sp. nov., a strictly anaerobic bacterium that reductively dechlorinates tetra- and trichloroethene in an anaerobic respiration. *Arch. Microbiol*. 169: 313-321

Holliger, C., Schraa, G., Stams, A.J., Zehnder, A.J. 1993. A highly purified enrichment culture couples the reductive dechlorination of tetrachloroethene to growth. *Appl. Environ. Microbiol*. 59: 2991–2997.

Jackson, B. E., McInerney, M. J. 2002. Anaerobic microbial metabolism can proceed close to thermodynamic limits. *Nature*. 415: 454-456

Johnson, D. R., Brodie, E. L., Hubbard, A. E., Zinder, S. H., Alvarez-Cohen, L..2008. Temporal transcriptomic microarray analysis of "*Dehalococcoides ethenogenes*" strain 195 during the transition into stationary phase. *Appl. Environ. Microbiol.* 74: 2864-72.

Krajmalnik-Brown, R. 2005. Genetic identification of reductive dehalogenase genes in Dehalococcoides. Ph.D. Dissertation. Georgia Institute of Technology.

Krumholz, L. R. 1997. *Desulfuromonas chloroethenica* sp. nov. uses tetrachloroethylene and trichloroethylene as electron acceptors. *Int. J. Syst. Evol. Microbiol*. 47: 1262-1263.

Lendvay, J. M., Löffler, F.E., Dollhopf, M., Aiello, M. R., Daniels, G., Fathepure, B. Z., Gebhard, M., Heine, R., Helton, R., Shi, J., Krajmalnik-Brown, R., Major, C.L. Jr..,Barcelona, M. J., Petrovskis, E., Hickey, R., Tiedje, J.M., Adriaens, P. 2003. Bioreactive barriers: a comparison of bioaugmentation and biostimulation for chlorinated solvent remediation. *Environ. Sci. Technol*. 37: 1422-1431.

Liu, C., Zachara, J. M. 2001. Uncertainties of Monod kinetics parameters nonlinearly estimated from batch experiments. *Environ. Sci. Technol*. 35: 133-141.

Löffler ,F.E., Sun, Q., Li, J., Tiedje, J. M. 2000. 16S rRNA gene-based detection of tetrachloroethene (PCE)-dechlorinating *Desulfuromonas* and *Dehalococcoides* species. *Appl. Environ. Microbiol*. 66: 1369-1374.

Löffler, F.E., Tiedje, J. M, Sanford RA. 1999. Fraction of electrons consumed in electron acceptor reduction and hydrogen thresholds as indicators of halorespiratory physiology. *Appl. Environ. Microbiol*. 65: 4049-4056.

Luijten, M. L. G. C., de Weert, J., Smidt, H., Boschker, H. T. S., de Vos, W. M., Schraa, G., Stams, A. T. M. 2003. Description of *Sulfurospirillum halorespirans* sp. nov., an anaerobic, tetrachloroetherespiring bacterium, and transfer of

Dehalospirillum multivorans to the genus *Sulfurospirillum* as *Sulfurospirillum multivorans* comb. nov. *Int. J. Syst. Evol. Microbiol.* 53: 787-793.

Maillard, J. 2004. Molecular characterization of key enzymes involved in dehalorespiration with tetrachloroethene. Ph. D. dissertation. Swiss Federal Institute of Technology.

May, H. D., Miller, G. S., Kjellerup, B. V., Sowers, K. R. 2008. Dehalorespiration withpolychlorinated biphenyls by an anaerobic ultramicrobacterium. *Appl. Environ. Microbiol*. 74: 2089–2094.

Maymó-Gatell, X., Chien, Y., Gossett, J. M., Zinder, S. H. 1997. Isolation of a bacterium that reductively dechlorinates tetrachloroethene to ethene. *Science*. 276: 1568-1571.

McCarty, P. L. 1975. Stoichiometry of biological reactions. *Prog. Water Technol. 7*: 157-172.

McCarty, P.L, Semprini, L. 1994. Ground water treatment for chlorinated solvents. In: RD Norris et al. (Eds.), Handbook of bioremediation. Lewis Publishers, Boca Raton, FL. 87-116.

Miller, E., Wohlfarth, G., Diekert, G. 1997. Comparative studies on tetrachloroethene reductive dechlorination mediated by *Desulfitobacterium* sp. strain PCE-S. *Arch. Microbiol.* 168: 513-519.

Mohn, W.W., Tiedje, J. M. 1992. Microbial reductive dehalogenation. *Microbial Reviews*. 56: 482-507.

Müller, J. A., Rosner, B. M., von Abendroth, G., Meshulam-Simon, G., McCarthy, P. L., Spormann, A. M. 2004. Molecular identification of the catabolic vinyl chloride reductase from *Dehalococcoides* sp. strain VS and its environmental distribution. *Appl. Environ. Microbiol*. 70: 4880-4888.

Nijenhuis, I., Nikolausz, M., Köth, A., Felföldi, T., Weiss, H., Drangmeister, J., Großmann, J., Kästner, M., Richnow, H. H. 2007. Assessment of the natural attenuation of chlorinated ethenes in an anaerobic contaminated aquifer in the Bitterfeld/Wolfen area using stable isotope techniques, microcosm studies and molecular biomarkers. *Chemosphere*. 67: 300-311.

Nonaka, H., Keresztes, G., Shinoda, Y., Ikenaga, Y., Abe, M., Naito, K., Inatomi, K., Furukawa, K., Inui, M., Yukawa, H. 2006. Complete genome sequence of the dehalorespiring bacterium *Desulfitobacterium hafniense* Y51 and comparison with *Dehalococcoides ethenogenes* 195. *J. Bacteriol*. 188: 2262–2274.

Ritalahti, K. M., Löffler, F. E. 2004. Populations implicated in the anaerobic

reductive dechlorination of 1,2-dichloropropane in highly enriched bacterial communities. *Appl. Environ. Microbiol*. 70: 4088-4095.

Ritalahti, K. M., Amos, B. K., Sung, Y., Wu, Q., Koenigsberg, S. S., Löffler, F. E. 2006, Quantitative PCR targeting 16S rRNA and reductive dehalogenase genes simultaneously monitors multiple Dehalococcoides strains. *Appl. Environ. Microbiol*. 72: 2765-2774.

Rittmann, B. E., McCarty, P. L. 2001. Environmental Biotechnology: Principles and Applications. McGraw-Hill Inc. NewYork.

Robinson, J. A, Tiedje, J. M. 1983. Nonlinear estimation of Monod hrowth kinetic parameters from a single substrate depletion curve. *Appl. Environ. Microbiol*. 45: 1453-1458.

Scholz-Muramatsu, H., Neumann, A., Messmer, M., Moore, E., Diekert, G. 1995. Isolation and characterization of *Dehalospirillum multivorans* gen. nov., sp. nov., a tetrachloroethene- utilizing strictly anaerobic bacterium. *Arch. Microbiol*. 163: 48-56.

Seshadri, R., Adrian, L., Fouts, D. E., Eisen, J. A., Phillippy, A. M., Methe, B. A., Ward, N. L., Nelson, W. C., Deboy, R. T., Khouri, H. M., Kolonay, J. F., Dodson, R. J., Daugherty, S. C., Brinkac, L. M., Sullivan, S. A., Madupu, R., Nelson, K. E., Kang, K. H., Impraim, M., Tran, K., Robinson, J. M., Forberger, H. A., Fraser, C. M., Zinder, S. H., Heidelberg, J. F. 2005. Genome sequence of the PCE-dechlorinating bacterium *Dehalococcoides ethenogenes*. *Science*. 307: 105-108.

Smatlak, C. R., Gossett, J. M., Zinder, S. H. 1996. Comparative kinetics of hydrogen utilization for reductive dechlorination of tetrachloroethene and methanogenesis in an anaerobic enrichment culture. *Environ. Sci. Technol*. 30:2850–2858.

Smidt, H., de Vos, W. M. 2004. Anaerobic Microbial Dehalogenation. *Annu. Rev. Microbiol.* 2004. 58: 43–73

Smits, H. M., Devenoges, C., Szynalski, K., Maillard, J., Holliger, C. 2004. Development of a real-time PCR method for quantification of the three genera *Dehalobacter, Dehalococcoides*, and *Desulfitobacterium* in microbial communities. *J. Microbiol. Methods*. 57: 369–378.

Smidt, H., Akkermans, A. D. L., van der Oost, .J., de Vos, W. M. 2000. Halorespiring bacteria—molecular characterization and detection. *Enzyme Microbiol. Technol.* 27: 812–20

Stuart, S.L., Woods, S.L., Lemmon, T.L., Ingle, J. D. Jr. 1999. The effect of redox potential changes on reductive dechlorination of pentachlorophenol and the degradation of acetate by a mixed methanogenic culture. *Biotechnol. Bioeng*. 63: 69-78.

Sun, B., Cole, J. R., Sanford, R. A., Tiedje, J M. 2000. Isolation and characterizationof *Desulfovibrio dechloracetivorans* sp. nov., a marine dechlor.inating bacterium growing by coupling the oxidation of acetate to the reductive dechlorination of 2-chlorophenol. *Appl. Environ. Microbiol.* 66: 2408–13

Sung, Y., Fletcher, K. E., Ritalahti, K. M., Apkarian, R. P., Ramos-Hernández, N., Sanford, R. A., Mesbah, N. M. Löffler, F. E. 2006. *Geobacter lovleyi* sp. nov. Strain SZ, a Novel Metal-Reducing and Tetrachloroethene-Dechlorinating. *Appl. Environ. Microbiol*.72: 2775-2782

Supida Piwkhow. 2007. Theoretical and experimental evaluation of acetate thresholds as a monitoring tool for in situ bioremediation. M.S. Thesis. University of Maryland.

Suyama, A., Iwakiri, R., Kai, K., Tokunaga, T., Sera, N., Furukawa, K. 2001. Isolation and characterization of *Desulfitobacterium* sp. strain Y51 capable of efficient dehalogenation of tetrachloroethene and polychloroethanes. *Biosci. Biotechnol. Biochem*. 65: 1474-81.

Tang, Y.J., Yi, S., Zhuang, W. Q., Zinder, S. H., Keasling, J. D., Alvarez-Cohen, L. 2009. Investigation of carbon metabolism in "*Dehalococcoides ethenogenes*" strain 195 by use of isotopomer and transcriptomic analyses. *J. Bacteriol.* 191: 5224-5231.

Utkin, I., C. Woese, C., Wiegel, J. 1994. Isolation and characterization of *Desulfitobacterium dehalogenans* gen. nov., sp. nov., an anaerobic bacterium which reductively dechlorinates chlorophenolic compounds. *Int. J. Syst. Bacteriol*. 44: 612-619.

van Doesburg, W., van Eekert, M. H., Middeldorp, P. J., Balk, M., Schraa, G., Stams, A. J. 2005. Reductive dechlorination of beta-hexachlorocyclohexane (beta-HCH) by a *Dehalobacter* species in coculture with a *Sedimentibacter sp*. *FEMS Microbiol. Ecol.* 54: 87-95.

Verce, M. F., Gunsch, C. K., Danko, A. S., Freedman, D. L. 2002. Cometabolism of cis-1,2-dichloroethene by aerobic cultures grown on vinyl chloride as the primary substrate. *Environ. Sci. Technol.* 36: 2171-2177.

Vogel, T. M, Criddle, C.S., McCarty, P.L. 1987. Transformation of halogenated aliphatic compounds. *Environ. Sci. Technol*. 21: 722-736.

Wackett, L. P. Hershberger, C. D. 2001. *Biocatalysis and Biodegradation, Microbial Transformation of Organic Compounds*. ASM Press: Washington, D.C., p 228.

Westermann, P., Ahring, B. K., Mah, R.A. 1989. Threshold acetate concentrations for acetate catabolism by aceticlastic methanogenic bacteria. *Appl .Environ. Microbiol*. 55: 514–515.

Wild, A., Hermann, R., Leisinger, T. 1997. Isolation of an anaerobic bacterium which reductively dechlorinates tetrachloroethene and trichloroethene. *Biodegradation.* 7: 507-511

Wilhelm, E., Battino, R., Wilcock, R. J. 1977. Low pressure solubility of gases in liquid water. *Chem Rev*. 77: 219–262.

Wu, Q. Z., Watts, J. E. M., Sowers, K. R., May, H. D. 2002a. Identification of a bacterium that specifically catalyzes the reductive dechlorination of polychlorinated biphenyls with doubly flanked chlorines. *Appl. Environ. Microbiol*. 68: 807–812.

Wu, Q. Z., Milliken, C. E., Meier, G. P., Watts, J. E. M., Sowers, K. R., May, H. D. 2002b. Dechlorination of chlorobenzenes by a culture containing bacterium DF-1, a PCB dechlorinating microorganism. *Environ. Sci. Technol*. 36: 3290–3294.

Yang, Y. R., McCarty, P. L. 1998. Competition for hydrogen within a chlorinated solvent dehalogenating anaerobic mixed culture. *Environ. Sci. Technol.* 32: 3591–97

Yang, Y., Pesaro, M., Sigler, W., Zeyer, J. 2005. Identification of microorganisms involved in reductive dehalogenation of chlorinated ethenes in an anaerobic microbial community. *Water Res.* 39: 3954–3966.